REGIONAL SEDIMENT MANAGEMENT PLAN

APPENDICES

APPENDIX A

BIBLIOGRAPHY

Bibliography

1. Barry, J., et al. (1997), A New Broad Band Frequency Modulated Subbottom Profiling Developed for Hawaii, paper presented at Seventh Annual International Offshore and Polar Engineering Conference

2. Society of Offshore and Polar Engineers (ISOPE), Honolulu, HI, 1997.

3. Cacchione, D., et al. (2002), Sand transport within a reef channel off Kailua, paper presented at Ocean Science Meeting, American Geophysical Union, Honolulu.

4. Campbell, J.H. (1972), Erosion and Accretion of Selected Hawaiian Beaches, 1962-1972: Honolulu, NOAA Sea Grant Program, p. 1-30.

5. Chien, Y., and C. Murray (1999), Sand Thickness Exploration Model - Kailua Bay, Pacific Northwest National Laboratory.

6. Coastal Engineering Manual (2006), EM 1110-2-1100, USACE, Coastal and Hydraulics Laboratory.

7. Conger, C. L. F., C.H., and M. Barbee (2005), Artificial neural network classification of sand in all visible submarine and subaerial regions of a digital image, Journal of Coastal Research, 21, 1173-1177.

8. Department of Planning and Permitting, City and County of Honolulu (2000), Ko`olaupoko Sustainable Communities Plan, Ch 3, 1-47.

9. Edward K. Noda and Associates Inc., and DHM inc (1989), Hawaii shoreline erosion management study, 34-75 pp, Hawaii Coastal Zone Managment Program, Honolulu.

10. Ericksen, M. C., et al. (1997), Sub-bottom imaging of the Hawaiian shelf. , in Sea Technology, edited, pp. 89-92.

11. Fletcher, C. H., et al. (1996), Coastal erosion management on the island of Oahu., 102-111 pp, University of Hawaii, DLNR, Honolulu.

12. Fletcher, C. H., et al. (1997), Beach loss Along Armored Shorelines on Oahu, Journal of Coastal Research, 13, 209-215.

13. Gerritsen, F. (1978), Beach and Surf Parameters in Hawaii: Honolulu, NOAA Sea Grant, p. 1-178.

14. Grossman, E. C., and C. H. Fletcher (2004), Holocene Reef Development Where Wave Energy Reduces Accommodation Space. Kailua Bay, Windward Oahu, Hawaii, USA, Journal of Sedimentary Research, 74, 49-63.

15. Hampton, M. A., et al. (2004), Carbonate Sediment Deposits on the Reef Front Around Oahu, Hawaii, Marine Georesources and Geotechnology, 22, 65-102.

16. Harney, J. N. (2000), Carbonate Sedimentology of a Windward Shoreface: Kailua Bay, Oahu, Hawaiian Islands, 232 pp, University, Honolulu.

17. Harney, J. N., and C. H. Fletcher (2003), A budget of Carbonate Framework and Sediment Production, Kailua Bay, Oahu, Hawaii, Journal of Sedimentary Research, 73, 856-868.

18. Harney, J. N., et al. (2000), Age and composition of carbonate shoreface sediments, Kailua Bay, Oahu, Hawaii, Coral Reefs, 19, 141-154.

19. Harney, J. N., et al. (1999), Standing crop and sediment production of reef-dwelling foraminifera on Oahu, Hawaii, Pacific Science, 53, 61-73.

20. Hawaii State Department of Health (2001), Total Maximum daily Loads Estimated for Waimanalo Stream - Island of Oahu, Hawaii-, 35 pp, U.S. Environmental Protection Agency Specifications, Hawaii.

21. Ho, F. P., and L. A. Sherretz (1969), A preliminary study of ocean waves in the Hawaiian area, 36 pp, University of Hawaii, HIG-69-16, Seagrant 69-2, Honolulu.

22. Hwang, D. (1981), Beach changes on Oahu as revealed by aerial photographs: Honolulu, Urban and Regional Planning Program and Hawaii Institute of Geophysics, p. 1-146.

23. Isoun, E. (2001), A remote sensing study of coral reefs; Kailua bay, Oahu, 99 pp, University of Hawaii, Honolulu.

24. Isoun, E., et al. (2003), Multi-spectral mapping of the reef bathymetry and coral cover Kailua Bay, Hawaii, Coral Reefs, 22, 68-82.

25. Krock, H. J., and H. Sundararaghavan (1993), Kailua Bay Circulation (KB-5), 24 pp, Univ. of Hawaii, Water Resources Research Center, Honolulu.

26. Laevastu, T., Avery, D. E., Cox, D. C. (1964), Coastal currents and sewage disposal in the Hawaiian Islands: Honolulu, Department of Planning and Economic Development, State of Hawaii, p. 1-101.

27. Laevastu, T., et al. (1964), Coastal currents and sewage disposal in the Hawaiian Islands., 36-38 pp, Univ. of Hawaii, HIG-64-1, Honolulu.

28. Lander, J. F., and P. A. Lockridge (1989), United States Tsunamis, 17-23 pp, National Geophysical Data Center, Boulder.

29. Laws, E. A., and L. Ferentinos (2003), Human Impacts on Fluxes of Nutrients and Sediment in Waimanalo Stream, Oahu, Hawaiian Islands., Pacific Science, 57, 119-140.

30. Laws, E. A., and L. Roth (2004), Impact of Stream Hardening on Water Quality and Metabolic Characteristics of Waimanalo and Kaneohe Stream, Oahu, Hawaiian Islands, Pacific Science, 58, 261-280.

31. Lipp, D.G. (1995), Changes in beach profiles due to wave reflections off seawalls at Lanikai, Hawaii [unpublished Masters thesis]: University of Hawaii, Honolulu, 76 p.

32. Moberly, R., Jr. et al. (1965), Source and Variation of Hawaiian Littoral Sand, Journal of Sedimentary Petrology, 35, 589-598.

33. Moberly, R., Jr. and T. Chamberlain (1964), Hawaiian Beach Systems, 64-65 pp, Univ. of Hawaii, Honolulu.

34. Mullane, Robert and D. Suzuki (1997), Beach Management Plan for Maui, County of Maui Planning Department, p. 1-35.

35. Norcross, Z.M. (2001), Large-scale alongshore meanders on a carbonate beach substitute for seasonal morphology in response to wave state [unpublished Masters thesis]: University of Hawaii, Honolulu, 37 p.

36. Norcross, Z. M., et al. (2002), Annual and terannual changes on a reef-fringed pocket beach: Kailua Bay, Hawaii, Marine Geology, 190, 553-580.

37. Pararas-Carayannis, G., and J. P. L. Calbaugh (1977), Catalog of Tsunamis in Hawaii, 25, 29, 50 pp, World Data Center A for Solid Earth Geophysics, Report SE-4, Boulder.

38. Regional Sediment Management (RSM) Demonstration Program Technical Note, U.S. Army Corps of Engineers Engineer Research and Development Center, ERDC/RSM-TN-2, June 2003.

39. Richmond, B. M., et al. (2002), Sand transport within a reef channel off Kailua, Oahu, Hawaii, paper presented at Ocean Science meeting, American Geophysical Union, Honolulu.

40. Sea Engineering Inc. (1989), Oahu Shoreline Study, Part 2, Management Strategies: Waimanalo, HI.

41. Sea Engineering Inc. (1993), Beach Nourishment: Waimanalo, HI, p. 1-33.

42. Shaw, S. L. (1981), A history of tropical cyclones in the central North Pacific and the Hawaiian Islands 1832-1979, 125 pp, NOAA, National Weather Service, Silver Spring.

43. Smith, D.A. (2003), Effect of particle shape on grain size, hydraulic, and transport characteristics of calcareous sand [unpublished dissertation]: University of Hawaii, Honolulu, 94 p.

44. Smith, T. D. and J. R. Hayes, Southeast Oahu Regional Sediment Management: Identifying Sediment Pathways in the Vicinity of Wailea Point, Regional Sediment Management, Winter/Spring 2006

45. Tetra Tech EM Inc (2003), Kailua Waterways Improvement Plan, 95 pp, Kailua Bay Advisory Council, Honolulu.

46. US Army Corps of Engineers (2004), Regional Sediment Management Primer.

47. Walker, D. A. (1994), Tsunami Facts, 31-37 pp, University of Hawaii, SOEST Tech. Report 94-03, Honolulu.

48. Wyrtki, K., et al. (1969), Current observations in the Hawaiian archipelago, 1-27 pp, Univ. of Hawaii, Office of Naval Research - Contract nonr-3748(06), Honolulu.

APPENDIX B

SOUTHEAST OAHU REGIONAL SEDIMENT MANAGEMENT DEMONSTRATION PROJECT SCOPE OF WORK

SOUTHEAST OAHU REGIONAL SEDIMENT MANAGEMENT DEMONSTRATION PROJECT

Regional Beach Management Plan
Scope of Work

August 7, 2006

BACKGROUND: The Southeast Oahu Regional Sediment Management (SEO/RSM) demonstration project is being conducted to (1) document long-term trends in wave climate for the windward side of Oahu, Hawaii, (2) develop a regional sediment budget and a geographic information system (GIS) for three littoral cells along the southeast Oahu coast, (3) identify suitable sand sources, and (4) develop/calibrate a sediment transport model for the region. The SEO region is located on the southeast shoreline of the island of Oahu, Hawaii. There are three littoral cells, Kailua in the north, Lanikai in the middle, and Waimanalo in the south part of the study area. There are geologic controls (both sub-aerial and offshore) affecting sediment transports within these cells. The offshore region is a sloping reef along which waves break on its outer edge. Waves are depth-limited by the reef as they approach the shoreline. SEO/RSM investigations are being conducted to determine if there is sediment transport between the cells. Long-term (decadal or more) shifts in wind, wave direction, and wave period may shift sediment transport patterns and magnitudes. As a result, sediment transport processes of these beaches are difficult to understand, and RSM solutions are not readily apparent. The final products from this study will be a sand source inventory, web-enabled GIS platform and regional beach management plan for the SEO region.

REGIONAL BEACH MANAGEMENT PLAN: The work to be performed under this task order is the preparation of the SEO/RSM Regional Beach Management Plan (RBMP) report. The RBMP report will document all of the activities that have been conducted since the beginning of the SEO/RSM investigations in fiscal year 2005 (see attached SEO/RSM scope of work). Work that has been performed by the Honolulu District, Coastal & Hydraulics Laboratory, Geotechnical and Structures Laboratory and the University of Hawaii (UH) will be documented in the RBMP report along with the results of the study workshops (the next workshop is to be held on August 23, 2006). Descriptions of the various tasks that have been completed are provided as attachments to this document. Reference is also made to the “Beach Management Plan for Maui” dated December 1997 as prepared for the County of Maui Planning Department by UH Sea Grant Extension Service. Many of the SEO/RSM products can be found online at the following web site.

http://gis.poh.usace.army.mil/rsm/pages/index.htm

RBMP Report: The RBMP report will consist at a minimum of the follow sections that compile the study results to date:

Executive Summary
Introduction
Regional Sediment Management
Southeast Oahu Regional Sediment Management Demonstration Project
Coastal Ecosystem
Coastal Erosion, Beach Loss and Coral Reef Degredation
Objectives
- Identification of Erosion Hotspots and Erosion Watchspots
- Guidelines for Shoreline Protection Measures
- Beach Nourishment
  - Sand Sources for Beach Nourishment
  - Pilot Beach Nourishment Project
- Dune Preservation and Restoration
- Coral Reef Ecosystems, Water Quality, and Upland Activities
- Shoreline Setbacks and Coastal Erosion Hazard Data
- Proactive Development of Coastal Lands
- Inter-agency Coordination
- Structures and Activities within the Shoreline Area
  - Minor Structures
  - Major Structures
- Beach Management Districts
- Public Awareness and Education

Coastal Processes Modeling
- Wave Climate
- Water Circulation
- Littoral Sediment Transport
- Regional Sediment Budget

Geomorphology
Shoreline Change
Sediment Trend Analysis
Sand Source Investigations
Workshops
Web-based GIS
Literature Search/Inventory
Potential Demonstration Projects (PDP)
PDP Alternatives (to be developed as part of this report)
Appendices (to include documentation of all study products covered in the attachments to this SOW and the SEO/RSM web site).

SPECIFICATIONS: The report is to be prepared in Microsoft Office Word as a "doc" file. All products generated in the process of report preparation will be provided to the Government upon completion of the task order work. Arial 12 font will be used for the text portion of the report.

MEETINGS: The A/E firm will meet individually with Oahu representatives having input into the various study products (such as employees of the Honolulu District, Hawaii Department of Land and Natural Resources (DLNR) and the University of Hawaii) to attain an in depth perspective on SEO/RSM related activities. The A/E will also make telephone contact with mainland contributors to the study. The A/E will arrange at least four progress meetings with SEO/RSM project delivery team (PDT members include Honolulu District, DLNR and UH personnel) to discuss progress on the report and issues to be resolved. The A/E will prepare draft minutes from each meeting and provide them to the PDT for review and comment. The A/E will prepare final meeting minutes based on comments received from the PDT.

DELIVERABLES: Deliverables will consist of meeting minutes as well as preliminary, draft and final RBMP reports. All products generated in the preparation of the final RBMP report will be provided to the Government prior to issuance of final payment.

SCHEDULE:

TASK	DATE
Preliminary FBMP Report	September 28, 2006
Draft FBMP Report	October 27, 2006
Final FBMP Report	November 30, 2006
Associated Products	November 30, 2006
Final Meeting Minutes	10 days after meetings

ATTACHMENT 1:

Regional Sediment Management
Southeast Oahu
Hawaii

Purpose: This study will (1) document long-term trends in wave climate for the windward side of Oahu, Hawaii, (2) develop a regional sediment budget and a geographic information system (GIS) for three interconnected littoral cells along the southeast Oahu coast, (3) identify suitable sand sources, and (4) develop/calibrate a sediment transport model for the region. The final products from this study will be a sand source inventory, regional sediment management (RSM) plan and web-enabled GIS platform for the South East Oahu (SEO) Region.

Problem: The SEO Region is located on the southeast shoreline of the island of Oahu, Hawaii. There are three littoral cells, Kailua in the north, Lanikai in the middle, and Waimanalo in the south part of the study area (Figure 1). There are geologic controls (both subaerial and offshore) affecting sediment transport within these cells. The offshore region is a sloping reef along which waves break on its outer edge. Waves are depth-limited by the reef as they approach the shoreline. The cells are not believed to share sediment with each other. The long-term average rate of shoreline retreat is nominally 2 feet/year. Long-term (decadal or more) shifts in wind, wave direction, and wave period may shift sediment transport patterns and magnitudes. As a result, sediment transport processes of these beaches are difficult to understand, and RSM solutions are not readily apparent. In addition, sand sources for this region have not been identified.

Proposal: A description of the tasks is presented below. Figure 2 shows a timeline of the various tasks.
Total duration: 4 years.

Task 1: Develop long-term wave climate.
Time: 12 mos.
From observations of shoreline position on the northeast side of Oahu, it appears that there is a long-term trend (20 or more years) of erosion and accretion. These cycles of beach change may be caused by shifts in wave climate, including multi-decadal shifts in storm activity associated with the Pacific Decadal Oscillation. Task 1 will utilize or generate updated Wave Information Study hindcast for the project area. Directional wave buoy data are available for the years 2000-2002, and non-direction wave buoy data are available for more than 20 years. These data will be used for validation of the hindcast. This task will provide a regional wave climate for Task 5, regional shoreline modeling.

Task 2: Nearshore circulation.
Time: 8 mos.
Because waves are depth-limited as they approach the study area, it is believed that nearshore circulation (wave- and wind-induced) may be a significant process controlling sediment transport. This task will setup and run the Advanced Circulation model for the study area. There are no current data available for validation; thus, three separate drogue studies are planned under a range of wave and wind conditions.

Task 3: Geomorphic analysis of study area.
Time: 10 mos.
Historical shoreline position, beach profile, aerial photography, bathymetric, and geologic information for the study area will be evaluated to identify (a) long-term trends in shoreline position; (b) long-term trends in bathymetric change; (c) locations with possible sources of beach nourishment material, and (d) geologic controls on littoral processes. Historical shoreline position data are available from the University of Hawaii. Sand samples will be taken for each littoral cell, and sediment cores will be collected and analyzed for possible offshore sources of material. Because of the low hardness value of the sediment, it is possible that abrasion or mechanical disintegration is a significant process in shoreline retreat. The abrasive characteristics of beach sediments will be quantified. This task will provide data for Task 4, development of the regional sediment budget, and the calibration and verification data set for Task 5, regional shoreline modeling.

Task 4A: Develop a regional sediment budget.
Time: 10 mos.
Volumetric change for historical and present-day time periods will be developed for the active littoral region. These data, together with knowledge of the long-term wave and wind climate (Task 1) and regional shoreline modeling (Task 5), will be used to develop sediment budgets for each littoral cell. Sediment sources and sinks will be defined and quantified. A regional budget will be developed, including an assessment of whether long-term sand sharing between littoral cells occurs. The regional sediment budget will be used to develop a RSM plan, and a with-project regional sediment budget will be forecasted.

Task 4B: Develop a web-enabled GIS platform.
Time: 10 mos.
A web-based GIS platform will be developed for the SEO Region. The GIS will contain georeferenced maps, attributes and metadata corresponding to SEO Region RSM requirements. Aerial photography, digital elevation models, geotechnical information, survey data, wave parameters and other pertinent georeferenced information will be automated via the GIS. The GIS will utilize state-of-the-art web enabling software to provide real-time access of products through the internet. The GIS will reside at the Mobile District.

Task 5: Regional shoreline change modeling.
Time: 12 mos.
The regional shoreline change model presently in developmental testing, Cascade, will be calibrated and verified for the study region. The wave climate produced in Task 1 will drive the model, and shoreline positions, geologic controls, and bathymetric contours defined in Task 3 will be used for calibration and verification. The regional modeling will work hand-in-hand with development of the regional sediment budget (Task 4A). A RSM plan will be developed using results from each task. This RSM plan will document long-term trends in beach change, and identify possible sources of sand, to management of sediment within the region. Travel funding for trips to/from the mainland for various team members is also included in the estimate.

Task 6B: Sand source investigations.
Time: 4 years
Sand sources will be identified in areas offshore and upland of the region. Research and development of sand manufacturing techniques will also be carried out under the task.

Schedule and Funding: As indicated in Figure 2, the RSM demonstration project for the SEO Region will take four years to complete.

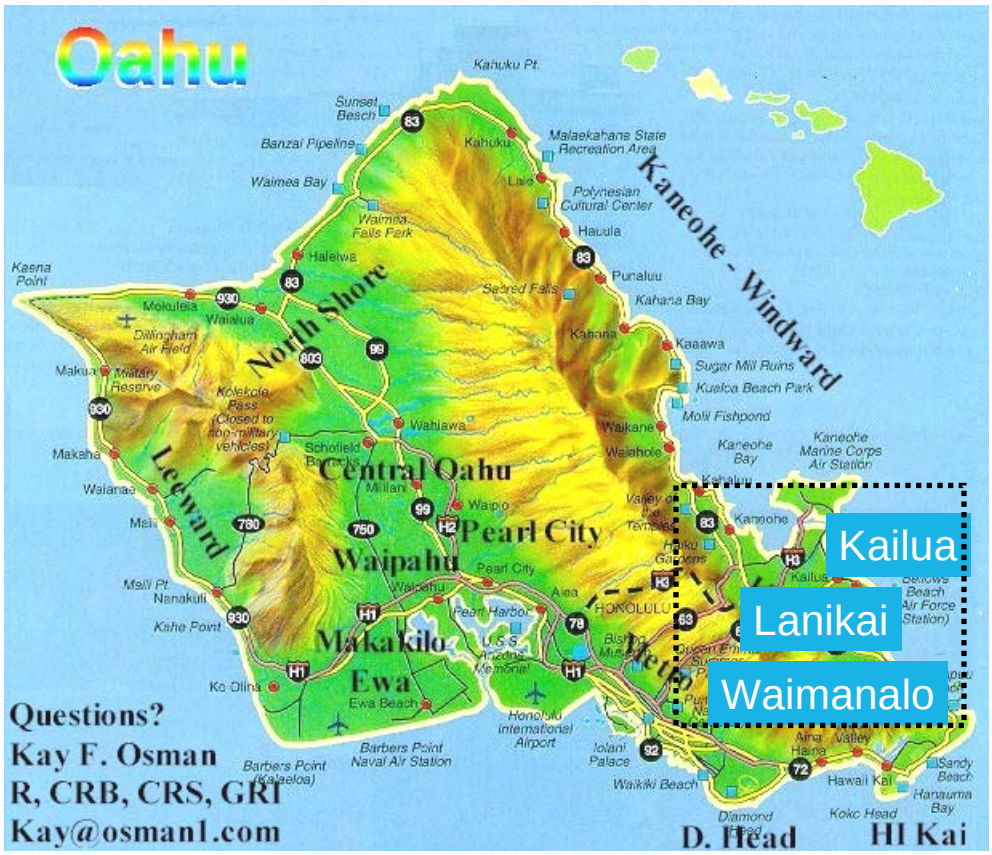

Figure 1. Project study area

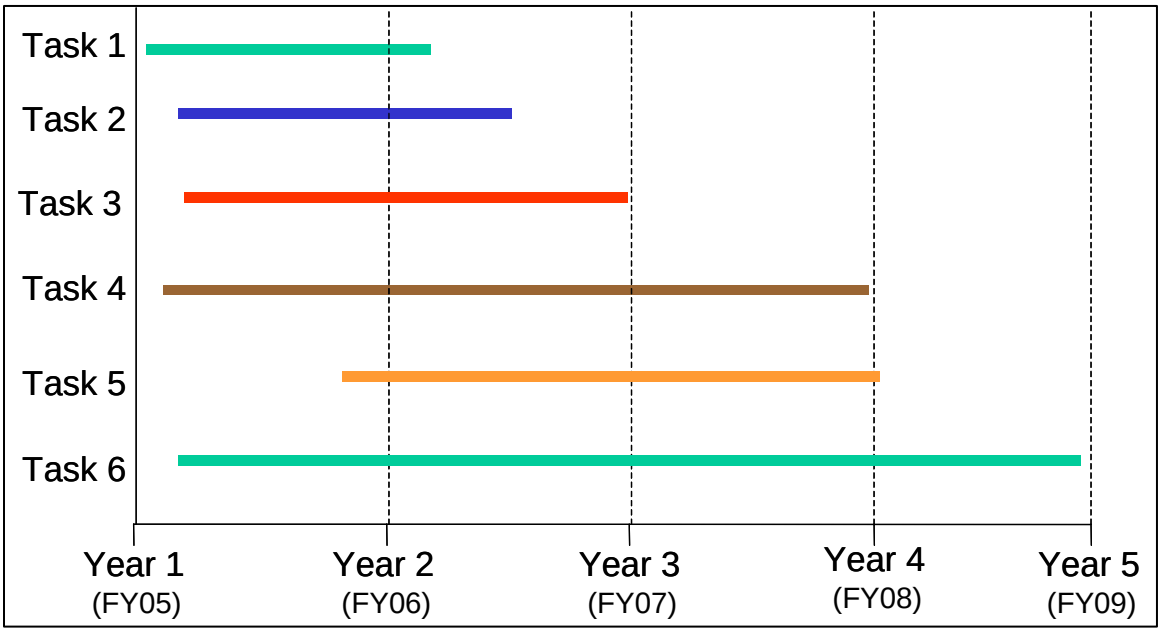

Figure 2. FY schedule and funding levels for the Southeast Oahu RSM demonstration project.

ATTACHEMENT 5

DRAFT Scope of Work
CHL Nearshore Circulation Modeling for Southeast Oahu, Hawaii

The proposed work includes six technical tasks: data collection/assessment, finite element and finite difference grid development, development of model forcing conditions, model calibration, model simulations, and simulation analysis. The tasks are linked and sequential, however, the first three tasks may be accomplished in parallel. The final product from these tasks is a calibrated hydrodynamic model for the project site. The models applied will be as follows:

a) Long-Wave Hydrodynamic Model – ADCIRC. The ADCIRC long-wave hydrodynamic model simulates the circulation and water levels associated with both tides and storms. A two-dimensional (depth-averaged) version of ADCIRC will be applied. ADCIRC has been extensively applied in the Atlantic and Pacific Oceans (and world wide) to simulate tidal circulation and associated storm surge and currents. The hydrodynamic modeling component will require the following tasks:

1. Grid development to include recent bathymetry and shoreline data.
2. Calibration and verification of the bathymetric grid to known tidal constituents. This phase of the investigation will provide circulation patterns for determining placement of water elevation and current measurement gages.
3. Re-verify model by comparison to measurements made for this study.
4. Development/selection of alternative forcing conditions.

b) Short-Wave Modeling – STWAVE. *STWAVE is a spectral wave transformation model, which is capable of representing wave-current interaction (wave-action equation, current-induced breaking, and wave blocking by a current). The ADCIRC and STWAVE models will be coupled to allow the interchange of radiation stresses from STWAVE to ADCIRC, and tide-, wind-, and wave-generated currents from ADCIRC to STWAVE. Application of STWAVE will require the following:*

1. Development of computational grid to simulate wave propagation.
2. Verification of calculated waves by comparison to measurements.
3. Generation of wave climate.

Study Phases

An approach toward development of a “turn-key” hydrodynamic modeling system should be pursued in a phased process. Activities including identifying and assembling data, grid development, tidal and wind-driven current and water level calibration, and nearshore wave transformation will be accomplished via a cooperative effort between POH and CHL personnel with in the field assistance provided by CHL.

Phase 1:

POH and CHL will jointly develop the geographic, bathymetric, hydrodynamic (waves and circulation), and meteorological data necessary to develop and calibrate the modeling system. An assessment of the quality of available data will aid in the specification of necessary additional field measurements. In addition, a decision will be reached as to what computer platform will be utilized to exercise the modeling system. CHL and POH will develop and calibrate the ADCIRC model for tidal constituent forcing, including in the field assistance if desired. Development of the finite element grid for the overall project will focus on a coarse resolution at the seaward, deep-water boundaries and detailed resolution in the nearshore regions of interest. Any recently collected bathymetric data will be evaluated and incorporated into the model grid and bathymetric databases will be used to supplement bathymetry for the grid domain.

Phase 2:
CHL will establish the range of atmospheric forcing required for accurate simulations. CHL and POH will develop and calibrate the STWAVE grid and perform an additional ADCIRC calibration including atmospheric forcing and coupling with STWAVE. This effort will include in the field assistance by CHL. These calibration simulations will utilize the POH current field measurement effort. Tidal forcing conditions will be developed for the ocean boundary condition using the LeProvost or OSU Pacific constituent database. Offshore wind and pressure fields generated by a combination of NCEP/NCAR winds and pressures adjusted for local observations will also be used as forcing conditions for the hydrodynamic model.

Phase 3:
CHL will assist POH in developing recommendations for alternative simulations, will document the methodologies and procedures, and will provide consultation in executing simulations and analyzing simulation results. The transfer of the completed modeling system to POH will be accomplished within the SMS framework.

ATTACHMENT 6:

Project: Southeast Oahu Regional Sediment Management Demonstration Project – Identification of Beach Quality Sand Sources and Investigation of Sand Manufacturing Techniques

Scope and Purpose: Carbonate sand is needed for the repair and restoration of beaches in Southeast Oahu, Hawaii. This project is directed to:

1) Locating sources of coral-based carbonate rock or gravel that can be ground to provide a clean carbonate sand.

2) Developing protocols for manufacturing carbonate sand by crushing and grinding coral-derived rock or gravel. Specifically this would involve the development of techniques for processing the carbonate to produce sand that will not re-cement when placed above the tidal zone on a beach.

3) Locating any alternate sand sources both onshore and offshore that could be used in beach construction. The goal of this project is to locate coral-reef derived carbonate material for the beach construction in sufficient quality to allow the development of a plan for the reconstruction effort and to determine the methods, equipment and material requirements needed for the production of a non-cementing carbonate beach sand. Additionally the project will complete a survey of the general availability of beach construction materials both on-shore and offshore. The time constraints and the level of funding for this phase of the work do not allow for dredging to obtain any new underwater carbonate samples.

Approach: A preliminary investigation of the carbonate supply problem will be undertaken to determine the availability of carbonate deposits using data developed in the investigations that have been undertaken by researchers from the U.S. Geological Survey, the University of Hawaii, and contractors. Archived sediment samples will be requested from past investigations. A preliminary assessment will be followed up with the collection of additional data and archived or stockpiled samples of the most promising deposits that occur within distances from the project area that make transport realistic economically.

Re-cementation of carbonate sand that is above sea level and subjected to leaching in fresh water is a significant problem. In Florida and Bermuda, natural carbonate beaches rarely have re-cementation problems that impact beach usage. The lack of dissolution of calcium carbonate and recrystallization of carbonate as cement is thought to be related to the presence of natural organic coatings on the carbonate sands. Extraction and analysis of organics from natural organic sands

shows that the surface of the grains has a coating of calcium salts of naturally occurring fatty acids (calcium stearate or calcium laurate). The coatings prevent the surface of the calcium carbonate from wetting effectively and disrupt any epitaxial growth of carbonate cements. In manufactured calcium carbonate sand, the freshly crushed material has clean surfaces that can act as templates form the formation of more crystalline calcium carbonate that can cement adjacent surfaces together. Additionally the presence of fine-grained material and sand-sized material with sharp edges and corners can contributed to the dissolution and reprecipitation that make beach rock out of beach sand.

The investigation of methods of manufacturing non-cementing beach sand will concentrate on the usefulness of using a well-sorted sand-sized particles that are tumbled to produce rounded grains and on the effects of adding coatings calcium salts of fatty acids. Phosphates in small quantities retard carbonate crystal formation and many fatty acids occur in nature with phosphate groups attached. As a coating material these compounds could be very effective crystal growth (cement) inhibitors. The systems proposed for investigation are all natural process that are being reintroduced into an manufactured sand to reproduce the non-cementing phenomenon occurring on normal carbonate beaches.

To support the development a sand manufacturing protocol, lab bench scale test will be set up to evaluate the importance of grain size and shape and the usefulness of coating materials. A test matrix will be developed with a variety of control samples to allow the evaluation of the separate properties of the sand treatments.

An overall assessment of aggregates (carbonate and non-carbonate and on-shore and off-shore) will also be included in this investigation. This survey of availability to assure that the most economical sources of material are located from the project and no useful resource that could make the project more effective or economical is overlooked. This phase of the investigation will allow the beach repair planners to optimize the use of resources and justify their selection of specific materials and specific sources. The program will include characterization of selected materials and estimates of amounts available and transport to the construction site.

APPENDIX C

SOUTHEAST OAHU
REGIONAL SEDIMENT MANAGEMENT
DEMONSTRATION PROJECT:
COASTAL PROCESS MODELING UTILIZING
NUMERICAL MODELS: ADCIRC AND STWAVE

Southeast Oahu

Regional Sediment Management Demonstration Project:

Coastal Processes Modeling Utilizing Numerical Models: ADCIRC and STWAVE

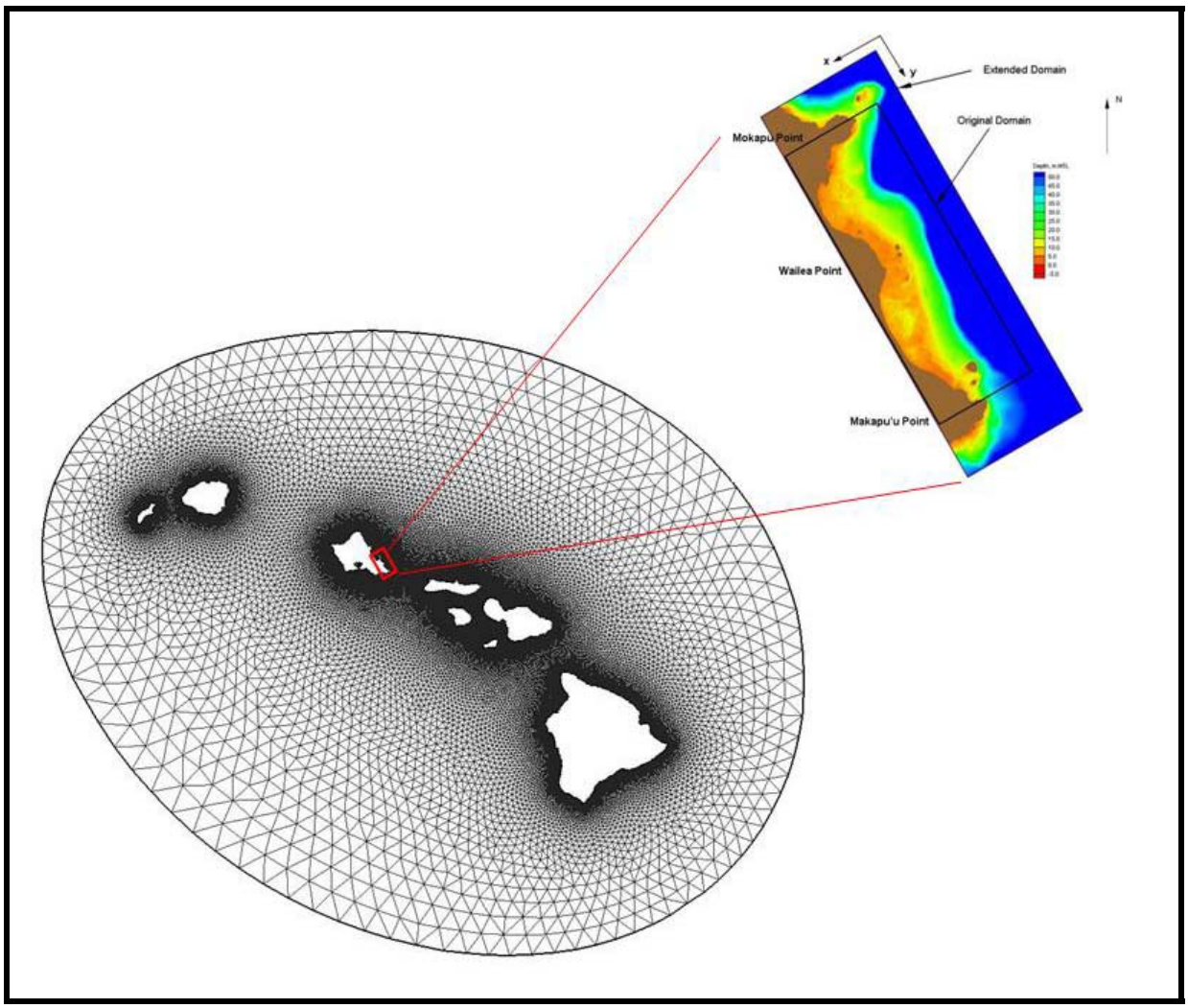

Nearshore Circulation Modeling for Southeast Oahu, Hawaii

The purpose of the nearshore circulation modeling study for the Southeast Oahu Regional Sediment Management (SEO/RSM) demonstration project was for the Engineer Research and Development Center (ERDC), Coastal and Hydraulics Laboratory (CHL) to provide the Honolulu District (POH) with a tool for understanding nearshore circulation and sediment transport in the study area (and at Wailea Point in particular). The ultimate goal for POH was then, to understand sediment transport potential in the region and determine the likelihood of accretional and erosional areas within the model domain. The nearshore circulation study project included six technical tasks: data collection/assessment, finite element and finite difference grid development, development of model forcing conditions, model validation, model simulations, and simulation analysis. The final product from these tasks was validated hydrodynamic and wave models for the SEO region. The scope of work for this effort is provided in Appendix A.

The ADvanced CIRCulation (ADCIRC) long-wave hydrodynamic model simulates the circulation and water levels associated with both tides and atmospheric conditions (Luettich et al. 1992). A two-dimensional, depth-averaged version of ADCIRC was applied in this study. ADCIRC has been extensively applied in the Atlantic and Pacific Oceans (and world wide) to simulate tidal circulation and associated storm surge and currents. The hydrodynamic modeling component for this study required: 1) grid development to include recent bathymetry and shoreline data, 2) validation of the bathymetric grid to known tidal constituents and wind forcing for April 2001, and 3) comparison of the bathymetric grid forced with known tidal constituents, wind, and waves to measurements for the field data collection time period. The application and validation of ADCIRC for the southeast Oahu study provides POH with the capability of simulating circulation in the study area for any required time period. NOTE: Conclusions provide later in the report should document why ADCIRC was not carried forward into the sediment transport analysis.

The STeady-state spectral WAVE model (STWAVE) is a spectral wave transformation model, which is capable of representing depth-induced wave refraction and shoaling, current-induced refraction and shoaling, depth- and steepness-induced wave breaking, diffraction, wind-wave growth, wave-wave interaction and whitecapping (Resio 1988, Smith et al 2001). The purpose of applying nearshore wave transformation models such as STWAVE is to describe quantitatively the change in wave parameters between the offshore and the nearshore because offshore time-series wave data is usually more commonly available; however, nearshore wave information is required for the design of almost all coastal engineering projects. STWAVE has previously been applied to numerous sites with a gently sloping seafloor or small areas of hardbottom. Due to the wide and relatively shallow reef fronting the shoreline of the SEO region, this application of STWAVE required the added feature of simulating wave transformation over a reef. Development of a bottom friction capability in STWAVE was completed to address this unique bathymetry specific to the island environment. Application of STWAVE for this project required development of a computational grid to simulate wave propagation, verification of calculated waves by comparison to measurements, and

generation of a wave climate. The ADCIRC and STWAVE models were then coupled to allow the interchange of radiation stresses from STWAVE to ADCIRC.

The approach toward development of a "turn-key" hydrodynamic modeling system for this region was pursued in a phased process. In the first phase, POH and CHL jointly developed the geographic, bathymetric, hydrodynamic (waves and circulation), and meteorological data necessary to develop and validate the modeling system. An assessment of the quality of available data aided in the specification of additional field measurements that were to be collected for this project. CHL developed and validated the ADCIRC model for tidal constituent forcing. Tidal forcing conditions were developed for the ocean boundary condition using the Oregon State University (OSU) Pacific constituent database. Development of the finite element grid for the overall project focused on a coarse resolution at the seaward, deep-water boundaries and detailed resolution in the nearshore region of interest. All recently collected bathymetric data, including SHOALS data collected in 2000, were evaluated and incorporated into the model grid, and bathymetric databases were used to supplement bathymetry for the grid domain.

In Phase 2, CHL established the range of atmospheric forcing required for accurate simulations. CHL developed the STWAVE grid, validated the STWAVE model, and performed an additional ADCIRC validation including atmospheric forcing and coupling with STWAVE. These validation simulations utilized the field measurement effort for comparison to model results. Tidal forcing conditions were developed for the ocean boundary condition with the LeProvost tidal constituent database (LeProvost et al 1994). (The LeProvost database was applied because it provided a stable solution for the linked model validation time period). Offshore wind and pressure fields generated by a combination of wind fields and pressures adjusted for local observations were used as forcing conditions for the hydrodynamic model, and are discussed in detail later in this report. Wave conditions from a Coastal Data Information Program (CDIP) buoy near the study site were used to generate forcing conditions for the wave model. STWAVE was validated by comparing model-predicted and field measurements of wave conditions at the field data collection locations. The bottom friction was adjusted in the model to represent the reef and non-reef areas until a close comparison was achieved. ADCIRC was validated by comparing model-predicted and field measurements of water level and velocity at the field data collection locations. A hybrid friction formulation and limited wave radiation stress gradients were applied to achieve the best comparison. In Phase 3, CHL assisted POH in developing recommendations for alternative simulations, documented the methodologies and procedures, and provided consultation in executing simulations and analyzing simulation results. The completed modeling system has been transferred to POH within the SMS framework and training has been provided to POH for future applications.

Field Data Collection

Wave and current data were collected for this project from 9 August to 14 September 2005 with two RD Instruments Workhorse ADCPs (Acoustic Doppler Current Profilers) and three Sontek Hydra ADVs (Acoustic Doppler Velocimeters). The field data

collection deployment period was dominated by tradewind weather (typically occurring from April through September in Hawaii) as characterized by consistent winds from the northeast and occasional swells from the southeast and southwest. Large wave events that would affect the windward coast are not typical during this season. Waves along the windward coast during these months are typically generated from local winds, and this is evident in the relatively small wave heights and northeasterly incident direction of the waves recorded during the deployment period. Instrument locations and additional information are shown in Figure 1 and Table 1. All recording gauges were referenced to UTC time.

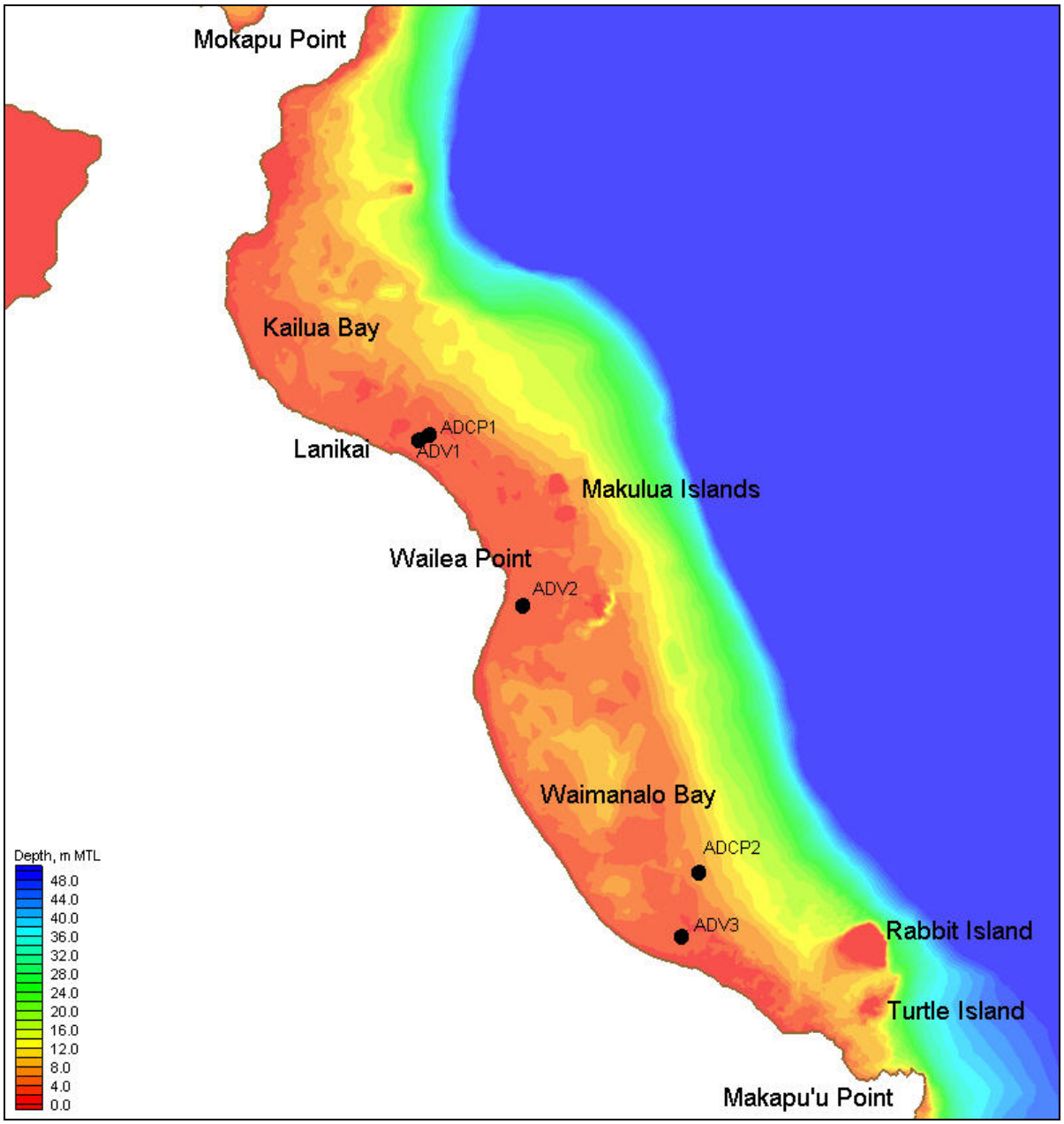

Figure 1. Instrument locations

Table 1. Instrument Identification and Location
Hawaii RSM Gage Locations, August - September 2005

Gage Type	Gage Name	Lat (deg min)	Lon (deg min)	Recording Time Period	Nominal Depth (m)
ADCP	ADCP1	21 23.905	157 42.994	9 August - 14 September	3.3
ADCP	ADCP2	21 20.318	157 40.786	10 August - 4 September	6.6
ADV	Y1	21 23.861	157.43.079	9 August - 14 September	2.5
ADV	G2	21 22.509	157 42.233	9 August - 14 September	2.7
ADV	R3	21 19.795	157 40.930	9 August - 14 September	2.5

ADCP Gauges:

For this study, two RD Instruments 1200 kHz Workhorse ADCP gauges were deployed for approximately one month. The ADCPs were bottom mounted, facing upward with the sensor head approximately 0.4 m off the bottom. The water depth at ADCP1 was approximately 3.3 m and the water depth at ADCP2 was approximately 6.6 m, which placed it near the seaward edge of the reef flat. These gauges have four acoustic transducers for measuring currents and a pressure sensor, from which horizontal and vertical current profiles were computed at 0.2 m vertical spacing. These instruments sampled at 2 Hz for directional wave measurements. Each hourly wave burst was approximately 34 minute long, starting at the top of each hour, and consisted of 4096 points. There is a 0.44 m blanking distance from the transducer head, and with a 0.2 m bin width this makes the first sample 0.72 m above the transducer, or about 1.12 m off the bottom. Current profiles were collected every 10 minutes from a 200 point average.

The ADCP deployments were on 9 August 2005 and retrieval was on 14 September 2005. ADCP2 was reprogrammed on 10 August so data collection started a day later than the other instruments, and the batteries were depleted on 4 Sep, about 10 days before retrieval of the all gauges. The ADCP2 data record was therefore, 11 days shorter than the other gauge records.

ADV Gauges:

In addition to the two ADCPs, three ADV gauges were deployed for the same one-month time period. ADV deployments were on 9 August 2005 and retrieval was on 14 September 2005. The three ADV gauges were Sontek's Hydra model that samples a single point current velocity (U, V, and W) and contained an external pressure sensor. The sample volume for the current measurement is approximately 1-2 cm in size and about 0.17 m above the center transducer. This instrument uses three beams to determine the three current components. Both the ADCP and ADV instruments and their mounts are shown in Figure 2. Figure 3 shows wave height, period, and direction for the three ADV gauges. Figure 4 depicts wave roses for the two ADCP gauges.

ADCP in frame (left) and close up of transducer head with biofouling (right).

Hydra ADV in frame (left) and closer view of the biofouled sensor head (right).

Figure 2. Images of gauges and mounts.

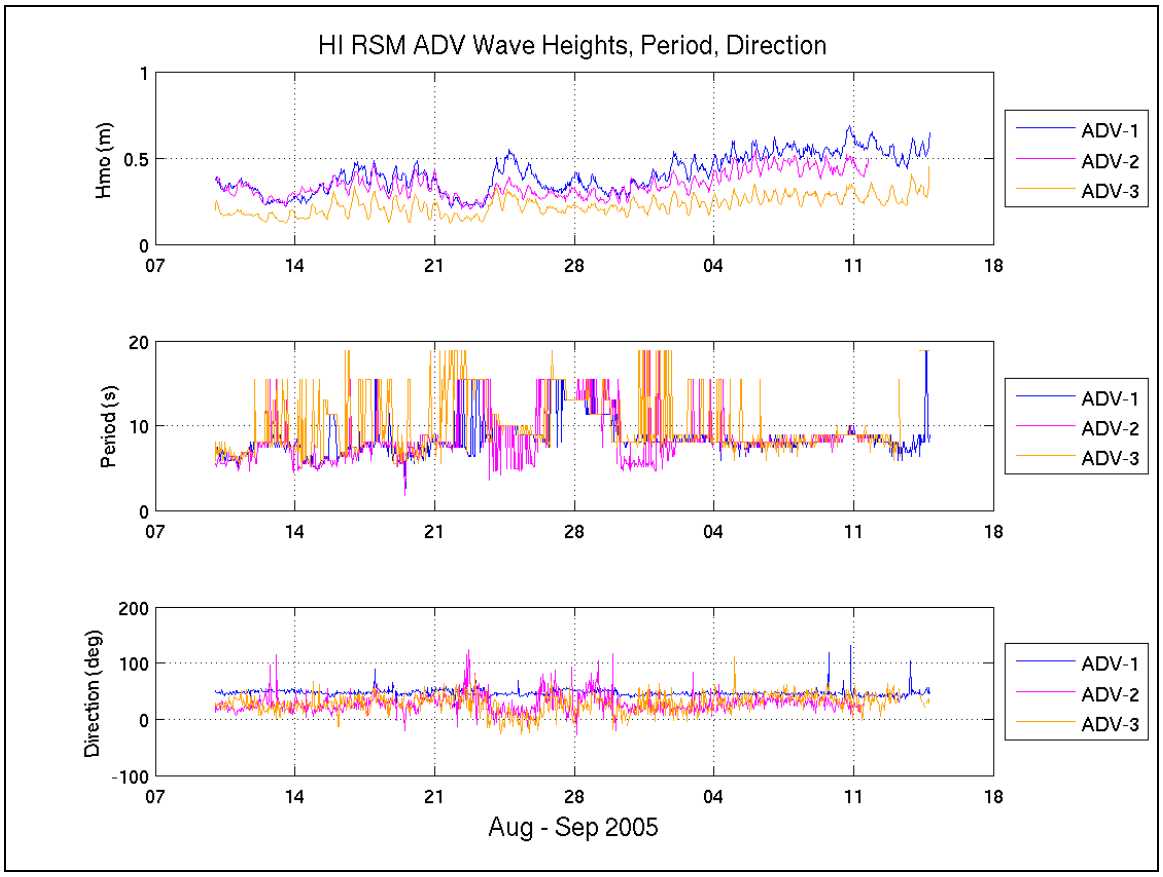

Figure 3. Wave height, period and direction from the three ADV gauges.

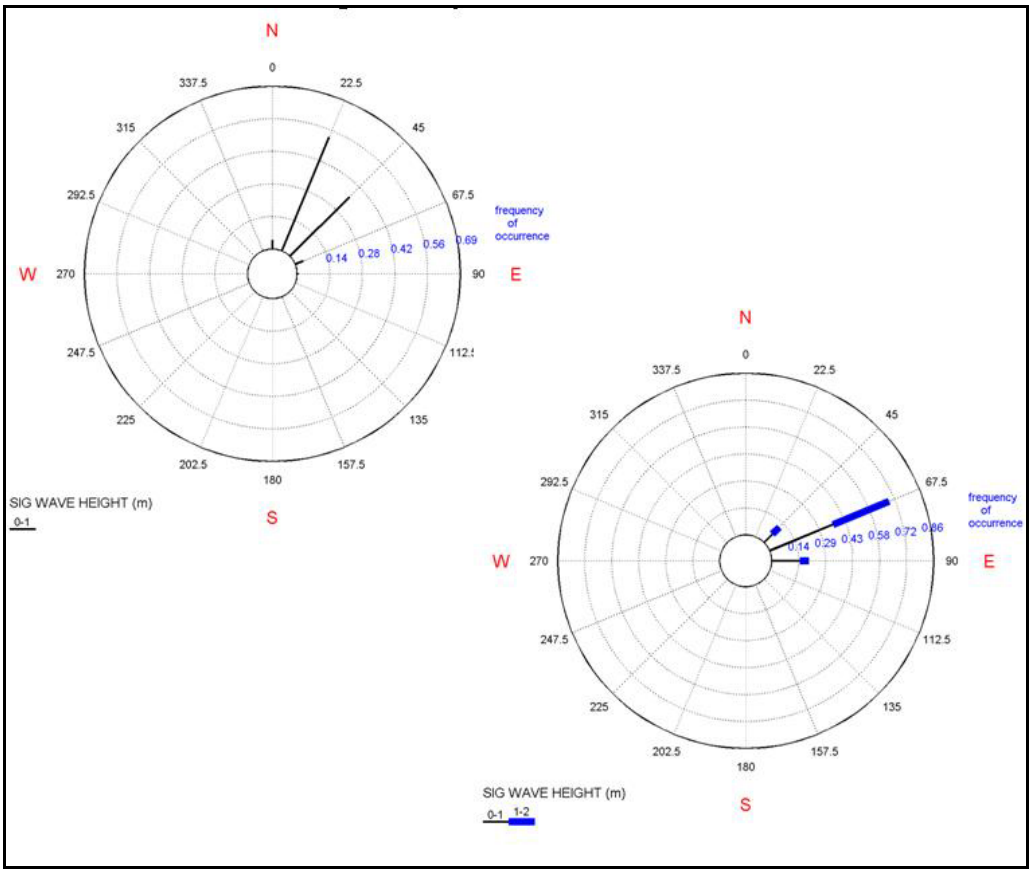

Figure 4. Wave roses for ADCP #1 (left) and #2 (right).

Current Drogues:

Four current drogues (drifters) were designed and built at the CHL Field Research Facility (FRF) for deployment at the beginning (10 August 2005) and end (13 September 2005) of the ADCP/ADV deployment period. The drogues were constructed with PVC pipe, vertical risers, rubber unions, hose clamps, and sails and used GPS receivers for tracking and radio telemetry for positioning. Difficulty with the radio tracking was experienced because it required line of sight to receive drifters. Since the drifters were in two different locations (Kailua Bay and Waimanalo Bay), partial tracking was all that could be accomplished. Also the antennas and connectors should have been constructed more robustly because two were broken during deployment.

Current drogue tracks for 10 August 2005 and 13 September 2005 are shown in Figure 5. There were two deployments on 10 Aug, hence the numbers 1 through 8. Some drogues were deployed in the vicinity of the ADV and ADCP gauges for inter-comparison. A track direction reversal of Drogue #2 was observed shortly after deployment on 13 September (Figure 6), starting off on a nearly due west track and then turning back to a south east trajectory. The nearshore drogues tended to track in a westerly (shoreward) direction at a rate of approximately 0.1-0.2 m/sec, which is comparable to model results. Drogues in Waimanalo Bay moved in a southerly direction during the two deployment periods.

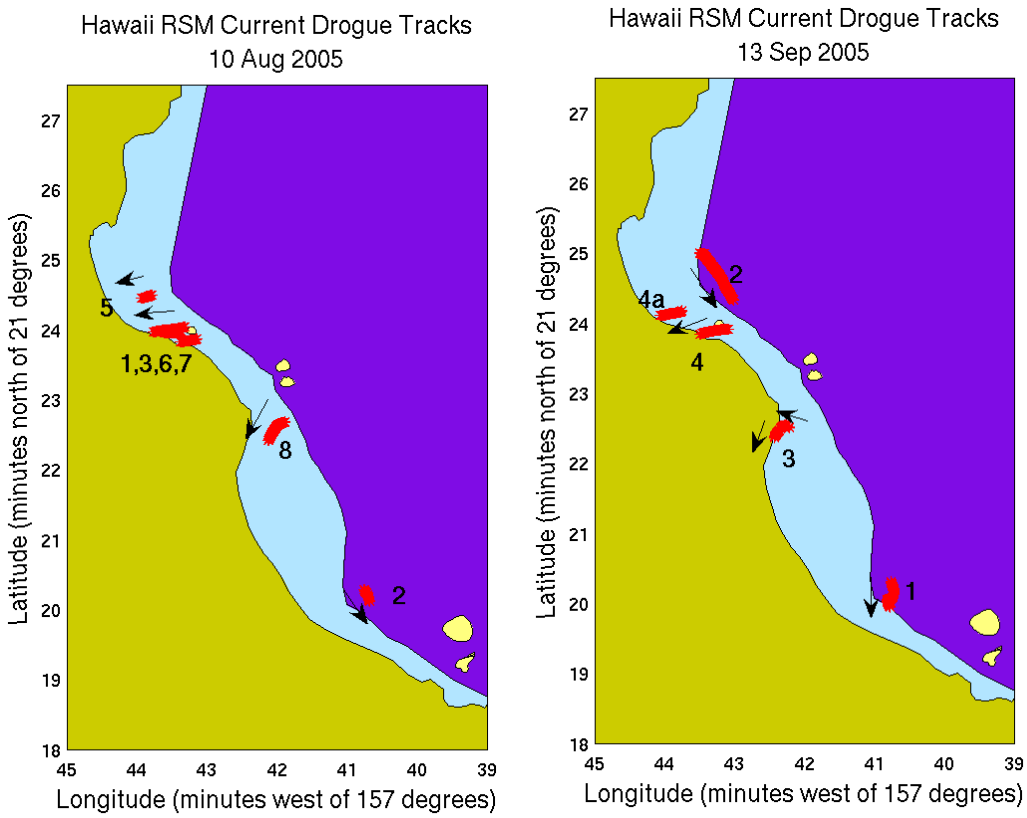

Figure 5. Drogue tracks with track number for 10 August (left) and 13 September (right).

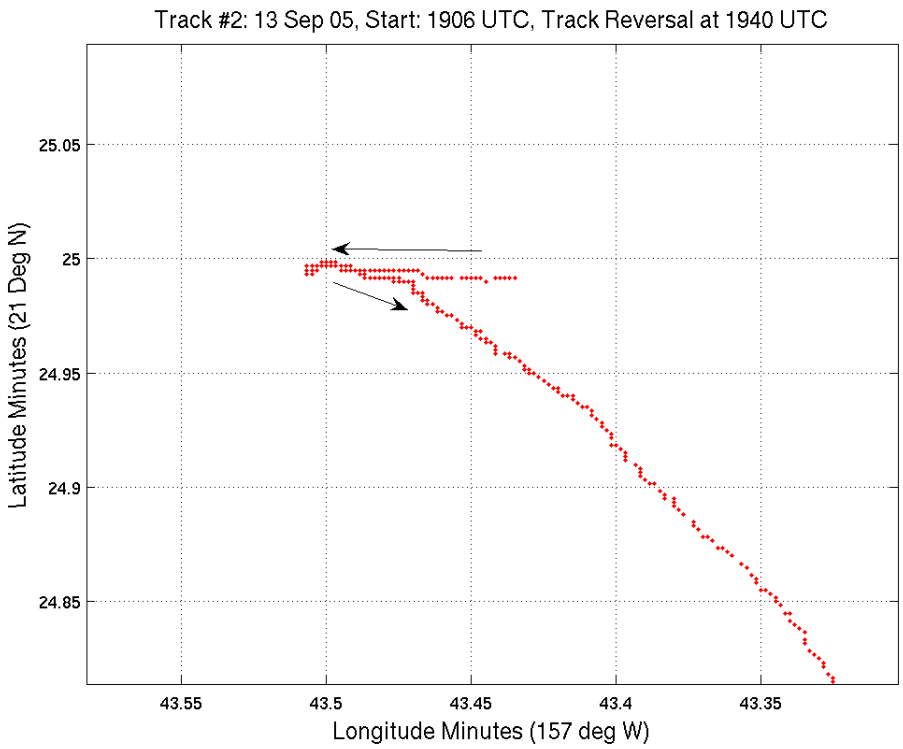

Figure 6. Drogue track reversal on 13 September.

ADCIRC

Grid Development

The ADCIRC numerical model, a regional two-dimensional (2-D) depth-integrated finite-element hydrodynamic circulation model, was applied in this study to provide water level and depth-averaged current (circulation) information for SEO. The model solves the shallow-water equations in full nonlinear form and can be forced with tide, wind, waves, and flux boundary conditions. Two ADCIRC model grids were developed in the course of this modeling initiative. The first grid was a large circular grid centered on the SEO region and extended from the central point approximately 21 degrees (2300 km) in all directions. Initial attempts at validation were unsuccessful because of the existence of two tidal amphidromes which were located in close proximity to the forcing boundary, shown in Figure 7. (An amphidrome is a location in the ocean where there is zero tidal amplitude due to canceling of tidal waves.) In order to eliminate the problem introduced by the tidal amphidromes, the spatial extent of the ADCIRC model domain was reduced.

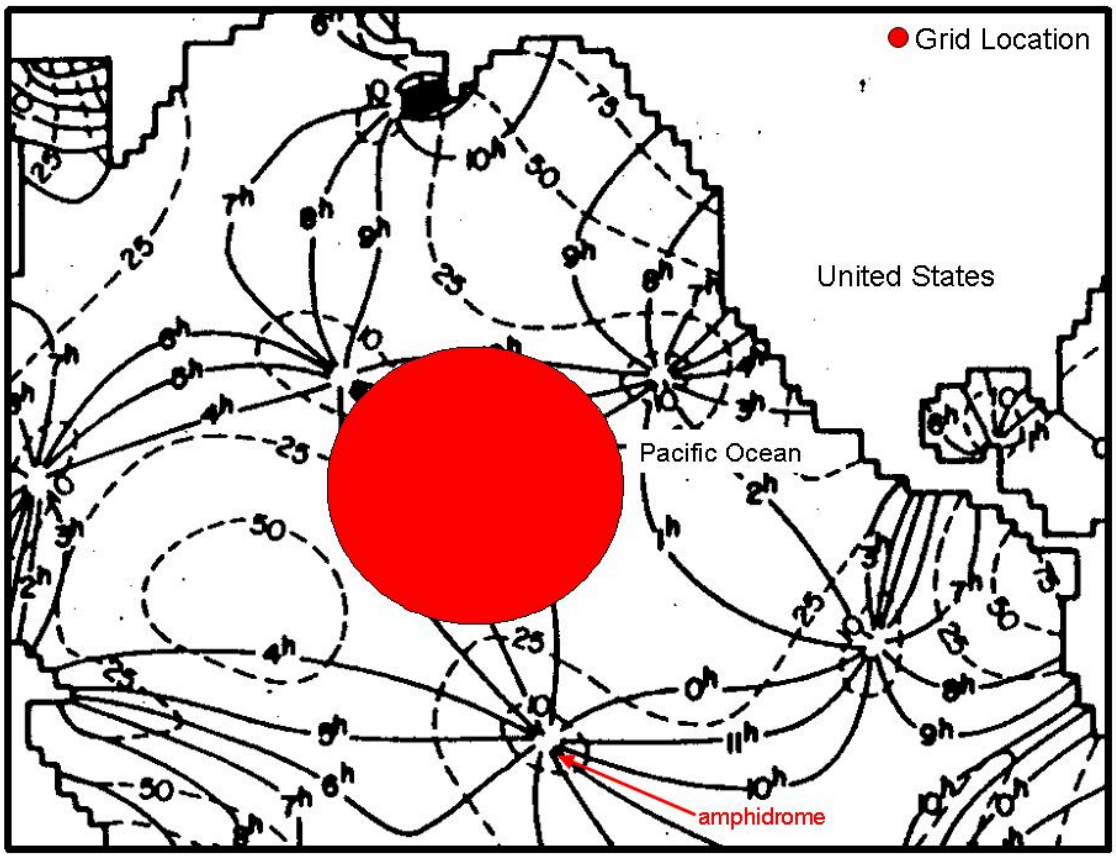

Figure 7. Approximate location of grid and amphidrome locations

The final ADCIRC mesh, shown in Figure 8, was a subdomain of the initial grid and is oblong in shape due to the orientation of the Hawaiian island locations. The mesh contains 73,305 computational nodes and 140,849 elements. Individual element area ranges from a maximum of 462,500 km^2 in deep water to a minimum of 60 m^2 surrounding many of the island features. High resolution was added to the existing ADCIRC mesh in the study area around bathymetric features, such as islands, entrances, and reefs. Depths on the mesh were referenced to mean tide level (mtl). This smaller grid had many improvements over the initial grid:

1. The ADCIRC grid mesh is forced along the open-water boundary that surrounds the Hawaiian Islands. Since the extent of the grid domain for the final grid is smaller than the grid extent for the initial grid, the forcing boundary for the final grid is far away from the influence of the tidal amphidromes shown in Figure 7.

2. The area of Honolulu Harbor is better resolved in the final grid, which improves the comparison between calculated and gauge data in this area.

3. Resolution around prominent features in the project reach was added, as well as topographic information for Rabbit and Turtle Islands located in the southern portion of the SEO region.

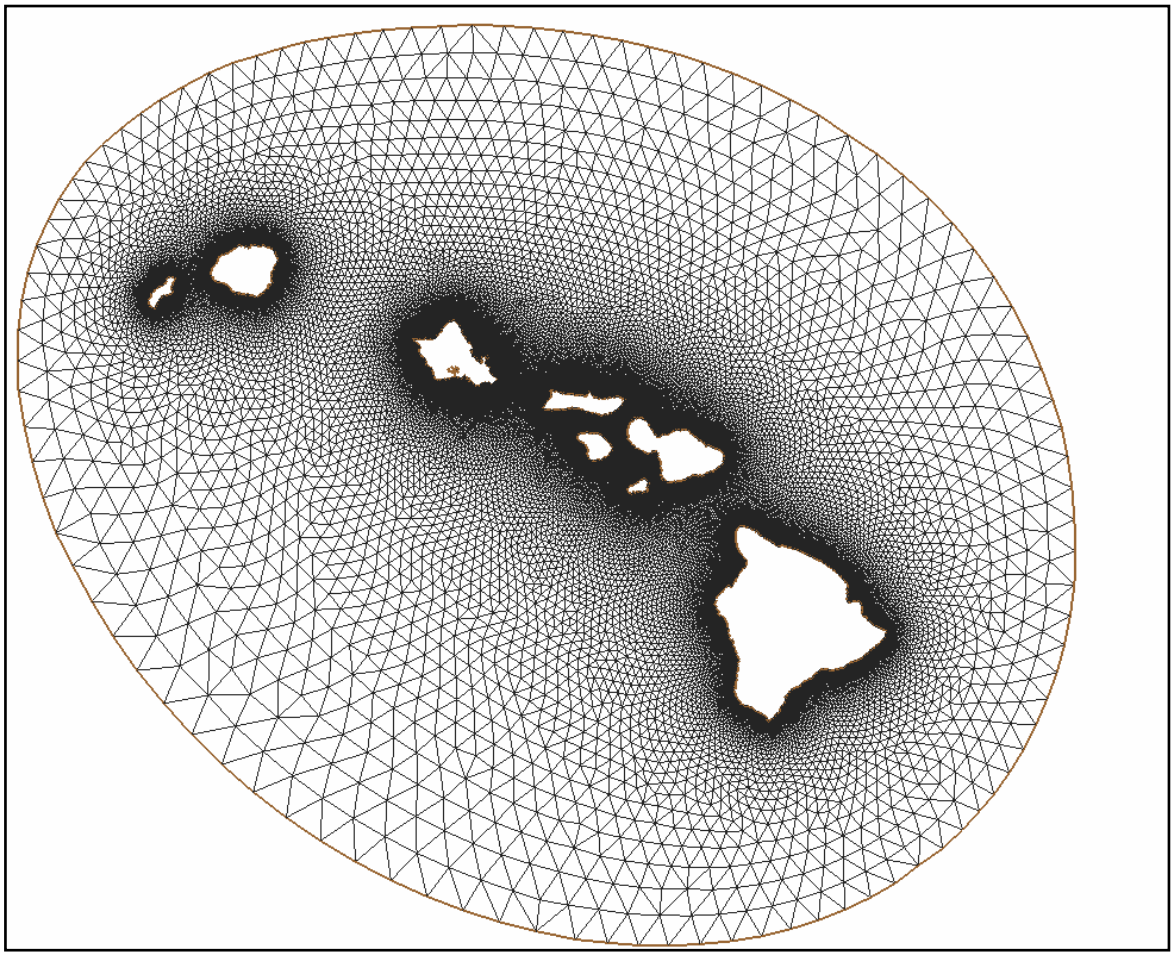

Figure 8. Final ADCIRC mesh domain

Wind Sources

Three wind sources were investigated as potential application as a forcing condition for the ADCIRC model: NOAA National Data Buoy Center (NDBC) Buoy 51001, National Centers for Environmental Prediction (NCEP) hindcast, and Oceanweather, Inc. (OWI) hindcast wind data. A comparison of the observed wind speed and direction at the NDBC Buoy 51001 and the nearest NCEP prediction point was performed for the period January to June 2001 (Figure 9). Wind directions compared well, however, the NCEP wind speed consistently exceeded the buoy observations by 5 to 10 percent. These differences can be attributed to the buoy anemometer height being 5 m, whereas the NCEP surface level winds are predicted at an elevation of approximately 10 m. The comparisons suggest that that long-term, historic NCEP winds can be applied in this project with a high degree of confidence for the initial validation time period.

A comparison of the NDBC Buoy 51001 winds to the OWI basin level Pacific hindcast (WIS) winds was also done for the month of April, 2001. A plot of this comparison is shown in Figure 10. Wind speed and directions compared well. These data suggest that WIS winds can also be applied to the project with a high degree of confidence. WIS winds were applied for the second validation (gauge deployment) time period.

ADCIRC Model Validation – Wind and Tide for Initial Validation Time Period

In the initial validation, the time period 10-24 April 2001 was selected for comparing model results to measured data. ADCIRC was forced along the open boundary with tidal information extracted from the Oregon State University (OSU) TPXO tidal database (Egbert, Bennett and Foreman, 1994). Wind speed and direction information were obtained from the NDBC Buoy 51001. The ADCIRC hydrodynamic time-step was 0.4 sec and results were reported hourly. Simulations were performed on the ERDC High-Performance Computer (HPC) system due to the size of the ADCIRC domain.

For this initial model validation, ADCIRC results for water level were compared with the two NOAA tide gauges available on the southern and eastern portion of the island of Oahu. Figure 11 shows the locations of the two gauges (red circles) and their proximity to the project area (black box). The calculated water levels from the ADCIRC simulation of the April 2001 time period compared relatively well in range and phase with the NOAA gauge measurements, considering that the locations of the gauges were well outside the area of high resolution in the project area. Water level comparisons of the ADCIRC validations to the two NOAA gauges, Honolulu Harbor and Kaneohe Bay, are shown in Figure12 and Figure **13**, respectively. Since these gauges were outside the project area and located in less resolved locations, it was determined that another validation would be made with the water level and current data received from ADV and ADCP gauges for the deployment time period from August 10 to August 31, 2005. Results of that validation are provided later in this document

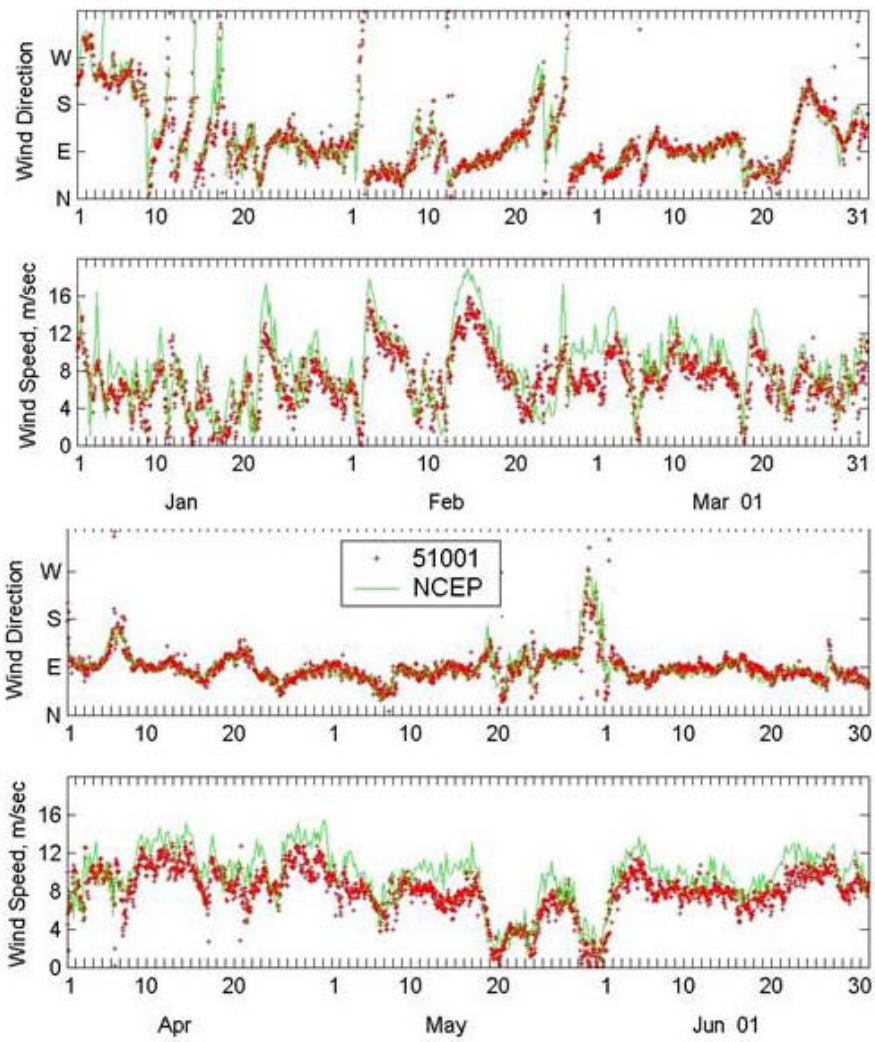

Figure 9. Comparison of observed (Buoy 51001) and predicted (NCEP) wind speed and direction

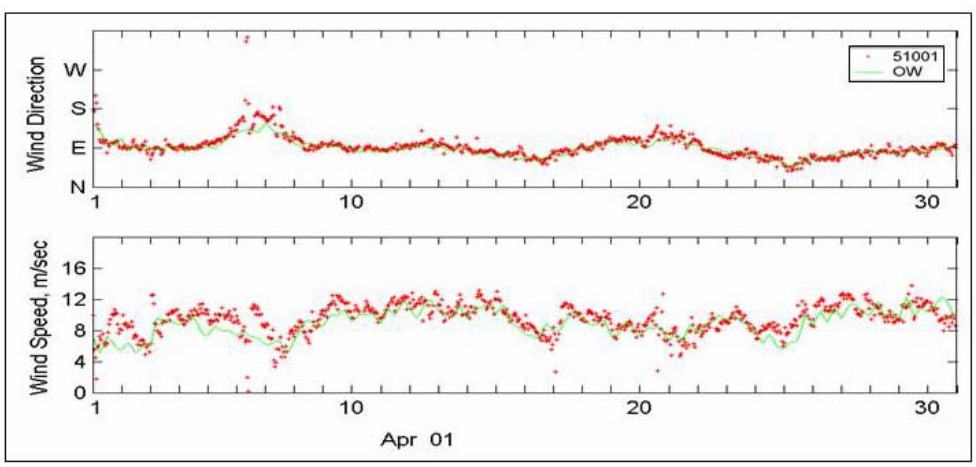

Figure 10. Comparison of observed (Buoy 51001) and predicted (OWI) wind speed and direction for April 2001

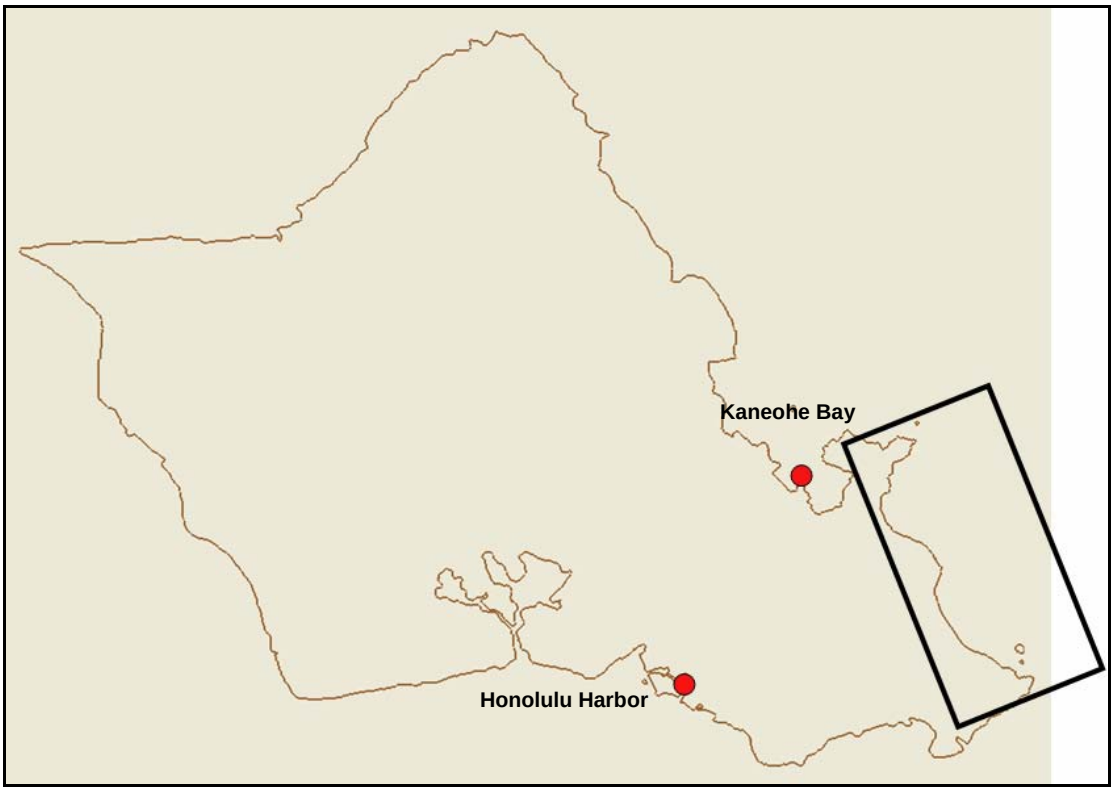

Figure 11. NOAA Gauge locations for initial validation time period. (Label project area)

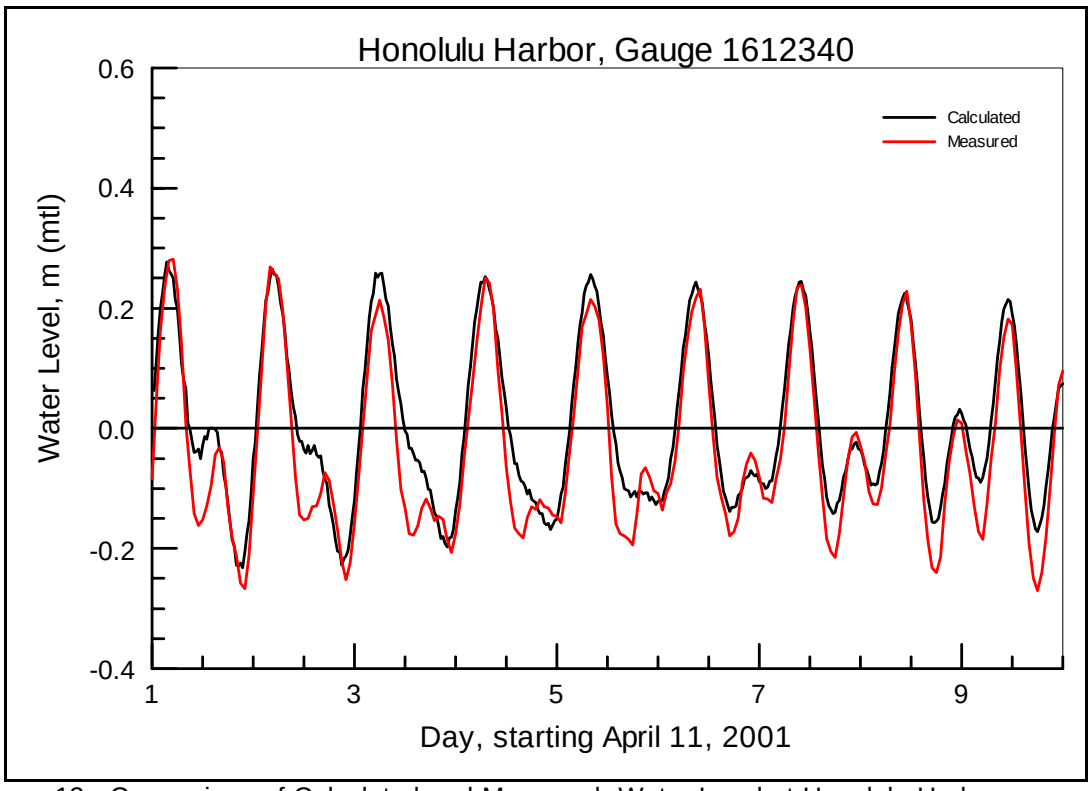

Figure 12. Comparison of Calculated and Measured Water Level at Honolulu Harbor gauge for initial validation period.

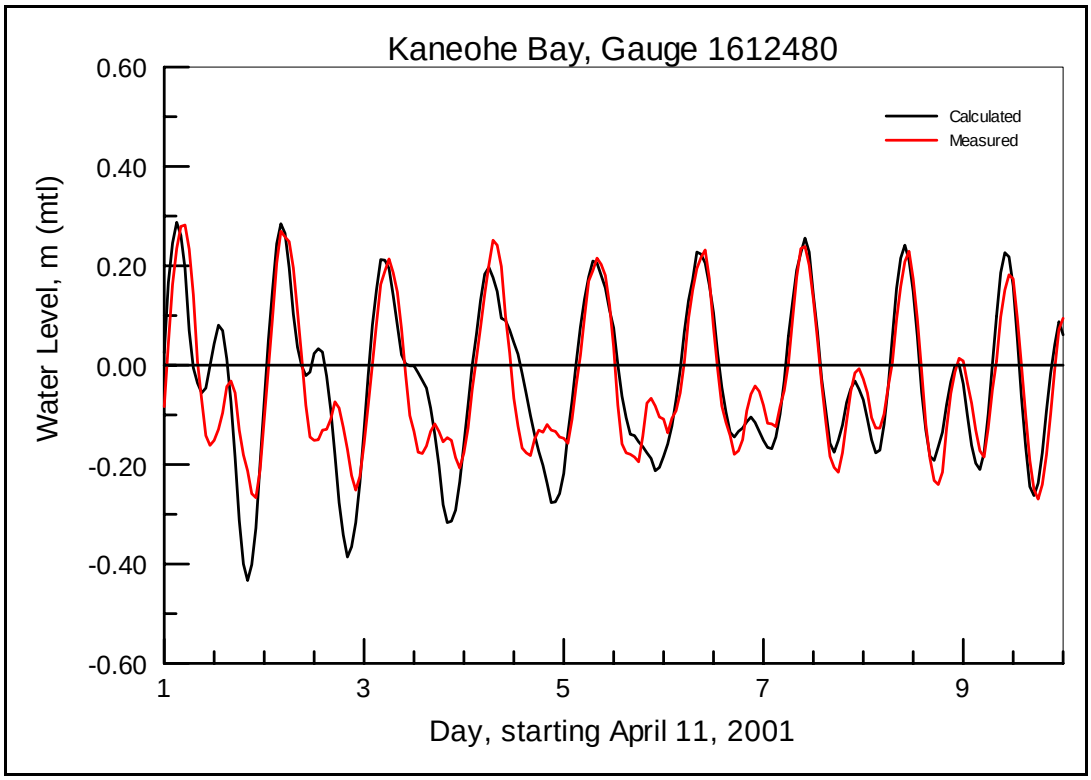

Figure 13. Comparison of Calculated and Measured Water Level at Kaneohe Bay gauge for initial validation period.

STWAVE

STWAVE is a steady-state, finite-difference model based on the wave action balance equation. STWAVE simulates depth-induced wave refraction and shoaling, current-induced refraction and shoaling, depth- and steepness-induced wave breaking, diffraction, wind-wave growth, wave-wave interaction and white-capping. The purpose of applying nearshore wave transformation models is to quantitatively describe the change in wave parameters between the offshore and the nearshore, and in this application included simulating wave transformation over a reef. As previously mentioned, development of a spatially-varying bottom friction capability in STWAVE was completed to enable application to the extensive reefs in the Southeast Oahu study area.

Grid Development

An STWAVE finite-difference grid was developed for the study area, with bathymetry interpolated from the ADCIRC grid mesh. The STWAVE grid resolution was 25 m x 25 m with a grid orientation of 210 degrees counter-clockwise from east. The original grid was 18 km (720 cells) in the alongshore direction by 6.2 km (248 cells) in the cross-shore direction and extended in the offshore to approximately the 100-m contour, with a maximum 344 m depth (Figure 14). After initial testing and consultation with POH, it was determined that the lateral extent of the grid should be expanded around the headlands and the offshore extent should be increased to get beyond the shallow water offshore from Mokapu Point and Makapu'u Point. The extended grid was 24.2 km

(968 cells) in the alongshore direction by 7.8 km (310 cells) in the crossshore direction and extended in the offshore to approximately the 300-m contour, with a maximum 480 m depth (Figure 14). The initial grid was applied for wave climate development and nearshore database generation. The extended grid was applied for comparison to field data and linkage to the ADCIRC model.

Wave Climate -- Model Forcing Conditions

Directional wave data were available at CDIP Station 098 (Mokapu Point) from August 2000 through 2004 (the study started in March 2005). Non-directional wave data were available at Station 034 (Makapu'u) from 1981 to 1996. Directional wave data were available for Station 099 (Kailua Bay) for two months (November-December 2000). Station locations are shown in Figure 15.

For this study, the long-term data record (2000-2004) for Station 098 was analyzed with the Coastal Engineering and Data Analysis Software (CEDAS) 3.0 – Nearshore Evolution Modeling System (NEMOS) software. Since the purpose of this procedure was to determine all conditions that occurred at Station 098, the longest record possible, including the incomplete years 2000 and 2004, were included in the analysis. (Note that there was a 3-month gap in the data in 2004 and that the small portion of 2005 data available at the time of study started (1 March 2005) were not included in the analysis.

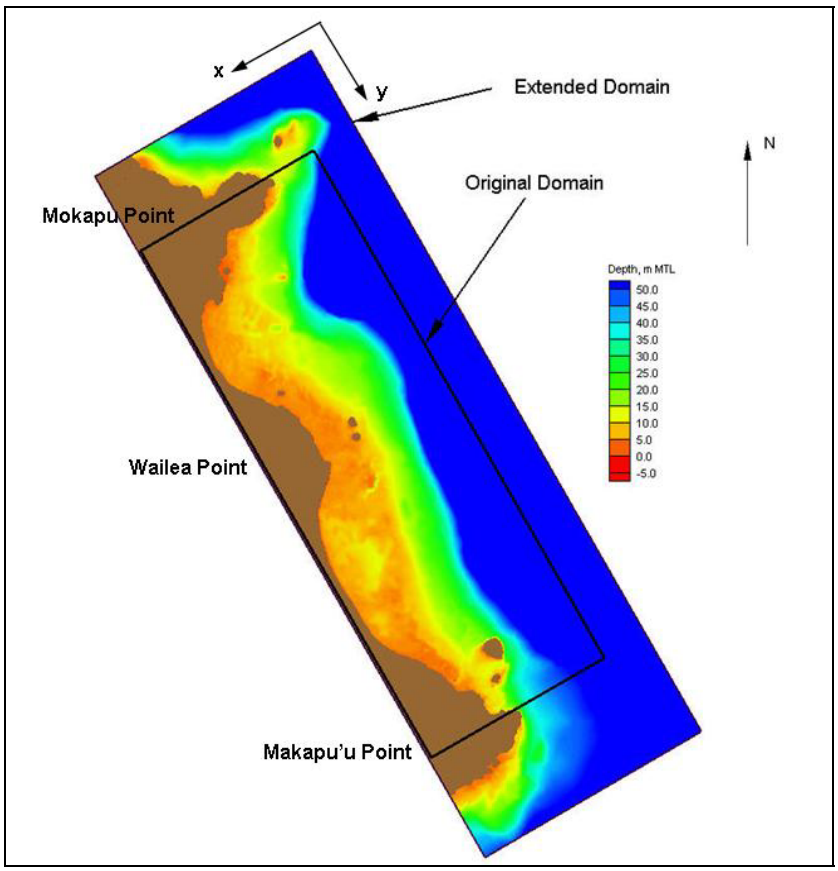

Figure 14. STWAVE grid domain

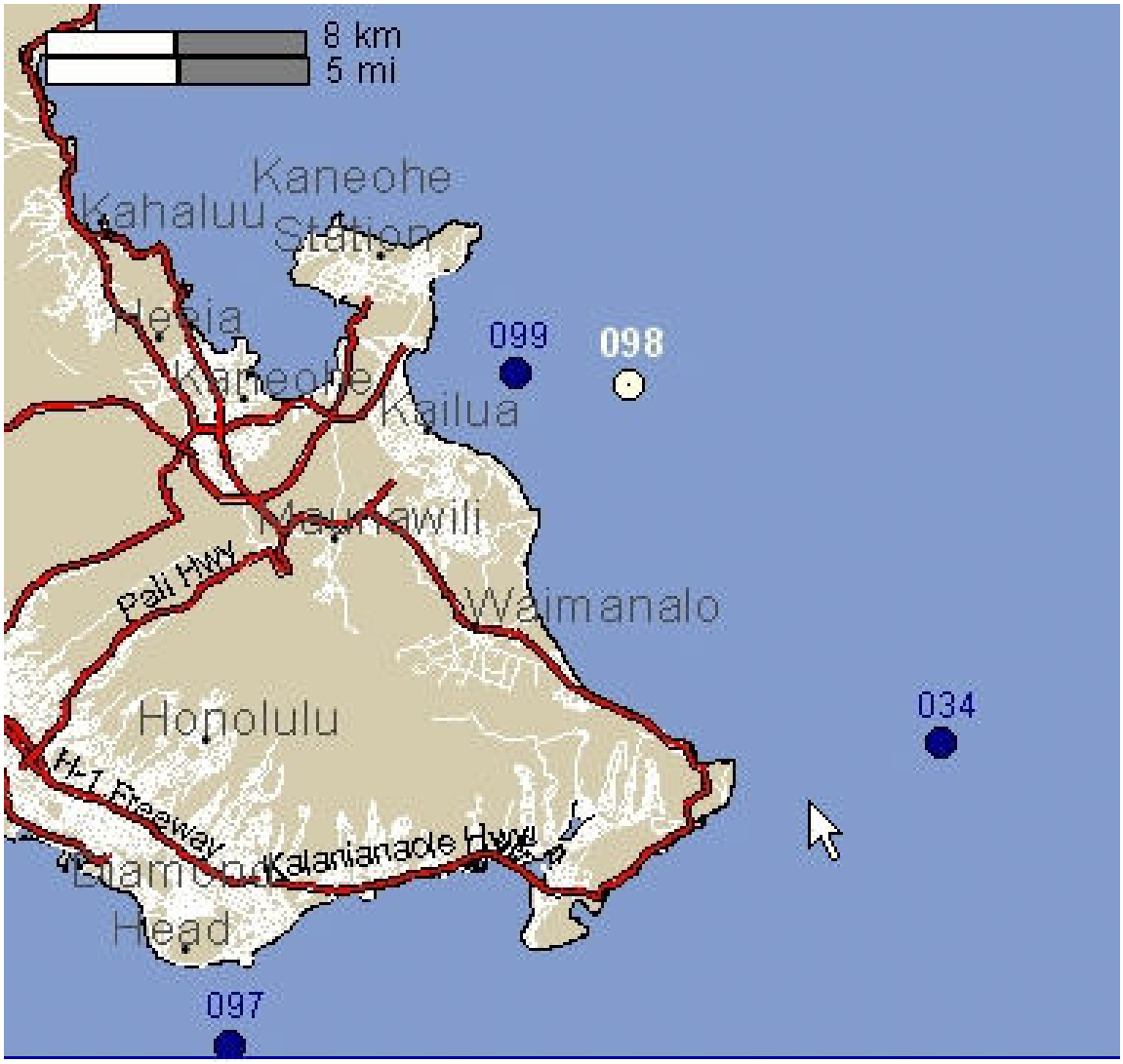

Figure 15. CDIP Buoy locations courtesy of CDIP web site (http://cdip.ucsd.edu)

Figures 16 and 17 show that waves are generally from the east-northeast quadrant and range in height from 0.5 to 6.0 m. Wave periods are generally 6-16 sec. From these tabulations, a set of discrete conditions was selected for simulation (Table 2). From the 216 possible height-period-direction combinations, 134 conditions occurred in the 2000-2004 time period. The wave height range was defined at 0.5-m intervals from 0.75 m to 2.75 m and at a 0.75-m interval to 3.5 m. The wave period range was 6 to 16 sec at a 2-sec interval. The wave directions were incremented every 22.5 deg from -22.5 deg to 90 deg, relative to True North. For each of the 134 selected wave conditions, TMA shallow-water spectra were generated by applying the SMS spectral wave generation software, and then wave transformation was simulated by applying STWAVE over the project domain.

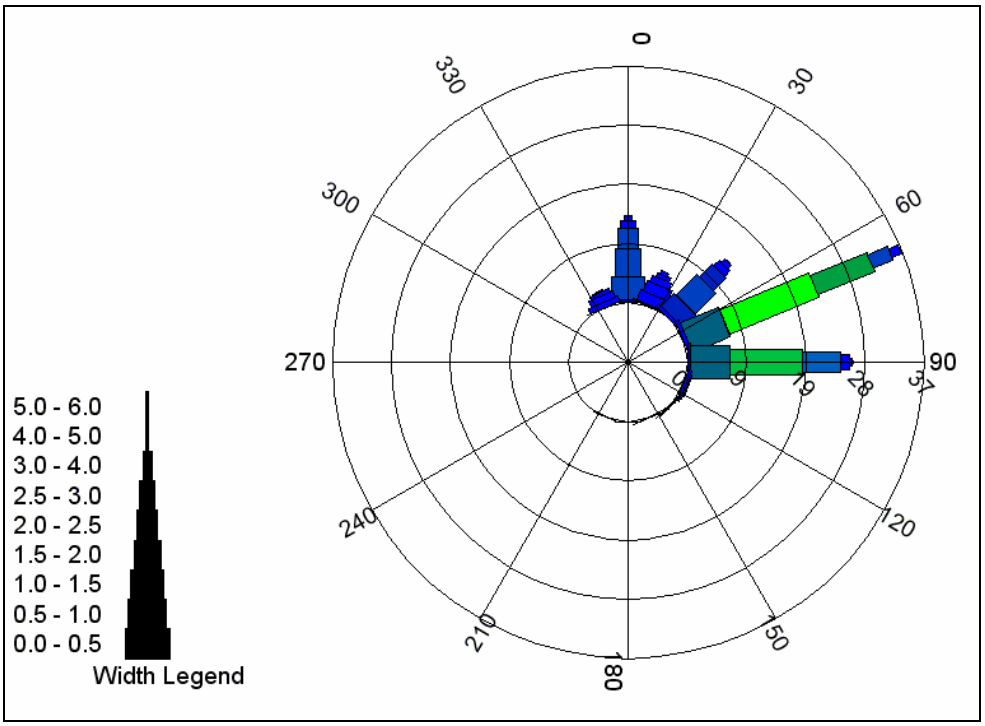

Figure 16. Wave height versus wave direction percent occurrence rose for CDIP Buoy 098 – Mokapu Point, HI (Data from August 2000 through December 2004)

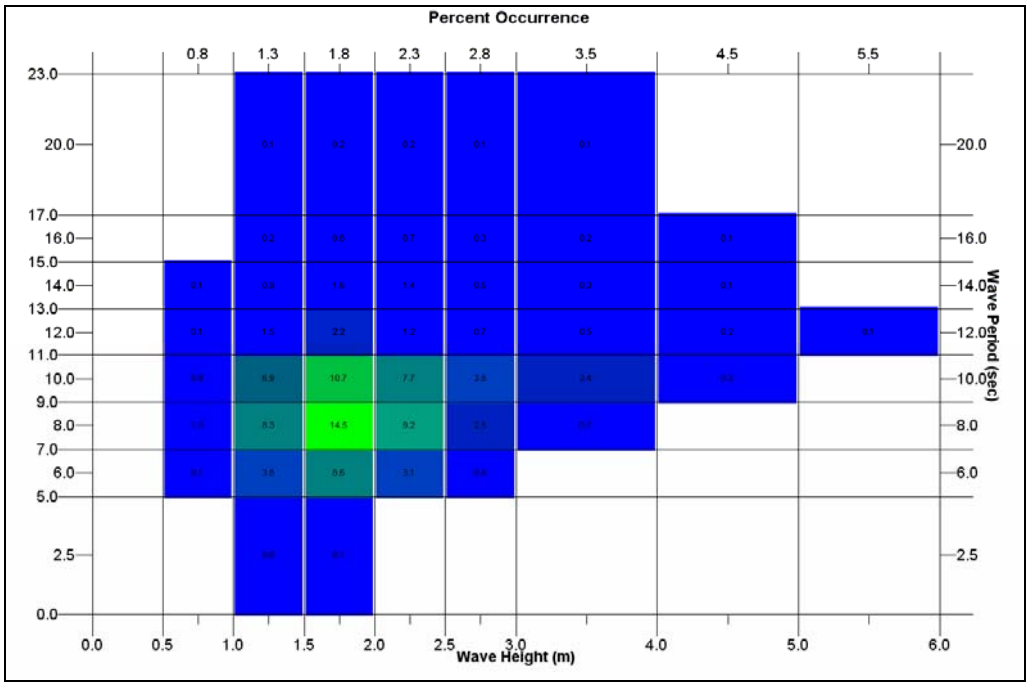

Figure 17. Block diagram of wave height versus wave period for CDIP Buoy 098 – Mokapu Point, HI (Data from August 2000 through December 2004)

Table 2. Wave Conditions			
Significant Wave Height, m	**Wave Period, sec**	**Wave Direction, deg from North**	**Wave Direction, deg from STWAVE axis**
.75	6	-22.5	82.5
1.25	8	0	60
1.75	10	22.5	37.5
2.25	12	45	15
2.75	14	67.5	-7.5
3.5	16	90	-30

Wave Climate Analysis

For demonstration purposes, nearshore conditions at a point in Waimanalo Bay (Figure 18, cell (229,506)) were extracted from the STWAVE model results for each of the 134 simulations. A transformation correlation between the offshore and nearshore condition was then determined for each of the 134 simulations. By applying the appropriate transfer function to each wave condition in the 2000-2004 offshore time series at Station 098, a long-term (2000-2004) nearshore time series was generated (Figure 19). Note that the 3-month gap in the time-series corresponds to 15 February to 19 May 2004 when the offshore CDIP Buoy 098 gauge was not operational. The

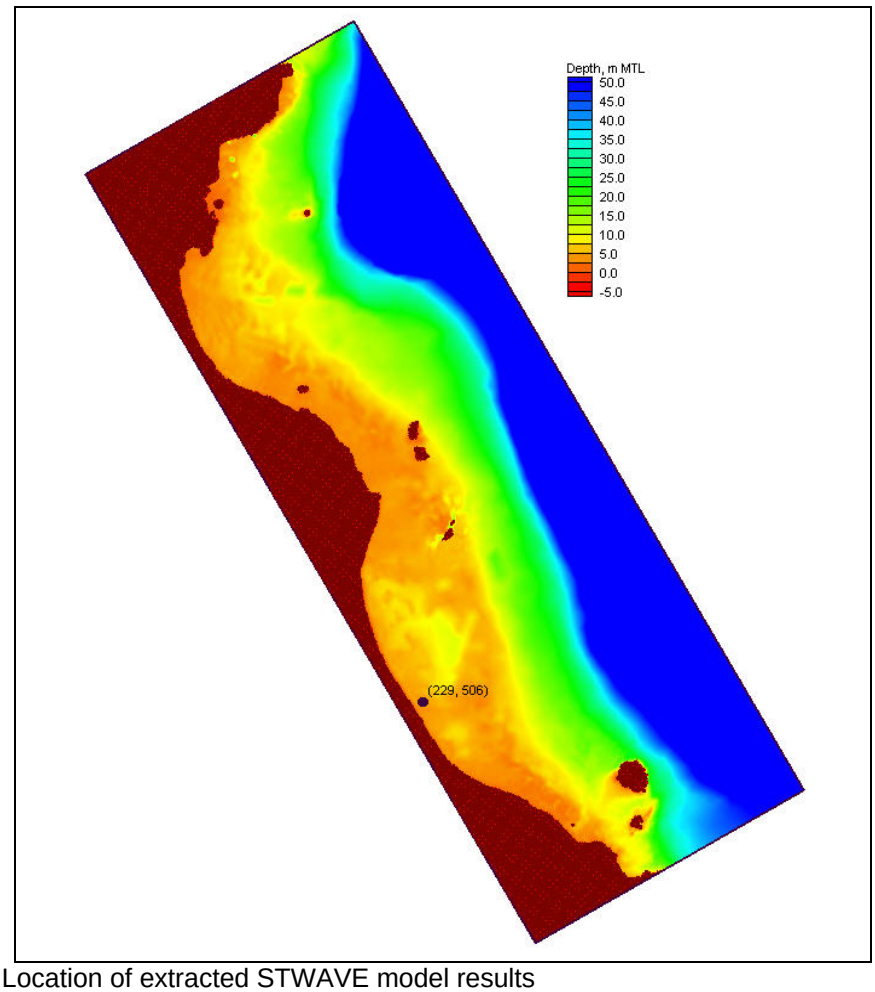

Figure 18. Location of extracted STWAVE model results

nearshore time series demonstrates that there is a reduction in wave height from the offshore location to the nearshore location, landward of the extensive reef system. The time series, however, appears generally contained or banded between the 1.25 and 2.25 m wave height bins that were selected to represent the overall wave climate. Further analysis was required to determine if a better representation of the offshore wave climate would better resolve the nearshore wave climate, and is discussed in the following.

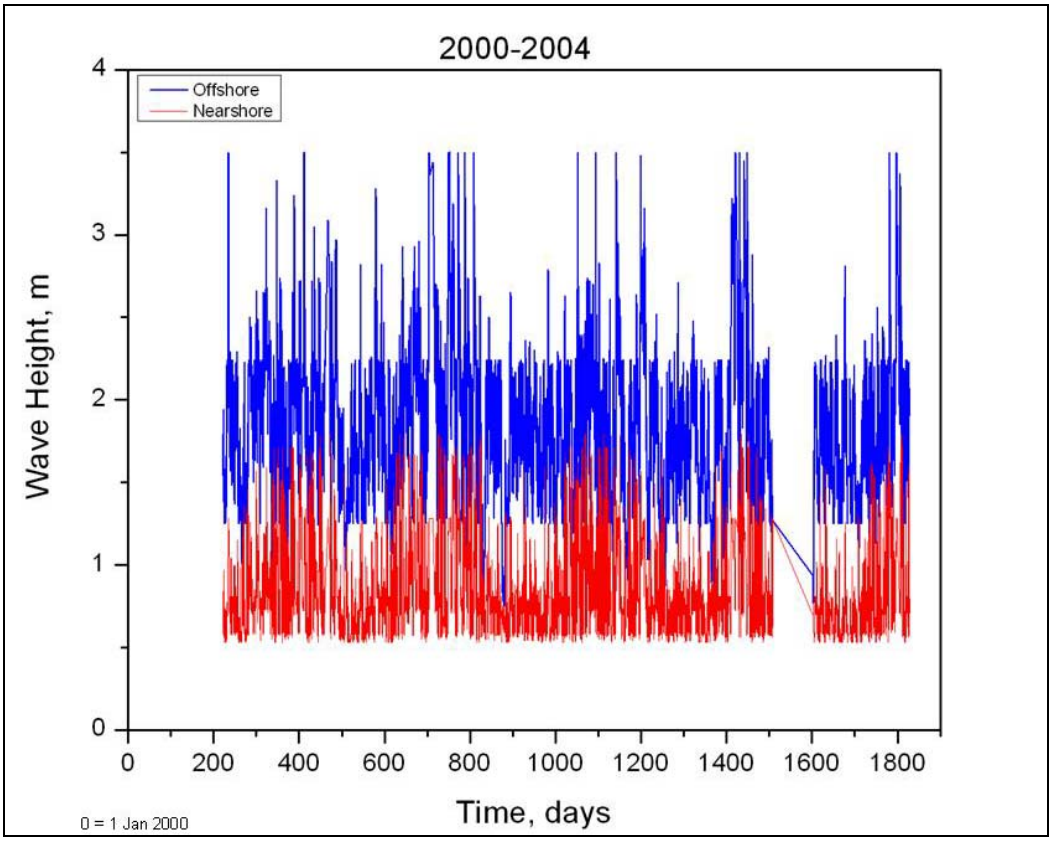

Figure 19. Nearshore time series generated from offshore time series with 134 correlation conditions

In order to capture the nearshore transformation time series more precisely and to include all wave conditions occurring in the time series, the range and refinement of the wave conditions simulated was expanded (Table 3). Wave heights ranged from 0.5 to 5.0 m with the finest increment being 0.25 m, wave periods were expanded to include 20 sec, and wave angles were expanded to include waves from the east-southeasterly direction (representing waves from 106-118 deg from True North) and were refined to 11.25 deg bands. For each of the 1274 selected wave conditions, TMA (shallow-water) spectra were generated by applying the SMS spectral wave generation software, then wave transformation was simulated by applying STWAVE over the project domain for each of the 1274 wave spectra. Again, nearshore conditions at cell (229,506) were extracted from the model results for each of the 1274 STWAVE simulations. A transfer function between the offshore and nearshore condition was then determined for each of the simulations. By applying the transfer function to each wave condition in the offshore time series at Station 098, a refined nearshore time series was generated (Figure 20),

which shows a more realistic undulation in the wave height. Note from the wave rose that wave directions converge to 35 to 73 deg relative to True North at the save point location located shoreward of the reef and are predominantly directed shore-normal (60 deg). (In a follow-on study, the 1274 STWAVE simulations included bottom friction and nearshore wave climates were developed for ten nearshore locations.)

Table 3. Expanded (1274) Wave Conditions

Significant Wave Height, m	Wave Period, sec	Wave Direction, deg from North	Wave Direction, deg from STWAVE axis
0.50	6	-22.5	82.5
0.75	8	-11.25	71.25
1.00	10	0	60
1.25	12	11.25	49.75
1.50	14	22.5	37.5
1.75	16	33.75	26.25
2.00	20	45	15
2.25		56.25	3.75
2.50		67.5	-7.5
2.75		78.75	-18.75
3.00		90	-30
3.50		101.25	-41.25
4.00		112.5	-52.5
5.00			

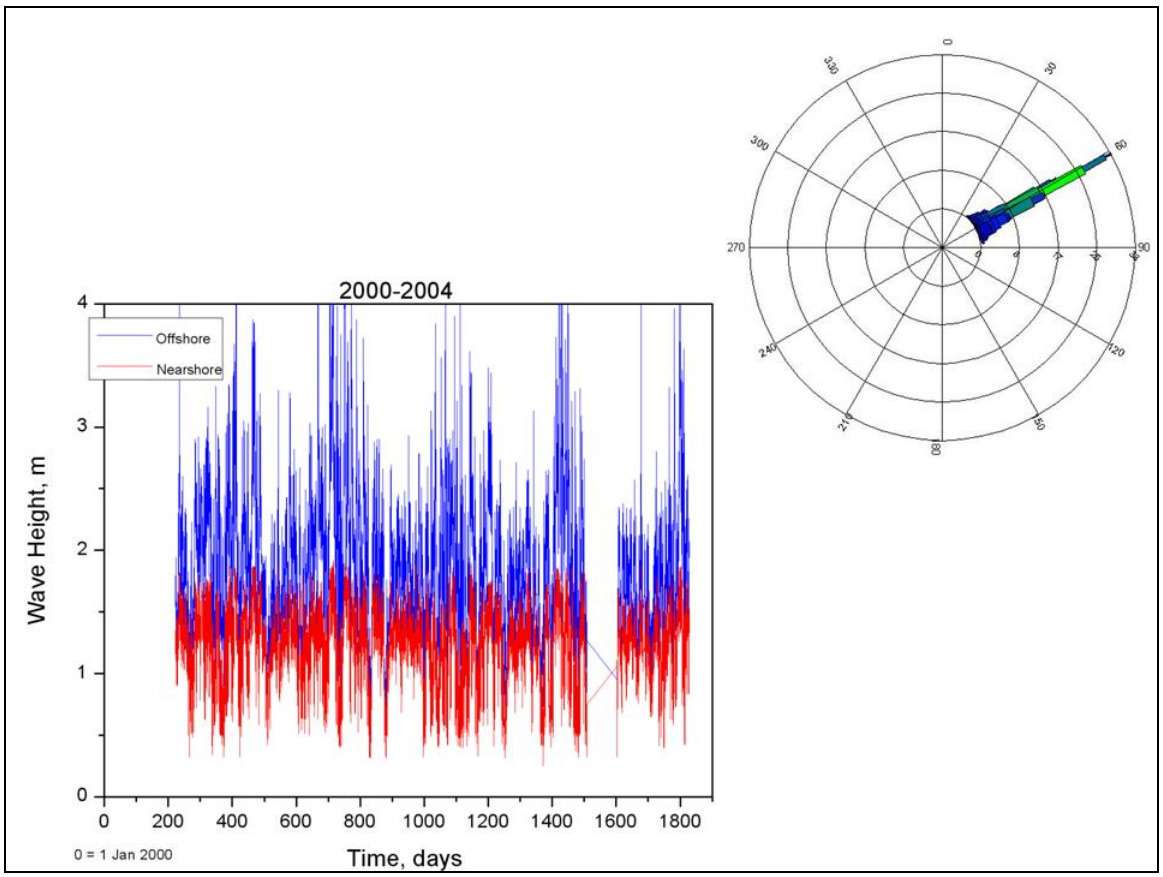

Figure 20. Nearshore time series and wave rose generated from offshore time series with 1274 correlation conditions

Bottom Friction

Development of a bottom friction capability in STWAVE was completed for application to the extensive reefs in the Southeast Oahu study area. The bottom friction source term in STWAVE is specified as:

$$S_{bf} = -\frac{1}{g} C_f \frac{\sigma^2}{\sinh(kd)^2} E(f,\theta)$$

where g is acceleration of gravity, C_f is the bottom friction coefficient, σ is angular frequency, k is wave number, d is total water depth (including surge), E is spectral energy density, f is frequency and θ is wave direction. The dissipation is summed over all frequencies and directions in the spectrum. Typical values of C_f for sandy bottoms range from 0.004 to 0.007 based on the JONSWAP experiment and North Sea measurements (Hasselmann et al. 1973, Bouws and Komen 1983). Values of C_f applied for coral reefs range from 0.05 to 0.40 (Hardy 1993, Hearn 1999, Lowe et al. 2005). Application of this model capability to a specific site requires validation to field data.

A single friction value can be applied to the entire STWAVE domain or a range of friction values can be applied on a cell-by-cell basis. As an example, the 134 wave conditions first simulated were repeated with the revised STWAVE, applying a bottom friction coefficient typical for reefs of 0.05 over the entire model domain. A comparison of nearshore waves at cell (229,506) was made (Figures 21 and 22). With the inclusion of bottom friction, wave height at the nearshore location ranges from 53 to 85% of the previous results that did not include bottom friction. On average, the wave height is 71% of the without bottom friction value at the selected location. Waves from the northeast refract slightly (1 deg) less with the inclusion of bottom friction. Waves from the east-southeast refract slightly (1 deg) more with the inclusion of bottom friction.

As another example, for each of the 1274 selected wave conditions simulated subsequently to achieve a more detailed wave climate, wave transformation *including spatially constant bottom friction* of 0.05 was simulated by applying STWAVE over the project domain for each of the 1274 wave spectra. Again, nearshore conditions at cell (229,506) were extracted from the model results for each of the 1274 STWAVE simulations. A transfer function between the offshore and nearshore condition was then determined for each of the simulations. By applying the transfer function to each wave condition in the offshore time series at Station 098, a refined nearshore time series with bottom friction was generated (Figure 23). A comparison of Figures 20 and 23 shows that the constant 0.05 value of bottom friction reduces nearshore wave heights by approximately 27%.

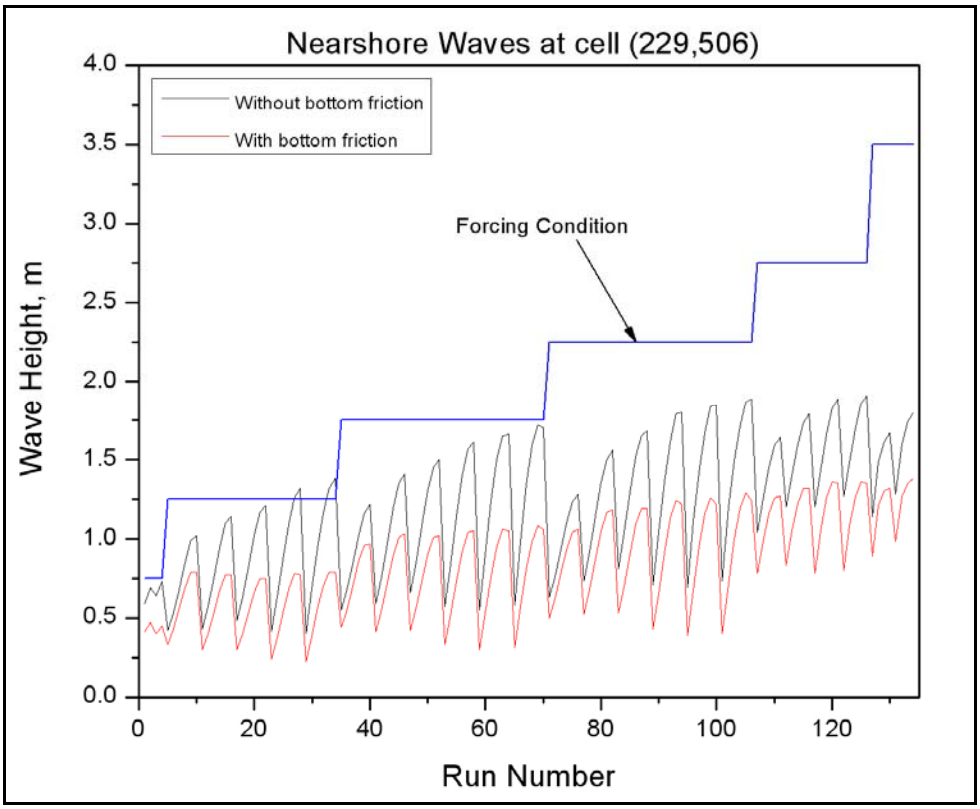

Figure 21. Comparison of predicted wave heights at cell (229, 506) with and without the STWAVE bottom friction feature

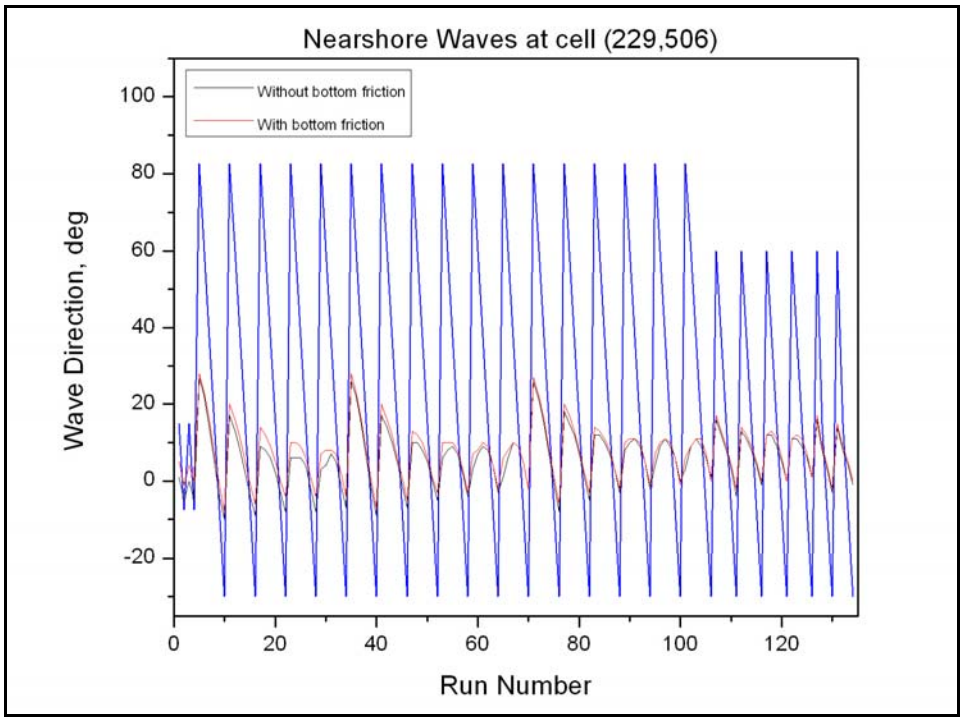

Figure 22. Comparison of predicted wave direction at cell (229, 506) with and without the STWAVE bottom friction feature

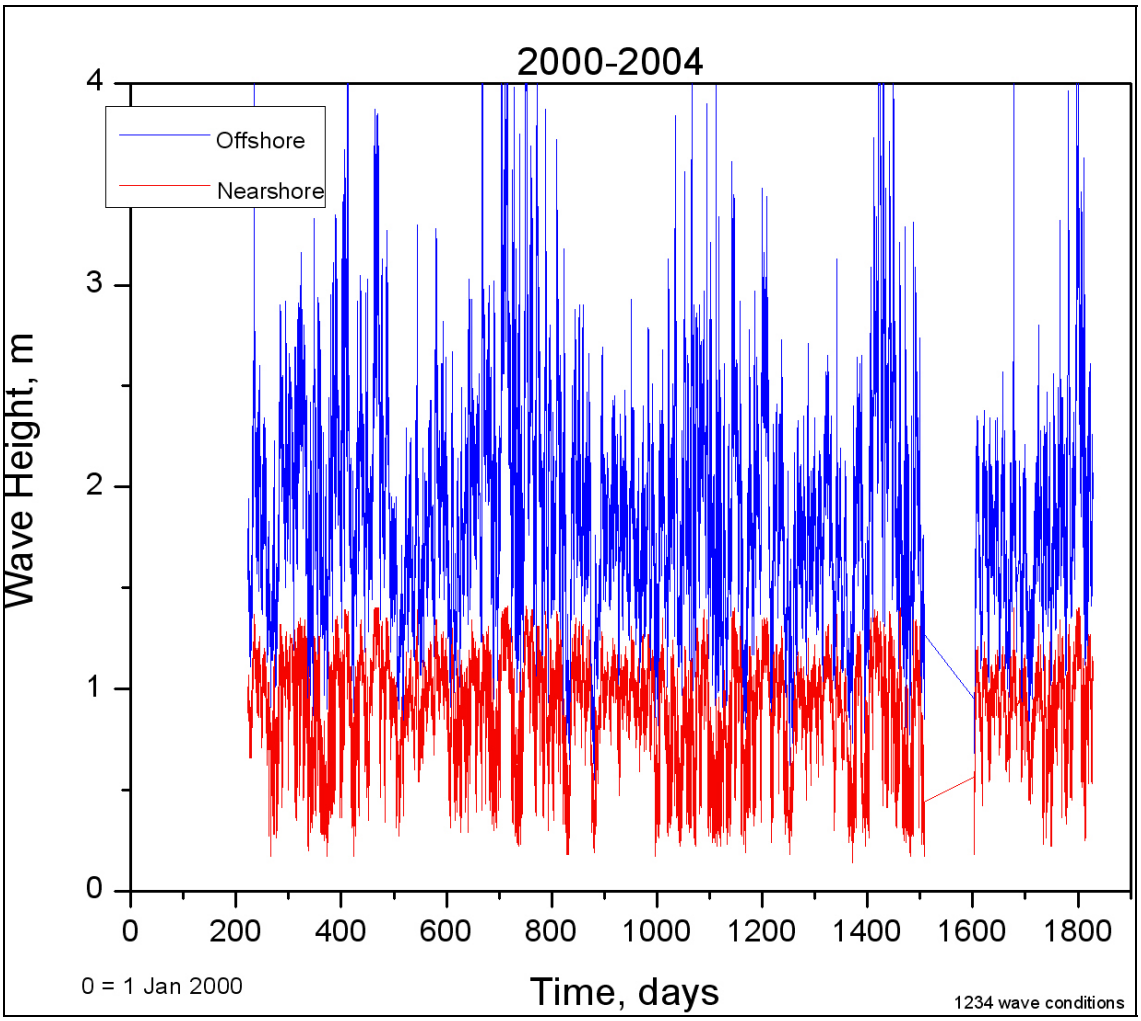

Figure 23. Nearshore time series (including spatially constant bottom friction) generated from offshore time series with 1274 correlation conditions

Model Validation

As previously discussed, the extended domain STWAVE grid was applied in the model validation process. The August 2005 model validation time period corresponded to a portion of the field data collection time period (9Augustthrough 14 September2005). CDIP Buoy data for August2005 (Figure 24) were extracted from the CDIP website for every 3-hr interval of August2005. For each of these measured wave conditions, TMA (shallow-water) spectra were generated by applying the SMS spectral wave generation software. These spectra were then applied to the offshore boundary of the model domain. Note that analysis was done to compare the waves at the 300-m depth STWAVE boundary and the 100-m depth gauge location by applying the University of Delaware Hydrodynamic Wave Calculator applet application (http://www.coastal.udel.edu/faculty/rad/wavetheory.html). It was found that the difference in wave height from the 300 m to 100 m depth is small (approximately 4% for periods <15 sec, which accounts for 98% of the waves) and the offshore gauge data were applied at the STWAVE boundary without back refracting to the 300 m water depth.

Initially, a constant bottom friction value was applied to each cell of the STWAVE domain. Several simulations with different constant bottom friction values ranging from 0.00 to 0.30 were made to examine the range of response (wave height) at the gauge locations. Figure 25 shows the wave height time series generated by STWAVE at the location where ADV1 was placed, without bottom friction and for 3 simulations with bottom friction. The bottom friction reduces wave height at ADV1's location by 20% for a bottom friction value of 0.05 (wave height is 80% of no bottom friction value) and by 72% for a bottom friction value of 0.30 (wave height is 28% of no bottom friction value). The range of response indicates the importance of selecting the appropriate bottom friction value to represent the reefs in the study area. In addition, a variable friction field with a larger friction value only applied over the extent of the reef areas would be the most appropriate representation of the study area.

In the validation simulation, a variable bottom friction field with 0.25 applied to the reef region, 0.35 around the offshore islands (for compatibility/linkage to the ADCIRC model), and 0.025 in the offshore regions was utilized. Figure 26 shows the wave field (heights) for one time period of the validation simulation. A comparison of field data collected at the three ADV locations (Figure 27) to the simulated wave heights is given in Figures 28 to 30. The model results for the ADV1 location follow the magnitude and trend of the data well. Model results at the ADV2 location tend to under-predict the measured wave height when the offshore waves are from the northeast and are smaller than 1 m). (Note that the wave direction for the period 23-26 August 2005 (Julian Days 235-238) was generally from the northeast (Figure 24). Model results at the ADV2 location show more of a signal (changing in wave height with time similar in pattern to the offshore forcing), whereas the measurements show much less variability (nearly constant wave height). Model results at ADV3 tend to over-predict the measured wave height when the offshore waves are greater than 1.3 m. Overall, all three measurement locations experience low wave energy relative to the offshore waves, likely due to the relatively mild tradewind conditions previously mentioned, and additional wave breaking over the reef. The field measurements range in wave height from 0.12 to 0.69 m for the data collection time period and the model results range from 0.04 to 0.71 m. The STWAVE model captures the large reduction in wave height from the offshore location to the three nearshore locations. It is noted that the coral reefs in this region are described as "mushroom fields". Some areas of the reef are more solid and some areas have gaps and holes in the reef. This level of detail was not applied to the friction representation of the reef. A possible improvement to the results, particularly at ADV3, could be made by reducing friction in the less solid reef areas (holes) and increasing friction in other areas. Overall, the wave height calculations compare well to the measured wave heights in the three measurements locations that are all located landward of the reef system.

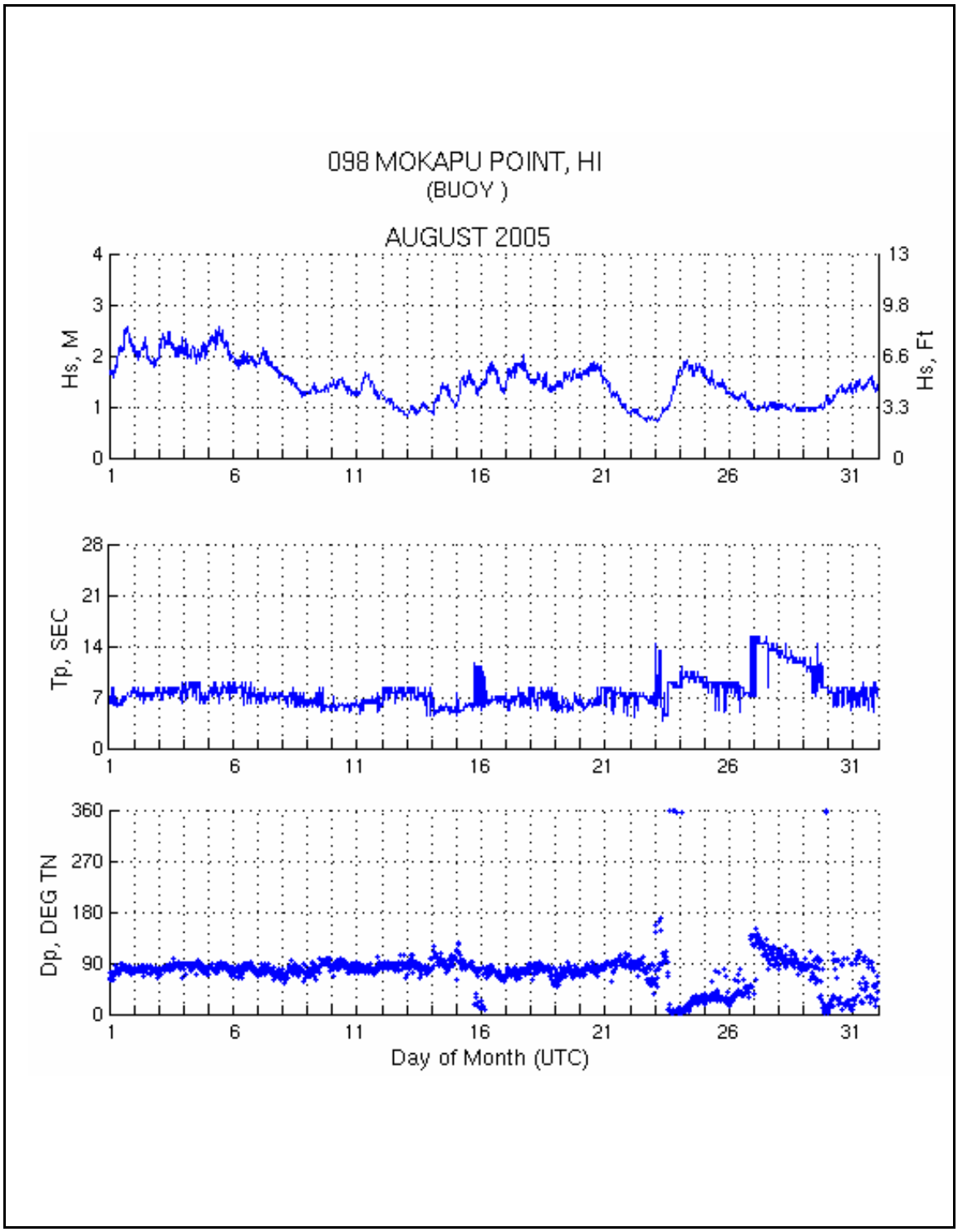

Figure 24. CDIP Buoy data for August2005

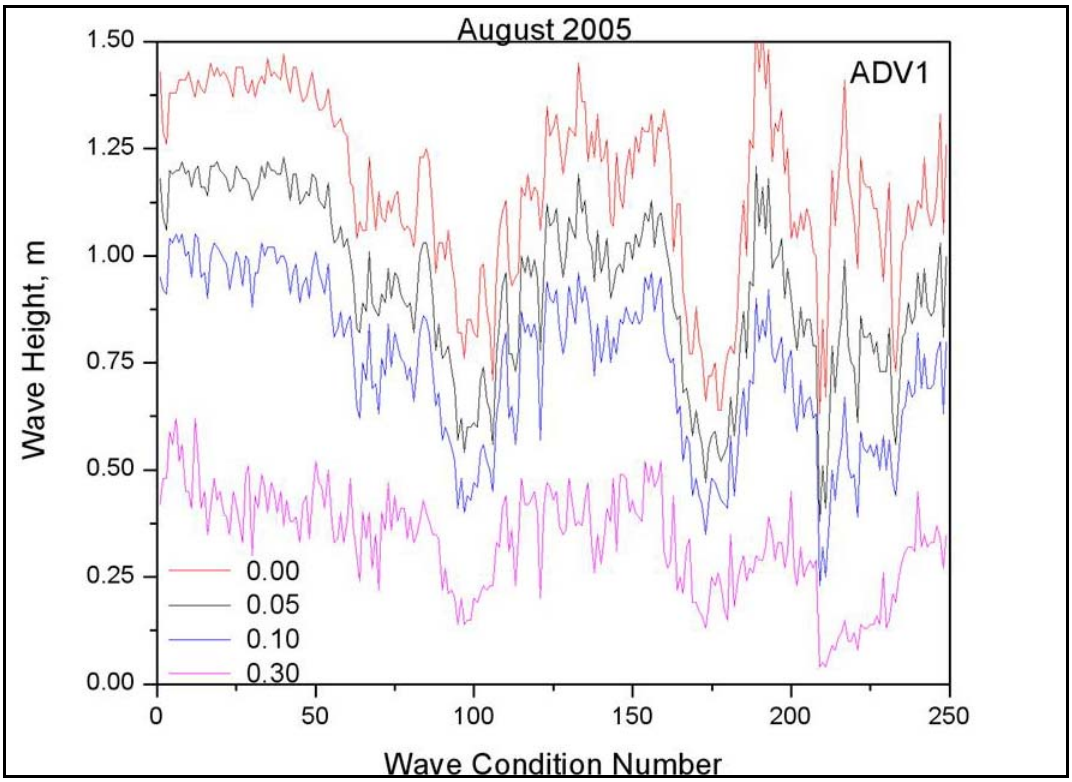

Figure 25. Simulated wave height time series at ADV1 with and without bottom friction

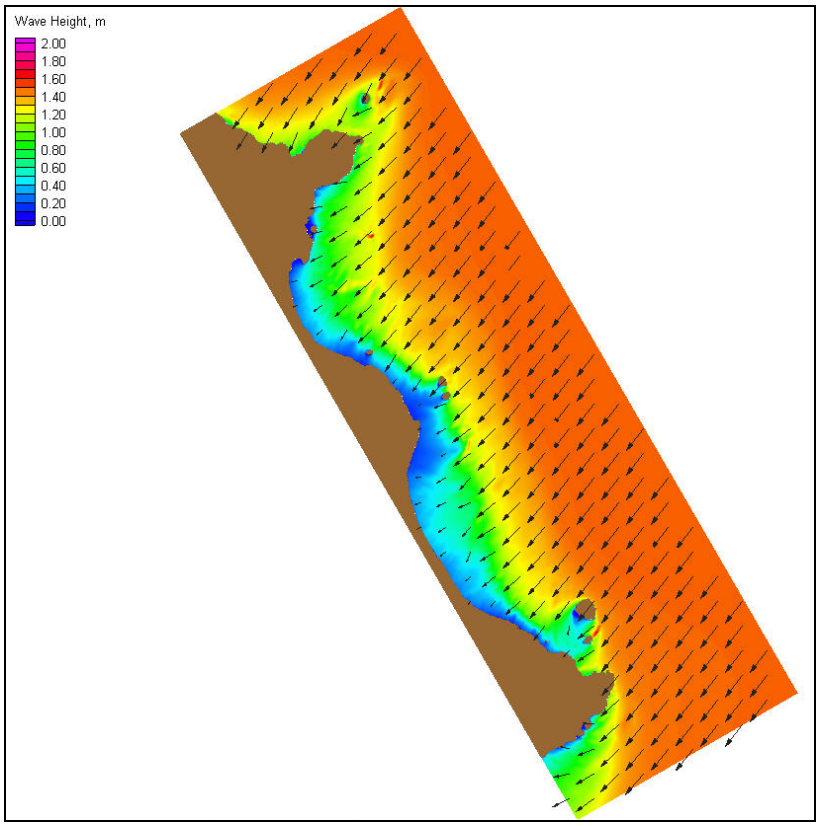

Figure 26. Wave field (heights) for one time period of the validation simulation

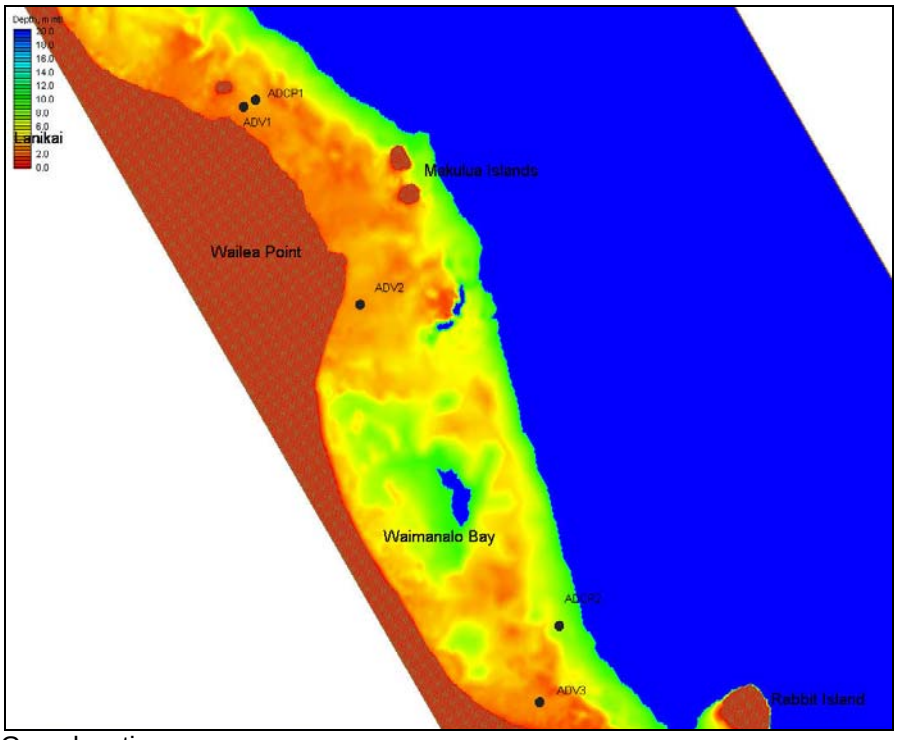

Figure 27. Gage locations

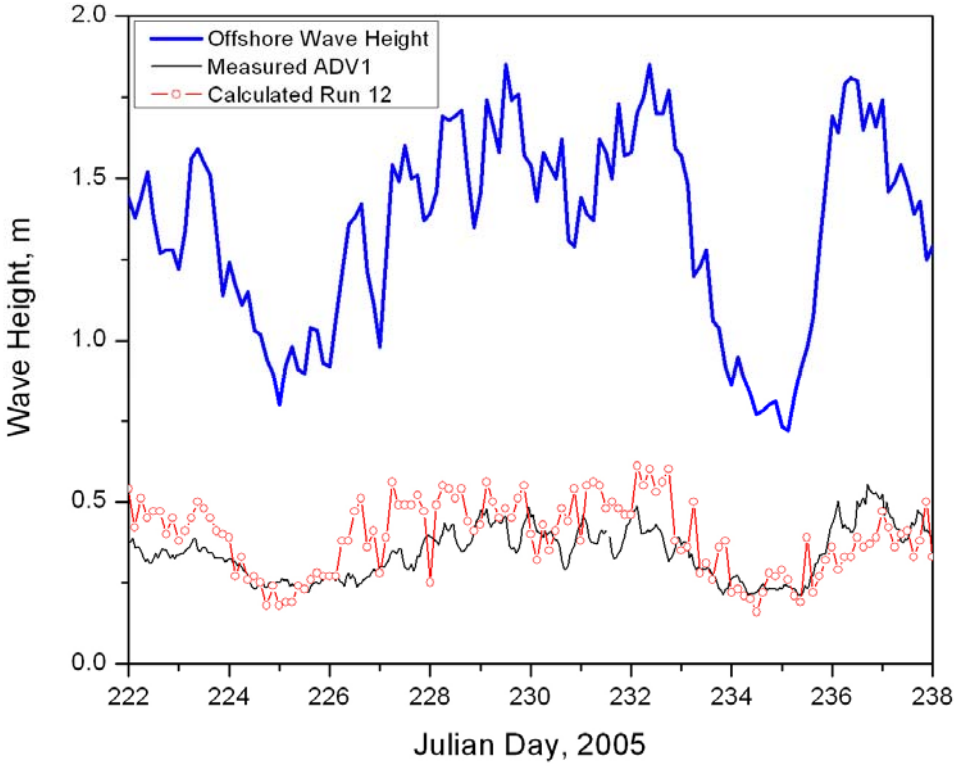

Figure 28. Comparison of measurements and STWAVE results at ADV1 for spatially-varying bottom friction

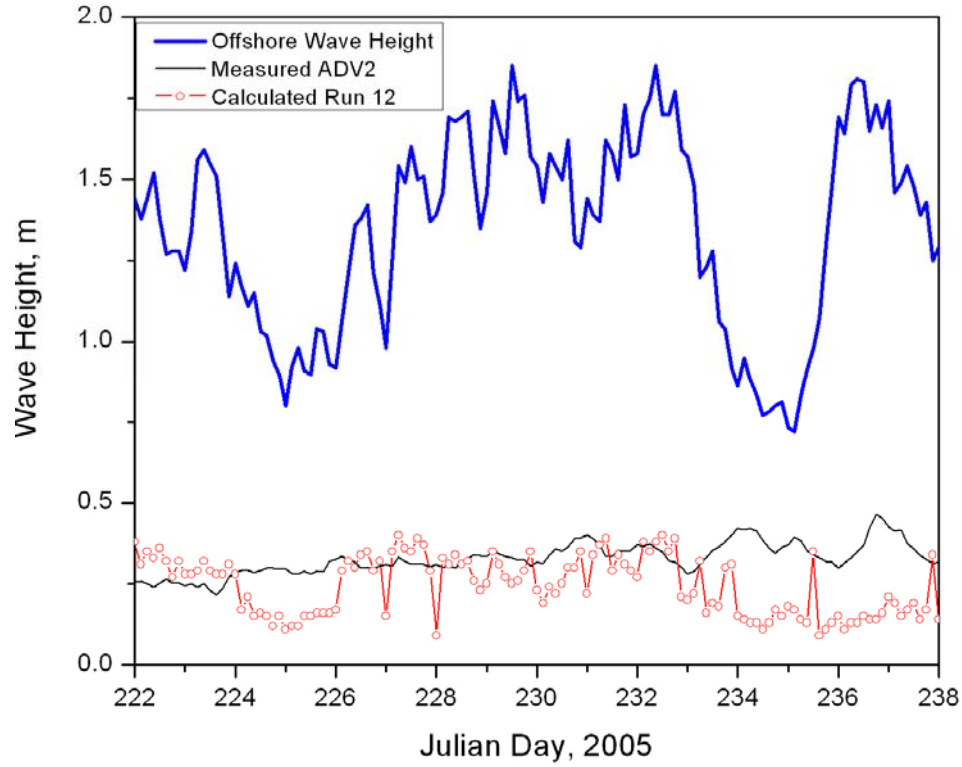

Figure 29. Comparison of measurements and STWAVE results at ADV2 for spatially-varying bottom friction

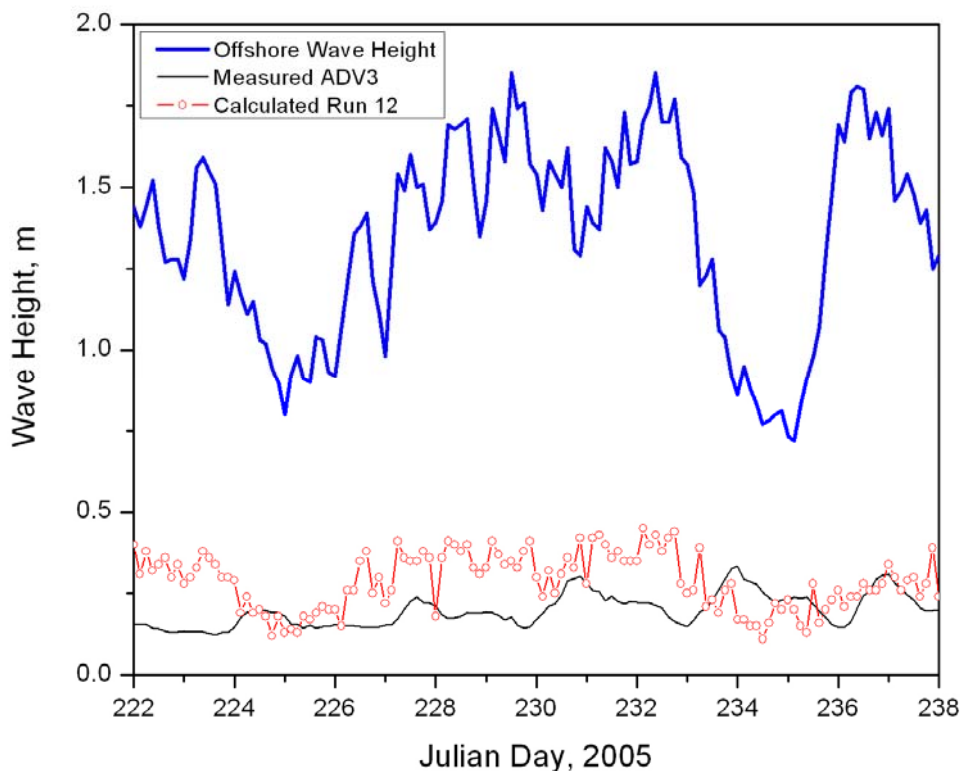

Figure 30. Comparison of measurements and STWAVE results at ADV3 for spatially-varying bottom friction

ADCIRC Validation – Wind, Tide, and Waves for Gauge Deployment Time Period

In the final validation, ADCIRC was applied to the study area for the August 2005 time period. This month overlapped the gauge deployment time period by approximately 2.5 weeks. ADCIRC was forced along the open boundary with tidal information extracted from the LeProvost tidal database. (The LeProvost database was applied because it provided a stable solution for the linked model validation time period.) Wind speed and direction information were obtained from the WIS winds described in the wind section earlier in this document. Wave forcing information was provided from the STWAVE simulation. (STWAVE was driven by CDIP buoy 98 data.) A series of ADCIRC simulations were run for the selected month in the validation procedure. The ADCIRC simulations varied in the hydrodynamic parameters, bottom friction values, as well as with and without wind and wave forcing as part of this validation process. There were some issues with the steep bathymetric gradients near the offshore island creating large radiation stress gradients which led to model instability. This was overcome by applying a large bottom friction value (0.035) in STWAVE near the offshore islands and limiting radiation stress gradients to a maximum of 0.0001. The final simulation applied a hybrid bottom friction formulation with a minimum C_f value of 0.003, then increased in value in shallow depths (less than 1.0 m). The eddy viscosity was set to 4.0 m^2/sec, and the time step was 0.4 sec.

Simulation Analysis

Currents and water levels were compared with field data obtained from the gauge deployment described earlier. Calculated water levels compared well in range and phase to measurements, but underestimated some lower peaks while overestimating some higher peaks. This may have been caused by unexpected interactions of the tides with the reefs surrounding the gauge locations. Water level comparisons with the three ADV gauges are shown below (Figures 31-33). A harmonic analysis may prove useful in obtaining a better comparison to the tidal constituents. However, since the current velocities measured are so small, an improved tidal constituent forcing would not greatly influence the total range of water level and therefore would not increase the current velocities significantly. Therefore, no harmonic analysis was performed.

Current velocity data from the three ADV gauges and two ADCP gauges were extremely small during the overlapping deployment time period – generally less than 10 cm/sec. Due to these small measured current magnitudes, current velocities calculated at these locations from the ADCIRC circulation model were not expected to compare well, however the range of velocity model results is within one order of magnitude and generally very close. Comparisons of ADCIRC circulation results to ADV and ADCP gauge measurements are shown in Figure 34-38. (Note that this analysis indicates that tidal and wave-induced currents for this time period were not significant enough in this region to bring forward to sediment transport analysis. This led to the conclusion that potential sediment transport mechanisms are more likely to be waves and storm-induced currents. A follow-on study to examine the effects of waves and storm-induced currents on sediment transport is ongoing.)

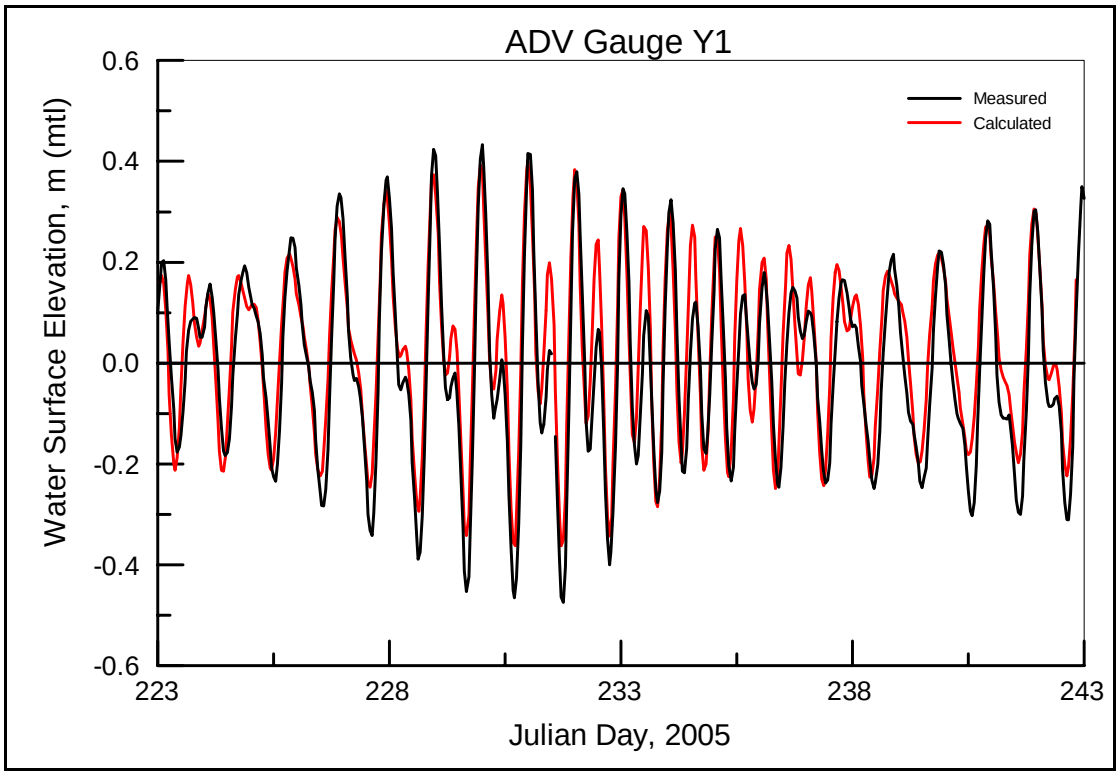

Figure 31. Water Level Comparison for ADV Gauge 1.

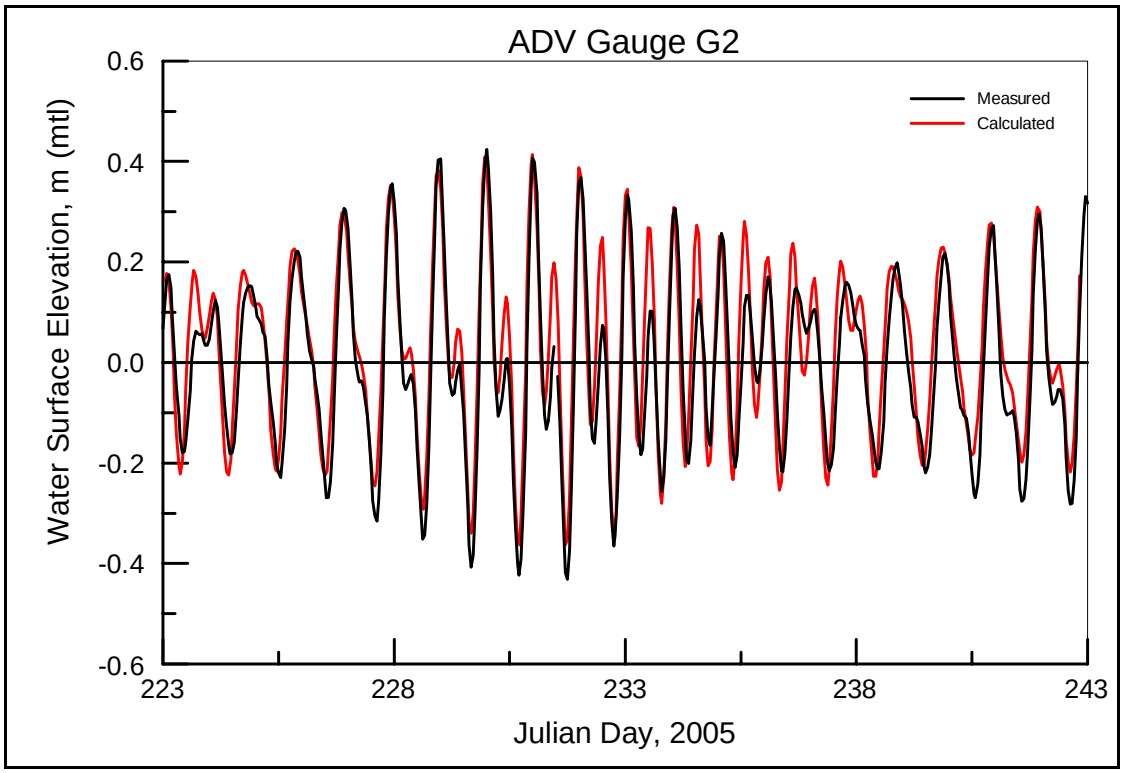

Figure 32. Water Level Comparison for ADV Gauge 2

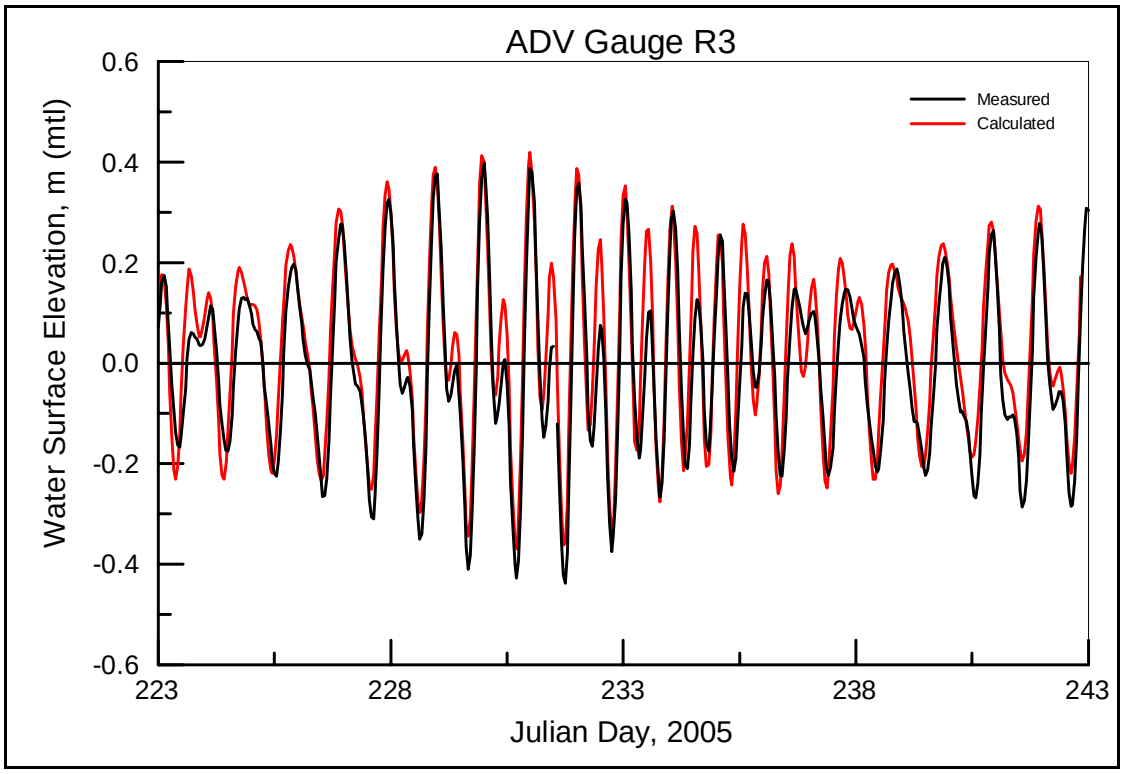

Figure 33. Water Level Comparison for ADV Gauge 3.

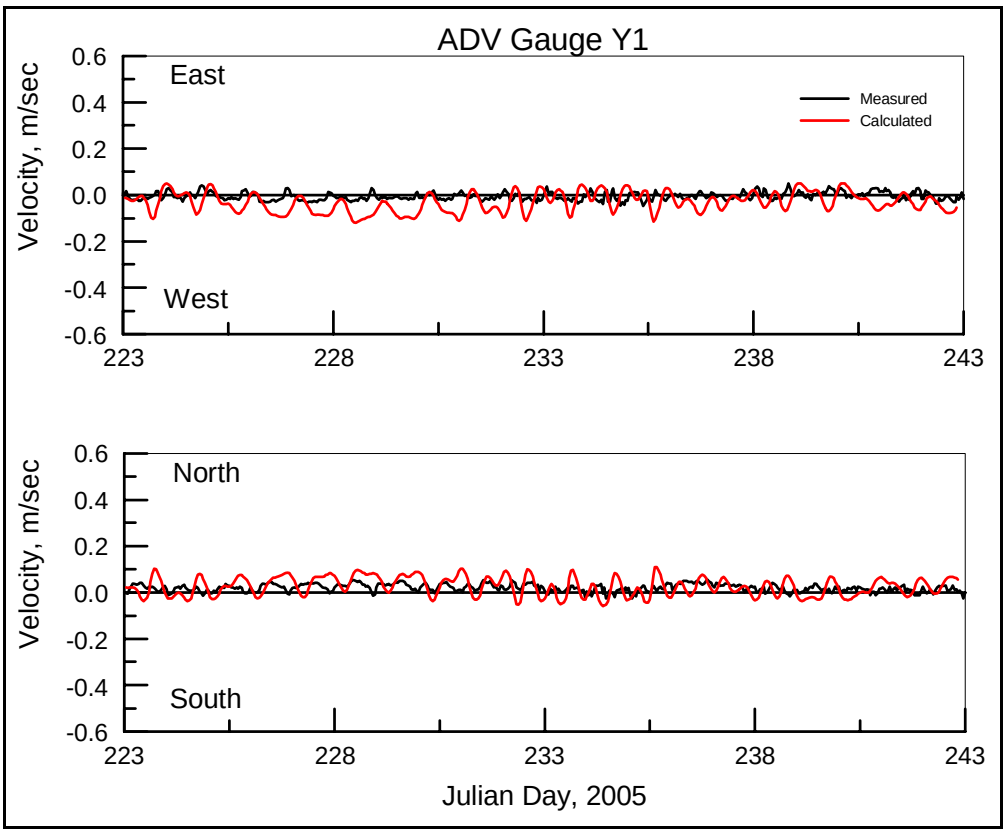

Figure 34. Velocity comparison for ADV Gauge 1

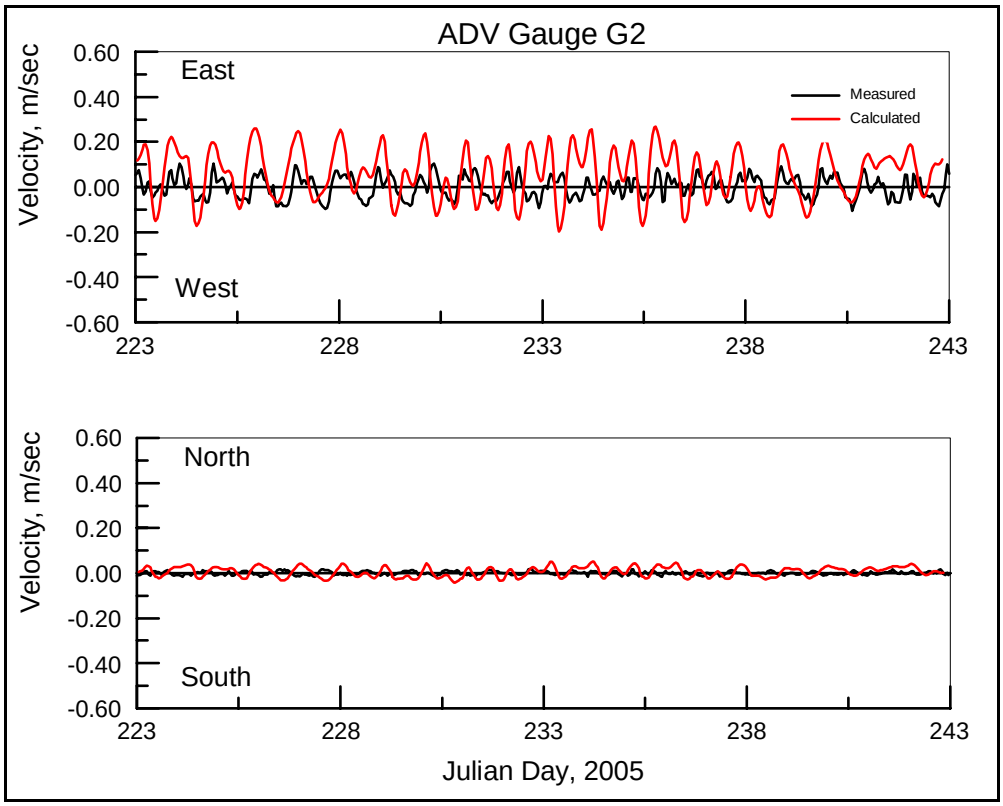

Figure 35. Velocity comparison for ADV Gauge 2

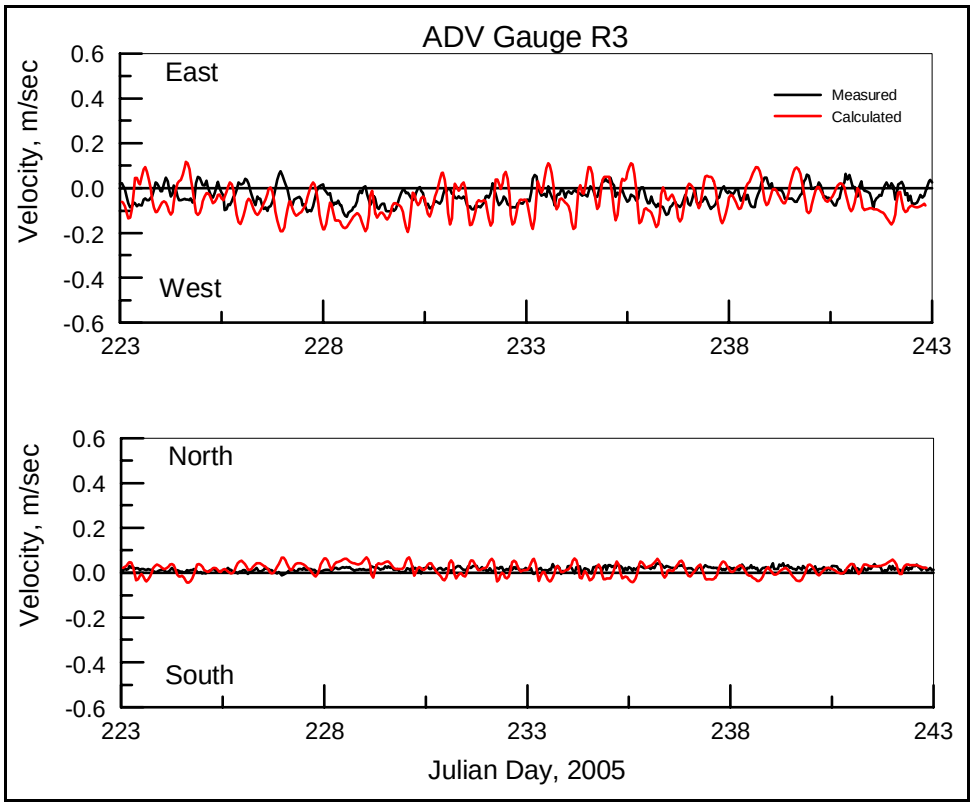

Figure 36. Velocity comparison for ADV Gauge 3

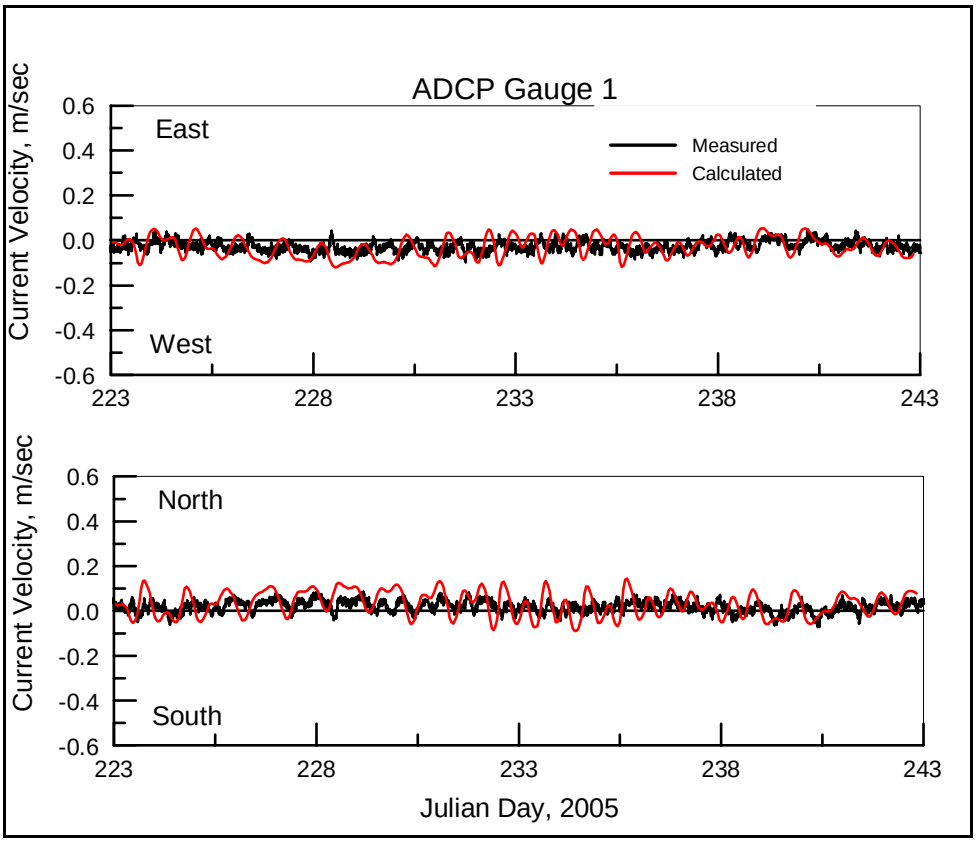

Figure 37. Velocity comparison for ADCP Gauge 1

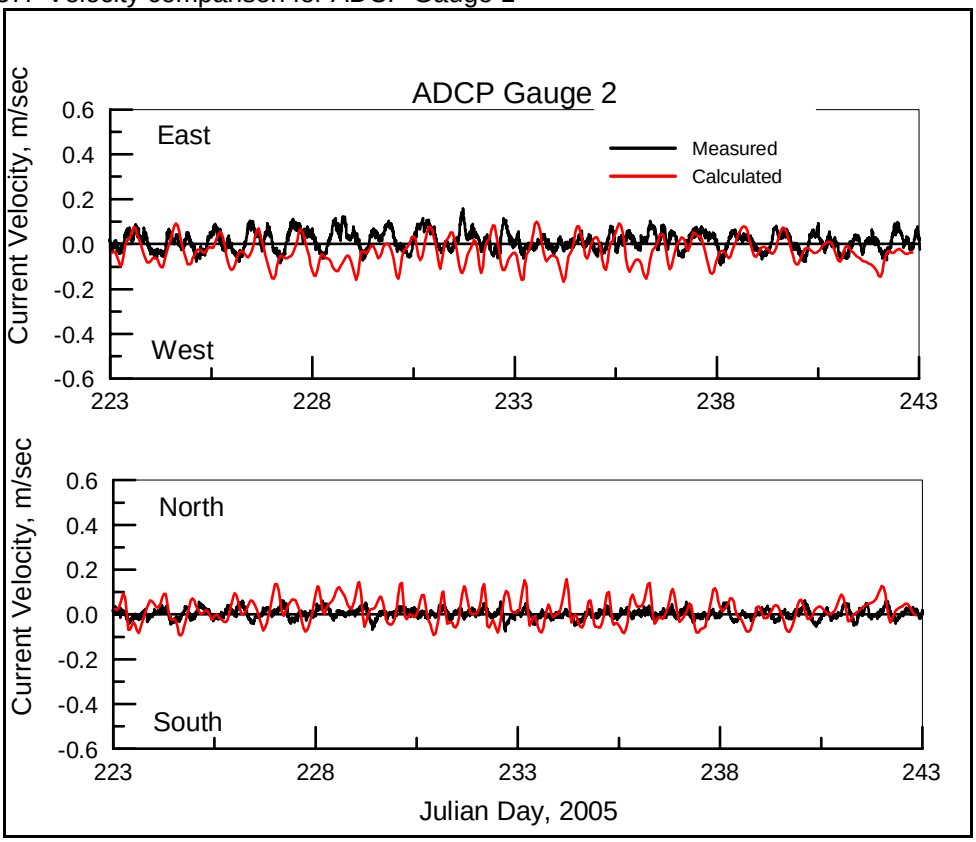

Figure 38. Velocity comparison for ADCP Gauge 2

Summary

The purpose of the study was to provide POH with validated hydrodynamic and wave models for the project site. POH could then apply the models with various forcing conditions to develop a better understanding of nearshore circulation and sediment transport potential in the region and determine the likelihood of accretional and erosional areas within the model domain. The nearshore circulation study included six technical tasks: data collection/assessment, finite element and finite difference grid development, development of model forcing conditions, model validation, model simulations, and simulation analysis.

In the field, data collection of waves, currents and water level were conducted for a one-month period with ADCP and ADV instruments. In addition, drogues were deployed on the two days that the ADCP/ADV were deployed and retrieved. Wave heights during the deployment period ranged from 0.12 to 0.69 m and were generally from the northeast direction, currents measured at the ADV and ADCP locations were small (generally less than 10 cm/sec), and water level ranged from +0.4 to -0.4 m, mtl. The drogue deployment provided general current trends for the two deployments.

A two-dimensional (depth-averaged) version of the hydrodynamic model ADCIRC was applied in this study. The ADCIRC modeling component for this study required grid development, validation of the bathymetric grid to known tidal constituents and wind forcing for April 2001, and comparison of the bathymetric grid forced with known tidal constituents, wind, and waves to measurements for the field data collection time period. The ADCIRC grid was developed as a circular mesh, encompassing the Hawaii Islands, but was revised to an egg-shaped mesh to avoid tidal amphidromes in the Pacific Ocean.

For the initial model validation, ADCIRC results were compared with two NOAA gauges on the eastern half of the island of Oahu. The calculated water levels from the ADCIRC simulation of the April 2001 time period compared relatively well in range and phase with the NOAA gauge measurements considering the locations of the gauges were well outside the area of high resolution in the project area. Since these gauges were outside the project area and located in less resolved locations, another validation was made by simulating the field data collection time period and comparing model results to field data collected in the study area, specifically for this project. Calculated water levels compared well in range and phase to measurements, but underestimated some lower peaks while overestimating some higher peaks. This may have been caused by unexpected interactions of the tides with the reefs surrounding the gauge locations. Current velocity data from the three ADV gauges and two ADCP gauges were extremely small during the overlapping deployment time period – generally less than 10 cm/sec. Velocities calculated at these locations from the ADCIRC circulation model were not expected to compare well to the measurements, however the range of velocity model results is within one order of magnitude and generally very close. The application and validation of ADCIRC for the southeast Oahu study provides POH with the capability of simulating circulation in the study area for any required time period.

The purpose of applying nearshore wave transformation models such as STWAVE is to describe quantitatively the change in wave parameters between the offshore and the nearshore because nearshore wave information is required for the design of almost all coastal engineering projects. STWAVE has been applied to numerous sites and this project has the added feature of simulating wave transformation over a reef. Development of a bottom friction capability in STWAVE was completed for application to the extensive reefs in the Southeast Oahu study area. Application of STWAVE for this project required development of a computational grid to simulate wave propagation, verification of calculated waves by comparison to measurements, and generation of a wave climate.

For demonstration of the wave climate development technique, nearshore conditions at a point in Waimanalo Bay, were extracted from the STWAVE model results for each of the 134 simulations. A transformation correlation between the offshore and nearshore condition was then determined for each of the 134 simulations. By applying the appropriate transfer function to each wave condition in the 2000-2004 offshore time series at Station 098, a long-term (2000-2004) nearshore time series was generated. The nearshore time series demonstrates that there is a reduction in wave height from the offshore location to the nearshore location, landward of the extensive reef system as expected. The time series, however, appeared generally contained or banded between the 1.25 and 2.25 m wave height bins that were selected to represent the overall wave climate. In order to capture the nearshore transformation time series more precisely and to include all wave conditions occurring in the time series, the range and refinement of the wave conditions simulated was expanded to 1274 wave conditions. The refined nearshore time series generated from analysis of these simulations shows a more realistic undulation in the nearshore wave height time-series.

Development of a bottom friction capability in STWAVE was completed for application to the extensive reefs in the Southeast Oahu study area. Values of the bottom friction applied for coral reefs range from 0.05 to 0.40. A single friction value can be applied to the entire STWAVE domain or a range of friction values can be applied on a cell-by-cell basis. As an example, the 134 wave conditions simulated in the initial climate development were repeated with the revised STWAVE, applying a bottom friction coefficient typical for reefs of 0.05. With the inclusion of bottom friction, wave height at the nearshore location ranges from 53 to 85% of the previous results that did not include bottom friction. On average, the wave height is 71% of the without bottom friction value at the selected location. Waves from the northeast refract slightly (1 deg) less with the inclusion of bottom friction. Waves from the east-southeast refract slightly (1 deg) more with the inclusion of bottom friction. As another example, for each of the 1274 selected wave conditions simulated for the revised wave climate, wave transformation *including bottom friction* was simulated by applying STWAVE over the project domain for each of the 1274 wave spectra. The constant 0.05 value of bottom friction reduces nearshore wave heights by approximately 27%.

The extended domain STWAVE grid was applied in the model validation process for the August 2005 model validation time period. Initially, a constant bottom friction value was applied to each cell of the STWAVE domain. Several simulations with

different constant bottom friction values ranging from 0.00 to 0.30 were made to examine the range of response (wave height) at the gauge locations. Bottom friction reduces wave height at the ADV1 location by 20% for a bottom friction value of 0.05 (wave height is 80% of no bottom friction value) and by 72% for a bottom friction value of 0.30 (wave height is 28% of no bottom friction value). The final validation decreased waves height from the without friction condition by 66% for a bottom friction value of 0.25. The range of response indicates the importance of selecting the appropriate bottom friction value to represent the reefs in the study area.

In the validation simulation, a variable bottom friction field with 0.25 applied to the reef region, 0.35 around the offshore islands (for compatibility/linkage to the ADCIRC model), and 0.025 in the offshore regions was utilized. Overall all three measurement locations experience low wave energy relative to the offshore waves. The STWAVE model captures the large reduction in wave height from the offshore location to the three nearshore locations. It is noted that the coral reefs in this region are described as "mushroom fields". Some areas of the reef are more solid and some areas have gaps and holes in the reef. This level of detail was not applied to the friction representation of the reef. A possible improvement to the results, particularly at ADV3, could be made by reducing friction in the less solid reef areas (holes) and increasing friction in other areas. Overall, the wave height calculations compare well to the measured wave heights in the three measurements locations that are all located landward of the reef system.

Lessons learned from this study include: 1) the technique of developing a nearshore wave climate by applying stwave for a large number (range) of offshore wave conditions provides a permanent "look up" table of nearshore wave conditions at any location in the computational domain and can be applied to any time period that offshore data is available, provided that bathymetric conditions within the model domain remain similar. (Note that the creation of a nearshore wave climate was applied to generate a nearshore time series for the 2000-2004 time period and POH is applying the database generated time series to develop sediment transport potential estimates in the project area. A follow-on study extended the time-series through 2005 and expanded to 10 save point locations.), 2) from the ADCIRC validation for the deployment time period and also from examination of the retrieved deployment data, it was concluded that the tidal and wave-induced currents in the project area are small and not sufficient to significantly transport sediment. A follow-on study is being conducted to examine simulation of higher energy (storm) conditions which may produce currents that are strong enough to transport sediment. This follow-on study also includes sediment transport modeling, and 3) an improved model capability was developed for this study. Bottom friction was added to STWAVE to simulate wave transformation over reefs. It was shown that bottom friction is extremely important and has a pronounced effect on modeling transformation over reefs, decreasing waves height from the without friction condition by 66% for a constant bottom friction value of 0.25. Simulation of the transformation process over reefs could be improved further by including wave ponding. This may be examined in future STWAVE model development and application.

CHL assisted POH by documenting the methodologies and procedures used in this study and providing consultation in executing simulations and analyzing simulation results. STWAVE and ADCIRC working sessions have been conducted at POH andthe completed modeling system was transferred to POH within the SMS framework.

References

Bouws, E., and G.J. Komen. 1983. "On the balance between growth and dissipation in extreme, depth limited wind-sea in the southern North Sea," Journal of Physical Oceanography, Vol 13, pp 1653-1658.

Egbert, G., Bennett, A., and Foreman, M. 1994. "TOPEX/Poseidon tides estimated using a global inverse model," Journal of Geophysical Research, vol. 99, No C12, pp. 24821 - 24852.

Hardy, T. A. 1993. The attenuation of spectral transformation of wind waves on a coral reef. James Cook University of North Queensland, Townsville, Queendsland, Australia, 336 pp.

Hasselmann, K., T.P. Barnett, E. Bouws, H. Carlson, D.E. Cartwright, K. Enke, J.A. Ewing, H. Gienapp, D.E. Hasselmann, P. Kruseman, A. Meerbrug, P. Muller, D.J. Olbers, K. Richter, W. Sell, and H. Walden. 1973. Measurements of wind-wave growth and swell decay during the Joint North Sea Wave Project (JONSWAP). Dtsch. Hydrogr. Z., A80(12), 95 pp.

Hearn, C. J. 1999. "Wave-breaking hydrodynamics within coral reef systems and the effect of changing relative sea level," Journal of Geophysical Research, vol. 104, No C12, pp. 30007-30019.

Lowe, R. J. Falter, J. L., Bandet, M. D., Pawlak, G., Atkinson, M. J., Monismith, S. G., Koseff, J. R. 2005. "Spectal wave dissipation over a barrier reef," Journal of Geophysical Research, vol. 110, No C04001, doi:10.1029/2004JC002711, 16pp..

Luettich, R.A., Jr., Westerink, J. J., and Scheffner, N. W. 1992. ADCIRC: an advanced three-dimensional circulation model for shelves coasts and estuaries, report 1: theory and methodology of ADCIRC-2DDI and ADCIRC-3DL, Dredging Research Program Technical Report DRP-92-6, U.S. Army Engineers Waterways Experiment Station, Vicksburg, MS, 137p.

Resio, D. T. (1988). A steady-state wave model for coastal applications. *Proceedings of the 21st Coastal Engineerring Conference*, ASCE, pp 929-940.

Smith, J. M., Sherlock, A. R., Resio, D. T. (2001). STWAVE: Steady-State Spectral Wave Model User's Manual for STWAVE, Version 3.0, SR-01-1, Coastal and Hydraulics Laboratory, U.S. Army Engineer Research and Development Center, Vicksburg, MS, 81p.

LeProvost, C. M., L. Genco, F. Lyard, P. Vincent, and P. Canceil, 1994. "Spectroscopy of the world ocean tides from a finite element hydrodynamical model," Journal of Geophysical Research, Vol 99, C12, pp 24777-24797.

APPENDIX D

GEOTECHNICAL INVESTIGATIONS

SAND SAMPLE MAP
SAND FROM CRUSHED CORAL RUBBLE

Geotechnical Investigations

SOUTHEAST OAHU REGIONAL SEDIMENT MANAGEMENT DEMONSTRATION PROJECT SAND SAMPLE MAP

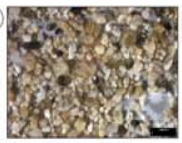

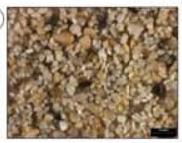

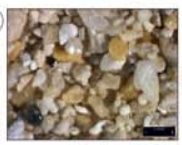

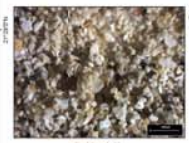

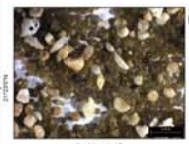

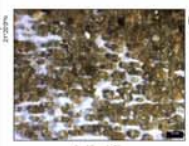

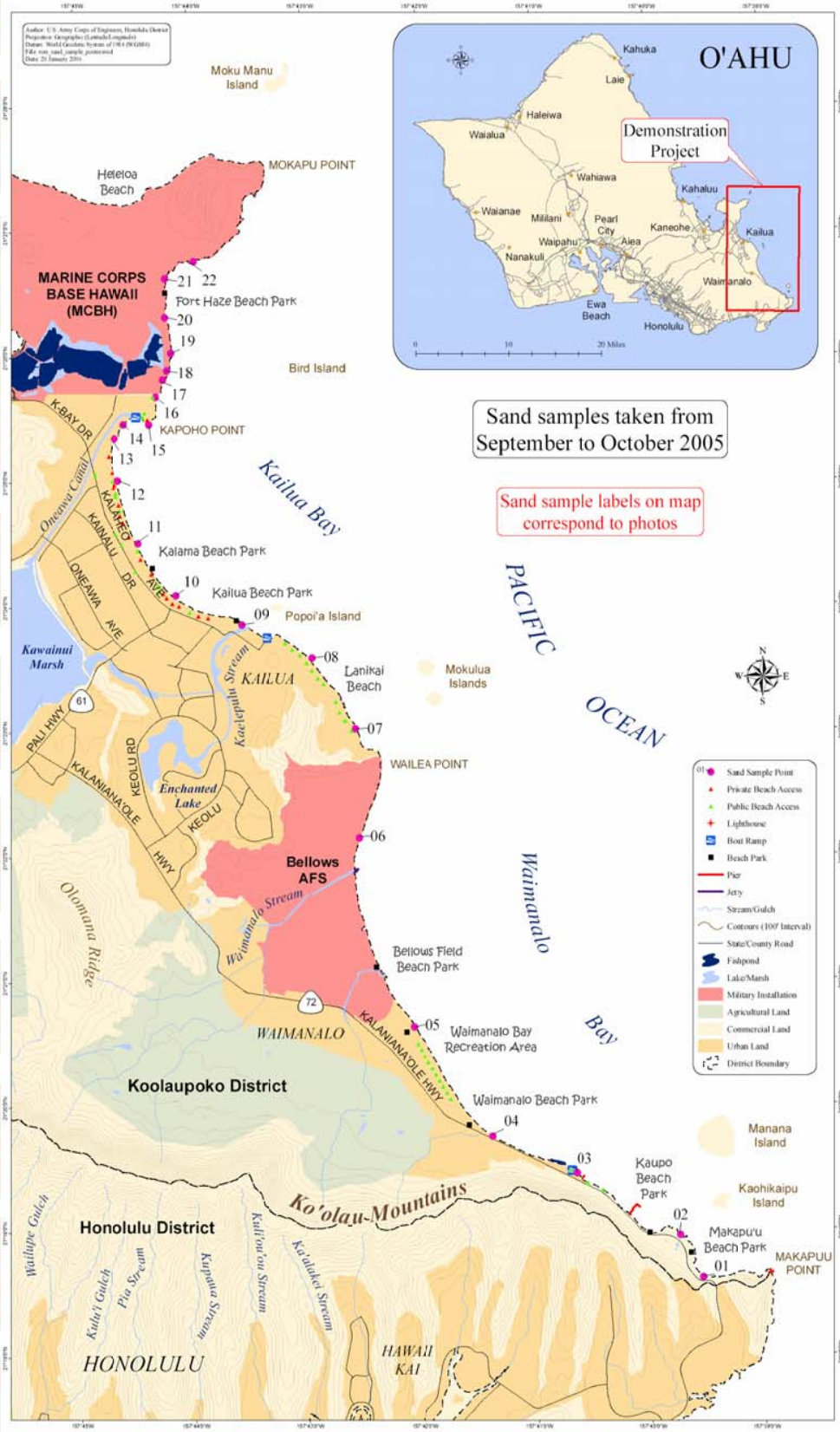

SAND
from
CRUSHED CORAL RUBBLE

Beachrock Formation

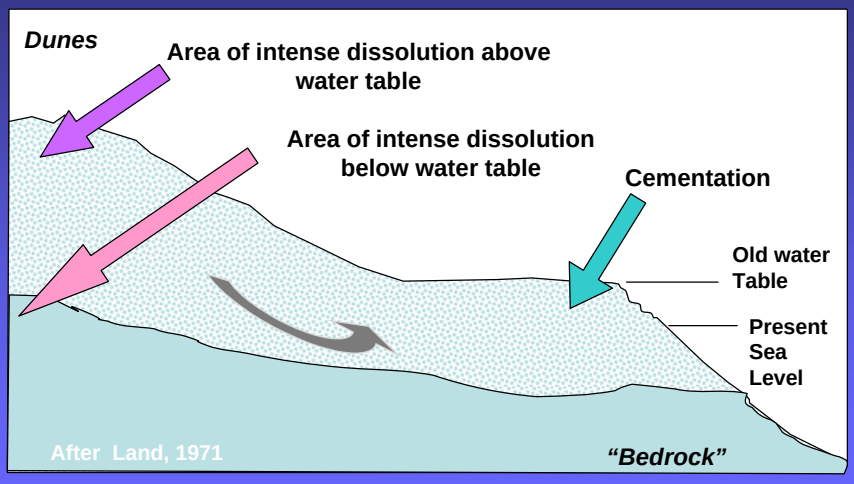

Washed Carbonate Sand Surface

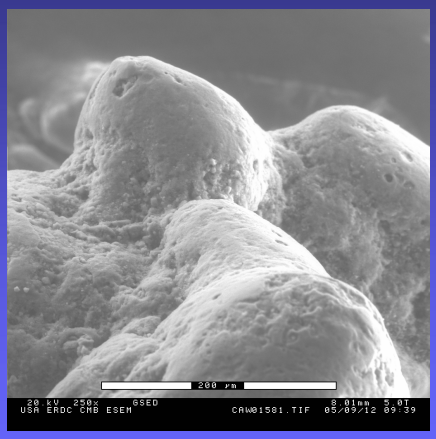

- Carbonate sand grains were treated by washing in boiling hydrogen peroxide to remove microbial overgrowth
- Surface is polished
- Fractures show porous skeletal carbonate structure

Overgrowth on Sand Surface

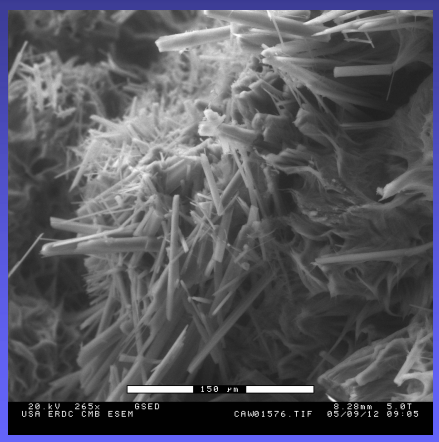

- Sand grain treated by using carbonate and calcium solution to produce overgrowth of aragonite needles on surface
- Grains are cemented into beachrock by carbonate overgrowth

Aragonite and Calcite Overgrowth

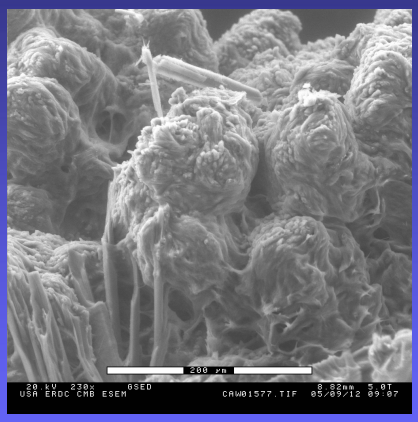

- Carbonate precipitation can produce calcite and aragonite overgrowth
- Aragonite is typically unstable and can redissolve and recrystalize as calcite
- Small crystals are less stable than large crystals and small crystals dissolve and large crystal grow larger (Ostwald crystal ripening).

Fatty Acids for Coating Materials

- Inexpensive, non-toxic
- Available in large quantities
- Available in all grades
- Slowly biodegradable
- React with and coat all carbonates
- End product is the calcium salt of the fatty acid (soap film)

What Loading Rate is Required?

- Assume the fine sediment is the source of the cement
- Three-micron diameter calcite fragments have a specific area of approx. 0.7 m^2/g
- Each molecule of stearic acid covers 20.5 sq. Å
- One gram of calcite has area of 7×10^{16} sq. Å
- Molecular wt of stearic acid = 284.5 (6×10^{23} molecules per mole)
- Approx. 6×10^{-9} moles stearic acid cover one gram
- Theoretically a metric ton of calcite requires less than 2 grams of stearic acid

Industrial Grade Fatty Acids

Commercial soaps are salts (typically sodium salts) of a mixture of fatty acids

Summary on Inhibiting Re-Cementing

- Coatings can isolate the surface of carbonate grains to make solution of carbonates and overgrowth of cements slower
- Process of preserving the sand mimics natural processes that inhibit re-cementing of carbonates
- Fatty acid coatings can promote clustering of fine-grained carbonates reducing turbidity
- Coating process is inexpensive and can be integrated into manufacturing sand along with crushing and sieving steps
- A sieved, coated sand should provide a better beach than quarry-run crushings

APPENDIX E

REGIONAL SEDIMENT MANAGEMENT
WEB ENABLED GIS PLATFORM
e-GIS

GIS and the Internet

All of the RSM geospatial data is available over the Internet with new "Online Mapping" Tools

Data Layers

Layers on the site include:

- satellite imagery
- watershed boundaries
- land parcels
- roads
- soil types
- wetlands
- hydrography
- shoreline profiles
- historical shoreline change
- shoreline structures
- coastal habitat & reefs
- sediment deposit information
- revetments
- bathymetry
- wave gauges
- nautical charts
- and much more!

What Am I Looking At?

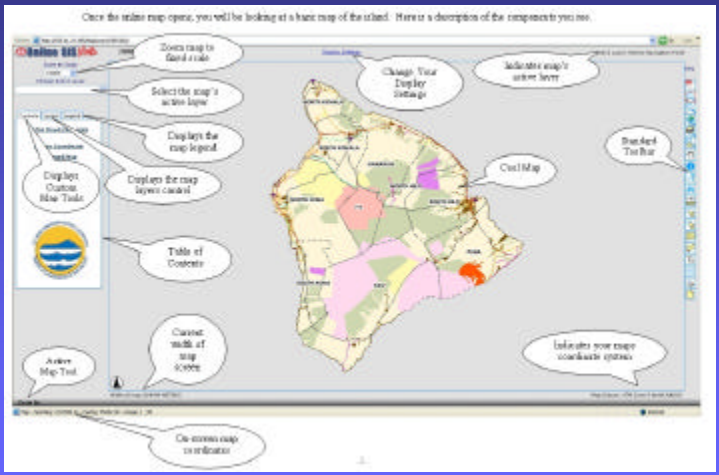

How Do I Turn a Layer On/Off?

1) Navigate to the Table of Contents , and click on the Layers tab (highlighted in red in the graphic to the right).

2) After you have activated the "Layers" tab, then just check (or uncheck) any of the square boxes (highlighted in purple in the graphic to the right). next to a layer to turn it on (off).

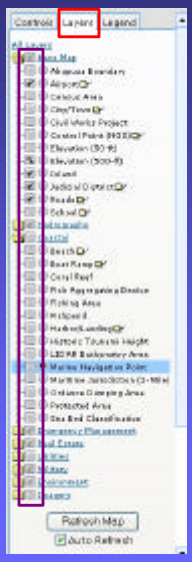

What Does the Standard Toolbar Do?

	Toggles the overview map on or off		Zoom-in on the map with user defined AOI		Zoom-out on the map with user defined AOI
	Zoom to the full extent of the map		Zoom to the extents of the active map layer		Zoom back to the previous extent of the map
	Pan the map in any direction		Retrieve attribute data by identifying a feature		Display standard query builder form
	Search the attributes of the specified layer		Measure linear distance on the map in specified units of measure.		Select map features and retrieve attribute data using a dynamically dragged window
	Select map features and retrieve attribute data by using a user defined polygon or line		Place a dynamic point on the map that is labeled with the point's coordinates		Calculate area of a user defined polygon in specified units of measure
	Add user defined text to the map where clicked		Place a user defined grid over the map with labeled rows and columns		Print the map
	Clears the map of any temporary selections.				

How Can I Calculate Acreage?

1) Zoom into the area on the map where you would like to calculate the area. This can be performed by using the "Zoom In" button , which is found on the Standard Toolbar.

2) After you have zoomed in to the area you would like to calculate, click on the "Calculate Area" button , which will activate the "Polygon Area" dialog box.

3) In the "Polygon Area" dialog box, set the Area Units you would like (acres, square feet, square meters, etc), as well as the fill color and transparency.

4) After you are happy with your settings, begin clicking on the map to designate the vertices of your area calculation. Before you reach your last vertex, click on the **Complete Polygon** button in the "Polygon Area" dialog box to auto complete the polygon.

5) The area information will appear on your map.

How Do I Print My Map?

1) Zoom into the area on the map where you would like to print. This can be performed by using the "Zoom In" button , which is found on the Standard Toolbar.

2) Add any coordinate labels, text, grids, etc that you want visible for printing.

3) After you have the map set just like you want, click on the "Print" button , which will activate the "Print Map" dialog box.

4) In the "Print Map" dialog box, type in your map title and any other comments you would like.

5) After you have your title and comments set, then select the paper size you want your map to print at.

6) After your paper size has been selected, click the **Generate Map** button.

7) Select File > Print to print the map out.

How Do I Save My Map?

1) Zoom into the area on the map where you would like to save. This can be performed by using the "Zoom In" button , which is found on the Standard Toolbar

2) Turn on/off any layers you would like visible/not visible.

3) Add any customized coordinate labels, text, grids, etc that you desire.

4) Right-click on the map, and select **Save Picture As…** from the context menu (highlighted in blue in the graphic to the right).

5) In the "Save Picture" dialog box, select where you would like the image saved, and then click the **Save** button.

6) Your image will be saved to your computer, and you can now insert it into e-mails, PowerPoint Presentations, project documents, etc.

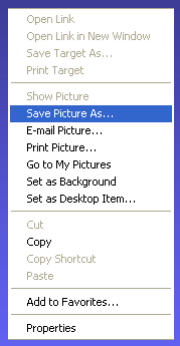

APPENDIX F

REGIONAL SEDIMENT PROCESSES

DEPARTMENT OF GEOLOGY AND GEOPHYSICS
UNIVERSITY OF HAWAII

A Reconnaissance of Reef Top Sediment Bodies in Windward Oahu, Hawaii

Draft (December 11, 2006)

by

Christopher Bochicchio

Charles Fletcher

Univeristy of Hawaii - Coastal Geology

Dept. of Geology and Geophysics

1680 East-West Rd.

POST 721a

Honolulu, HI 96822

Draft 06

INTRODUCTION

Fringing reefs in Hawaii display sand fields on their surfaces (Figure1) that potentially play a role in littoral sediment budgets, provide substrate for important components of reef ecology, and may serve as a resource for sand and gravel aggregate. These shallow sand fields may also potentially provide quantities of affordable sand for beach replenishment projects (Moberly et *al.*, 1975; Casciano and Palmer, 1969; Moberly and Chamberlain, 1964). However, the degree of sand storage they provide and their role in littoral sediment budgets has not been defined.

Past Studies: Several studies review offshore and onshore carbonate sand sources on the island of Oahu, Hawaii. Moberly et *al.* (1975) present a general survey of offshore sand resources surrounding Oahu in the 0 – 18 m depth zone. At three sites, Sand Island, North Shore, and Penguin Bank, sand thickness is measured using a sub-bottom seismic profiler and sand volumes are estimated. Ocean Innovators in conjunction with the US Army Corps of Engineers completed jet probe surveys and sediment sampling at a number of shallow and deep sand resource areas around Oahu (Ocean Innovators, 1977a – c, 1978a – b, 1979).

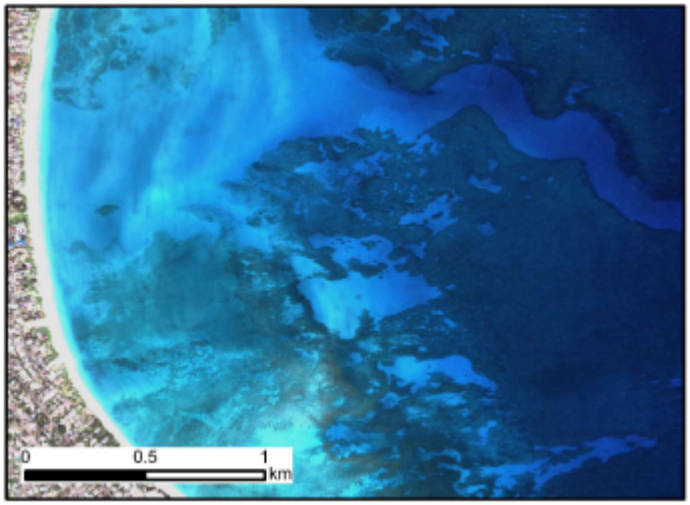

Figure 1. Bodies of sand fill depressions on the near-shore carbonate platform.

Coulbourn et *al.* (1988) perform detailed statistical analysis on sand samples taken by Ocean Innovators to identify grain size correlations to depth and depositional environment. Sea Engineering (1993) presents a summary of sand exploration studies performed around the island of Oahu as well as comparative ratings for exploitable deposits. Hampton et *al.* (2003) and Hampton et *al.* (2004) identify significant bodies of

sediment stored in the deep, 18 –100 m, fore-reef area at various Oahu locations using sub-bottom seismic imaging. Neither of Hampton's reports makes significant mention of sand bodies in water < 18 m.

The NOAA Benthic Habitat Mapping Program (Coyne et *al.* 2003) mapped sandy substrate from the shoreline to 30 m depth as part of a benthic habitat classification for the whole of Oahu. Conger et *al.* (2006) created detailed maps of sandy substrate to 20 m depth at sites around Oahu via supervised classification of multispectral satellite imagery, but these lack volume estimates.

Present Study: Past studies describe sand resources at sites around Oahu in varying degree of detail. The focus of this report pertains to three adjoining locations on the eastern Oahu shore: Kailua Bay, Lanikai, and Waimanalo Bay. Previous studies that provide detailed subsurface sampling within our area of interest include: Ocean Innovators (1978a), Coulbourn et *al.* (1988), Hampton et *al.* (2003), and Hampton et *al.* (2004). Sea Engineering (1993) provides a summary of data in Kailua Bay.

This study is an initial large-scope investigation of sediment volume within the study area. The intent of this study is to highlight areas of significant volume that could be the subject of more detailed measurement and study in the future. Here we report the results of 205 jet probe thickness measurements obtained from 54 distinct sand bodies in the 0 – 20 m depth zone across the reef platform of Kailua Bay, Lanikai, and Waimanalo Bay. Volume estimates and uncertainties are presented with discussion of sand body morphologies. The focus of this research is to quantify the volume geometry of reef-top sand bodies, improve our understanding of controls on variations in thickness of these sand resources, and infer the role of reef top sand bodies in littoral sediment processes.

STUDY AREA: KAILUA BAY, LANIKAI, AND WAIMANALO BAY

Wave Climate: Wave energy influences coastline stability, nearshore submarine sand transport, and mechanical abrasion on the reef. Hawaii's regional wave climate (Figure 2) is described in four components by Bodge and Sullivan (1999):

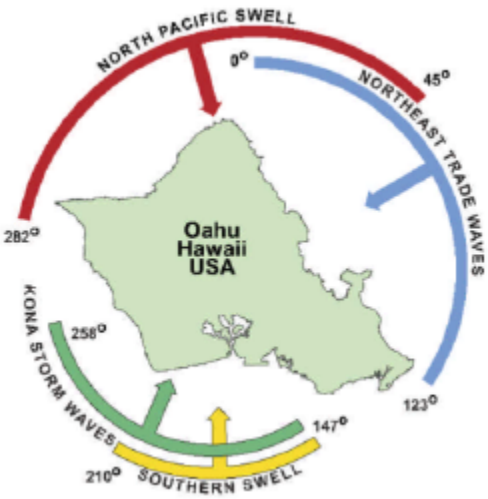

Figure 2. Components of Oahu's wave environment.

1) High-energy northeast Pacific swell created during the winter by storms north of Hawaii. Waves are incident on WNW to NNE shorelines; typical heights of 1.5 – 4.5 m and periods of 12 – 20 seconds.
2) Lower energy south Pacific swell between the months of April and October. Waves are incident on most south facing shorelines and have typical heights of 0.3 – 1.8 m and periods of 12 – 20 seconds.
3) Kona storms infrequently produce from the south and west wave heights of 3 – 4.5 m and periods of 6 – 10 seconds.
4) Trade wind waves consistently approach from the general northeast quadrant for 90% of the summer months and 55 – 65% of the winter months (Fletcher et *al.* 2002). Trade wind wave heights are 1.2 – 3 m with periods of 4 – 10 seconds.

Additionally, large but infrequent hurricane waves can have significant impact on the reef (Fletcher et. al, 2002). Rooney et *al.* (2004) discuss the occurrence of extraordinarily large winter swell associated with strong El Nino episodes. They conclude that these events exert control over fringing reef accumulation and have essentially terminated most shallow water accretion on north-exposed coasts in Hawaii since approximately 5,000 yrs B.P (before present).

The primary wave regime for our windward study area is governed by the consistent full strength of trade wind swell. This swell is modified by annual and decadal

North Pacific wave events that wrap around Mokapu Peninsula into the study area. Large south swell affects the study area to a lesser extent. Easterly storms may also impact the study with high winds and/or high waves approaching on an interannual basis from the northeast, east, or southeast. Calmest conditions in the study area occur during Kona wind conditions as trade winds diminish, frequently producing offshore air flow.

Shelf Origin: The underlying carbonate framework of the study area is the product of reef accretion over recent interglacial cycles. Specifically, the shallow shelf of Oahu is a fossil reef complex dating from Marine Isotope Stage (MIS) 7 (~190,000 – 210,000 yrs B.P., Sherman et *al.*, 1999; Grossman and Fletcher, 2004). The front of this shelf accreted separately during MIS 5a-d (ca. 80,000 – 110,000 yrs B.P.). Eolianites of late last interglacial age (ca. 80,000 yrs B.P., Fletcher et *al.*, 2005) are found on the nearshore and coastal plain regions of windward Oahu.

Modern Holocene reef accretion is limited to deeper environments on the front of the reef where wave energy is not destructive. Grossman and Fletcher (2004) and Conger et *al.* (2006) infer that rugosity in depths less than 10 m atop the fringing reef is the result of karstification of limestone during times of lower sea-level, most recently since the last interglacial. Modern wave scour has prevented accretion in this zone. In depths greater than 10 m the karst surface has largely been over grown by Holocene accretion (Conger et *al.*, 2005).

Coastal Plain: Harney and Fletcher (2003) provide a synthesis of drill cores and radiometric dating obtained in the Kailua coastal plain over the last 60 years. It is demonstrated that sediments underlying the town of Kailua and the Kawaianui Marsh reflect 5,000 years of coastal sedimentation during a sea-level highstand (+2 m) and subsequent declines in sea-level position (Grossman and Fletcher, 1988). A 3-10 m thick sandy accretion strand plain is deposited over lagoonal sediments (marine silt with shell and coral fragments) >40 m in thickness. Under modern Kawainui Marsh, cores penetrate 15 m of peat, terrestrial mud, and lagoonal sediments. The presence of lagoonal sediment is attributed to formation of a marine embayment ca. 3,500 yrs B.P. during the high-stand followed by formation of a terrestrial marsh following sea-level fall ca. 2,200 years B.P. (Kraft, 1982, 1984; Athens and Ward, 1991). The accretion strand

plain is lies between the marsh and the beach face of modern Kailua Bay and has an especially thick central portion attributed to shoreward expression of the offshore paleo-stream channel that has filled with sand (Harney and Fletcher, 2003). The strand plain formed by shoreline regression as sea-level fell to its modern position following the mid-Holocene highstand. Coastal plain deposits underlying Kawainui Marsh and the town of Kailua are found by Harney and Fetcher (2003) to contain 10,049 (+/- 1,809) x 10^3 m^3 of carbonate sand and silt of Holocene age.

General Sediment Characteristics: Moberly and Chamberlain (1964) characterize Kailua Bay, Lanikai, and Waimanalo Bay as having very poorly sorted highly calcareous beach sands and large but thin patches of offshore sand. Kailua and Lanikai sands are described as poorly sorted, with Kailua tending towards bimodality. Waimanalo sands are described as coarse- to medium- grained and vary from well sorted to poorly sorted with high *foraminifera* fractions. Landward of Kailua and Waimanalo beaches are modern vegetated dunes and older lithified eolianites, consisting of coarse well-sorted sand, in which *foraminifera* constitute the highest compositional fraction.

Sediment Production: Harney et *al.* (2000) completed a detailed study of beach, channel, and reef-top sand bodies in Kailua Bay. Harney determined >90% of sediments were biogenic carbonate, dominated by coralline (red) algal fragments. They identified two primary sources of sediment for Kailua Bay. The offshore reef platform is a primary source of framework sediments (coral and coralline algae) while nearshore hardgrounds and landward portions of the reef platform are sources of direct sediment production (*Halimeda*, mollusks, and benthic *foraminifera*).

Radiometric dating of sand grains indicate middle to late Holocene age for surficial sediment stored in Kailua Bay. Most surficial sediments were found to be older than 500 yrs, suggesting relatively long storage times in the immediate sediment budget. Harney et *al.* (2000) concluded that sand stored in Kailua Bay represents production under a higher sea-level stand (+ 2 m; Grossman and Fletcher, 1998) that retreated during the late Holocene.

Coralline algae, the primary compositional element of Kailua sands, are primary reef framework producers in high wave energy environments (Harney et *al*, 2000). High

coralline algae composition suggests that a strong wave environment is a major controlling factor on sediment production in Kailua Bay during the past 5000 yrs. Grossman (2001) and Rooney et *al.* (2004) analyzed drill cores from reef platforms exposed to strong modern north swell and concluded that positive fringing reef accretion was halted by an increase in wave energy ca. 5000 yr ago. Rooney et *al.* conclude the increase in northern swell ca. 5000 yr ago corresponds to amplification of El Nino/Southern Oscillation (ENSO), which is responsible for unusually large northern wave events in Hawaii during particularly strong El Nino episodes. It stands that sediment storage in Kailua Bay reflects a diminishing sediment production regime over the last 5000 years, brought on by stronger ENSO induced north swell and reduced accommodation space due to sea-level fall.

Benthic organism data collected at the Kailua sand channel by Harney (2003) shows a 50% decrease in living coral cover (57% to 7%) along the channel margin where depth decreases from 10 m to 3 m. This reduction in coral cover is the result of higher wave shear stress in shallower waters (Grossman, 2001) aided by higher suspended sediment concentrations. A combination of higher shear stress and less accommodation space likely led to reduced reef framework growth at shallow depths around windward Oahu (Grossman and Fletcher, 2004).

PREVIOUS SAND RESOURCE INVESTIGATIONS IN THE STUDY AREA

Onshore Resources: Inventory and mapping of sand resources in Kailua and Waimanalo began with Moberly and Chamberlain (1964). Kailua Bay, Lanikai, and Waimanalo Bay beach sands are described as very poorly sorted and highly calcareous. Offshore sand bodies are described as large but thin and patchy. Moberly et *al.* (1975) identify lithified eolianites in Kailua, Bellows, and Waimanalo as a potential source of beach sand. Moberly describes the deposits as the most extensive on windward Oahu, but adds that houses and beach parks cover a majority of these. As of 1975, island-wide deposits of lithified dune lacking development and available for mining were estimated at less than 2 x 10^6 m^3 (2.7 million yd^3). Existing modern vegetated dunes are mentioned, but considered a great deal more valuable intact than mined, as removed would yield

relatively small volumes of sand and have negative impacts on wildlife habitat and flood protection.

Pacific Rock & Concrete (PR&C) began crushing limestone mined in a Waimanalo quarry in the late 1960's. The intent of PR&C was to use the sand as material for beach replenishment (personal interview relayed by Casciano and Palmer, 1969).

Offshore Resources: Moberly et *al.* (1975) completed the first intensive survey of offshore sand resources around Oahu. Spatial extent of offshore sand fields was roughly mapped by aerial surveys. Major sand bodies from sea-level to 18 m depth were mapped for the Kailua and Waimanalo areas, however the survey of deeper sand bodies (18 m – 90 m) excluded the region between central Kailua and Koko Head. None of the areas selected for detailed thickness measurements were within the Kailua or Waimanalo regions.

Ocean Innovators (1978, 1979) completed a jet probe survey of the Kailua sand channel and an adjacent sand body for the U.S. Army Corps of Engineers in 1978. Jet probing was performed in a series of 13 transects perpendicular to the channel axis in depths of 5 to 24 m and 3 transects between 5 and 6 m in the adjacent sand body. Minimum volumes were estimated for the sand channel, 3.7×10^7 m^3 (4.84×10^7 yds^3), and the adjacent sand body, 2.08×10^6 m^3 (2.72×10^6 yds^3).

Surface and subsurface sampling in Kailua channel performed in the same locations revealed a variability in grain size, sorting and color with no discernable pattern. Median grain sizes of samples varied from fine to coarse sand (0.11 to 1.4 mm) with the percentage of samples finer than 0.15 mm varying between 1% and 81%. In only 7 out of 36 samples were less than 10% of the grains found to be finer than 0.15 mm. The average percentage of material finer than 0.15 mm was 38%. The color varied between slightly gray and yellow. Initial results indicated the sand channel contained very thick sand, in excess of 9 m in most instances and occasionally over 15 m. Sediment washed out by the jet probe initially appeared suitable for use in beach replenishment. However, subsurface samples analyzed by Casciano (US Army Corps of Engineers, 1978) concluded that the sand was highly stratified in terms of grain size and would ultimately be too fine for beach replenishment.

Sea Engineering (1993) conducted a beach nourishment viability study for the Hawaii Coastal Zone Management Program. The study synthesized all data taken on offshore sand resources around Oahu and scored each deposit based on site depth and wave exposure, interaction with adjacent littoral cells, deposit volume, and sediment grain size characteristics. Using these criteria it was concluded that the Kailua channel sand body was unsuitable for mining. The primary negative criteria were unsuitably fine grain sizes and the concern that reducing sediment volume in the channel posed a considerable risk to the stability of the immediate and adjacent littoral cells (Richmond, 2002).

Hampton et *al.* (2004) mapped sediment thickness in the Kailua sand channel using a tunable, swept-frequency (0.6 kHz to 3 kHz) acoustic profiler (see Barry et *al.* 1997 and Sea Engineering, 1993) supplemented by analysis of sediment recovered from 13 vibracores in 2000 and 14 vibracores in 1997. Thickness mapping in Kailua was performed in 60 -100 m of water. Sand deposits extend for about 4 km in an arc parallel to the Kailua reef front with a maximum thickness of 40 m, a mean thickness of 11 m, and is strongly skewed towards the smaller thickness. The total volume calculated for the deposit is 5.3 x 10^7 m^3 (6.9 x 10^7 yds^3). Grain size analysis of vibracored sediments revealed the sediment is finer than that which is usually used in beach replenishment. Compositional and abrasion analysis shows the sand has a low resistance to abrasion due to a high portion of *Halimeda* skeletal grains.

Conger et *al.* (in press) analyzes the surficial spatial distribution of benthic sand bodies across Oahu's insular shelf (to 20 m depth) at nine locations around Oahu, totaling 125 km^2 (39% of Oahu's shoreline). For each region, shallow benthic sand bodies are delineated, totaling 14,037 sand bodies for the study. Of the 125 km^2 of reef area studied 25 km^2 (~20%) was identified as sand, with a majority (64%) located in sand channels and fields. Sand bodies were classified in deposit shape classes by an automated classification algorithm accounting for a combination of individual shape characteristics such as area, orientation, and roundness. The resulting dataset of 14,037 sand body polygons was mapped to 2.4 m resolution, and each assigned a classification based on its shape.

A quantitative comparison of regional variations in sand bodies (number, shape, and size) to regional geomorphic setting (deep vs. wide reef) and wave climate (high,

medium, or low-energy) shows that the distribution of reef-top sediment is strongly influenced by reef geomorphology and, to a lesser extent, wave energy. Sand coverage is most extensive in two depth zones: <10 m depth zone (24% of total) and straddling the 10 m contour (72% of total). Conger et *al.* concludes that sand coverage is greatest in these regions because, the sub-10 m depth zone precludes the possibility of depressions being closed by modern reef growth due to high shear stress. Sand conduits crossing the 10 m depth contour provide both storage and transport between near and–offshore sand bodies. The 0-10 m depth range is also likely the zone of highest sediment production.

Reef types supporting the highest sand coverage are low wave-energy, have offshore sand bodies, and a wide shallow back reef. Least sand coverage is found in reefs with high wave-energy, no offshore sand bodies, and no wide shallow back reef. Study areas were categorized by sand coverage (highest to lowest): 1) Honolulu and Keehi Lagoon, 2) Lanikai and South of Laie Point, 3) Waianae, 4)Kailua, Kaneohe, Mokapu Point, and North of Laie Point. Lanikai is a medium-energy wide reef falling into the second highest category of sand coverage. Kailua is classified as a medium-energy deep reef falling into the lowest category of sand coverage.

Potential Effects of Sand Mining on Adjacent Beaches: The threat of increasing beach erosion through the mining of offshore sand bodies stems from the nature of a littoral cell as a naturally organized, interconnected, system of sand production, storage, and loss. An offshore sand body in Keauhou Bay, Hawaii was mined during 1977 as part of a two-month field test of a new sand mining and delivery system (Maragos et *al.,* 1977). A total of 10,000 m^3 of sand were mined from a sand body located 120 m offshore in 15 – 25 m of water. The sand body was 150 m wide by 300 m long and 6 m in thickness and surrounded by flourishing coral community. A detailed environmental survey was performed before, during, and after the mining operation, the results of which are presented in Maragos et *al.,* (1977). The study showed that mining sand had no immediate effect on nearby beaches at Kahaluu (1.5 km north) and Disappearing Sands (3.5 km north). It was noted that there exists no clear pathway between the sand deposit mined and either beach, suggesting that the mining of well-isolated and distant sand fields will not have an effect on nearby coastlines. Sea Engineering's 1993 sand resource viability study considered sand deposits offshore of a rocky shoreline and with low

proximity to a local beach littoral cell to be less hazardous mining objectives than deposits offshore of a sand beach near an active littoral sediment cell (Sea Engineering, 1993).

Moberly and Chamberlain (1964) state that sand channels potentially support circulation that delivers sand to adjacent beaches, seaward into deeper water, or a seasonal exchange between sand channels and the beach. Cacchione and Tate (1998) noted in a study of Kailua sand transport that fossil channels almost always connect to both nearshore and offshore sand fields and act as conduits for sand movement in both onshore and offshore directions. Cacchione and Tate showed sand ripples in the Kailua sand channel migrate shoreward at a rate of 0.5 m/day during trade wind conditions and seaward at a rate of 0.5 m/day during winter swell conditions. This is supported by common observations of sand ripples and well-sorted sediments fining in shoreward direction, both signs of active transport occurring between deep and shallow fields at the terminal ends of the channel. Special consideration should be taken with regard to removing sand from this type of sand body as sediment supply to a pre-existing shore face or littoral cell could be diminished (Cox, 1975; Dollar, 1979).

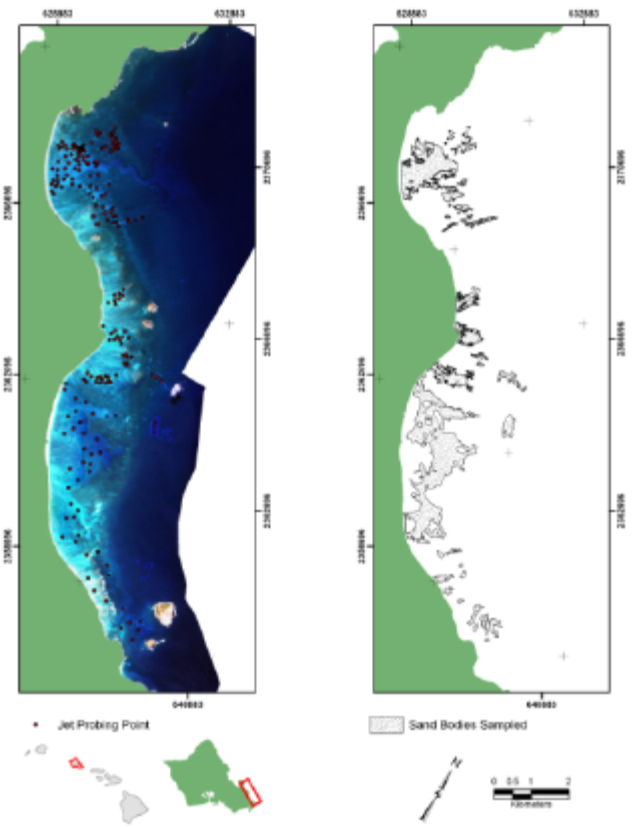

Figure 3. a) 205 jet probe measure were taken in the study area. b) 54 sand bodies are delineated for study.

MATERIALS AND METHODS

Boundaries of 54 sand bodies (Figure 3) in the study area were delineated for study using satellite imagery, LIDAR bathymetry, benthic slope maps (a product of LIDAR), NOAA benthic habitat maps, and sand classification maps produced by Conger et *al.*, 2005. Sand bodies were classified by morphology (Figure 4). Sampling with a jet probe (Figure 5) provided a total of 205 measurements of sand thickness. Thickness interpolation and griding of point data is accomplished using Kriging and Voronoi methods. Volumes estimates are calculated with for all sand bodies.

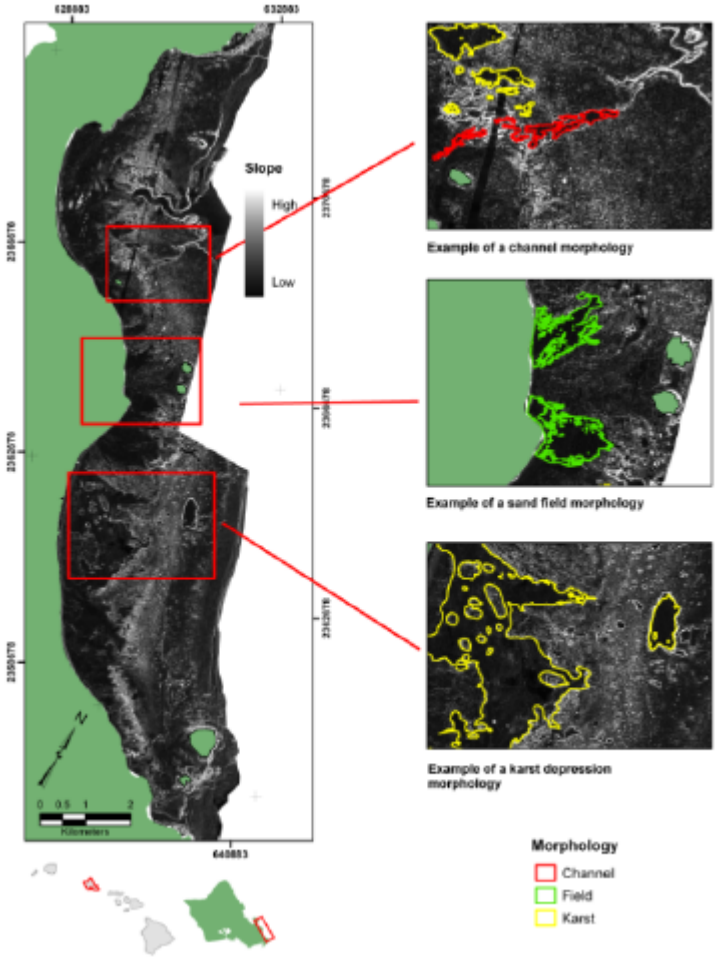

Figure 4. A slope map created from LIDAR bathymetry assists in classification of sand body morphology.

Morphology Classification: Conger (2006) determined antecedent topography to be the primary control on morphology of reef top sand bodies. Karstification of the carbonate platform during periods of lower sea-level creates depressions which, once flooded, serve as basins that accumulate sand. Variations in relief, shape, and orientation of depressions are likely due to differing processes of karstification.

Following the work of Conger, a generalized morphology classification has been created for this study. Sand bodies sampled are classified as one of three morphologies: Sand Field, Fossil Channel, or Karst Depression. Variance in topographic relief, distribution of thickness, and generalized shape are used as major distinguishing factors used to classify sand body morphologies. Segregating sand bodies in this manner adds a

morphology component to the process of interpolating measured thicknesses and constructing a coverage map of estimated thickness, thereby increasing estimation confidence.

In addition to field observations, slope maps generated from LIDAR bathymetry were used to evaluate the topographic relief between the reef platform and the surface of the sand body. Figure 4 illustrates distinctions between morphologies by highlighting examples on a slope map of the study area. Table 1 summarizes sand body morphology classifications and location.

NUMBER of SAND BODIES	Fossil Channel	Karst Depression	Sand Field	Total
Kailua Bay	7	26	0	33
Lanikai	1	3	4	8
Waimanalo Bay	0	5	8	13
Total	8	34	12	54

Table 1. Number of sand bodies organized by morphology (columns) and region (rows).

Sand Fields: Sand fields are defined, in this study, as areas of continuous sand cover deposited over a broad topographic swale in the reef platform. Boundaries generally have little to no topographic relief and irregular borders. Sand fields are generally found near to shore in shallow (0 - 5.0 m) areas, have broad landward openings toward the beach face that separate and thin into separate fingers of sand that continue seaward and terminate on shallow reef locations. Of the 54 sampled sand bodies, a total of 13 were designated as sand fields.

Fossil Channel: Fossil channels are seaward extensions of watershed systems, incised into the carbonate shelf during low sea-level stands. The high topographic relief of the channel allows fossil channels to act as effective traps for littoral sediment. Channels in Kailua and Waimanalo are typically shore-normal in orientation and cross the –10 m isobath. Major channels, such as the Kailua sand channel, have steep walls of fossil reef and widen shoreward into large sand fields that lack significant bounding relief. Shoreward transition from bounding walls to a more gradual surface occurs in water shallower than 5 m, at which point sand is no longer confined to a channel and spreads

out into a sand field. Large sand channels can contain sediment over 9 m thick (Ocean Innovations, 1978) and remain thickest along the axis of the channel, thinning to 1.0 – 1.5 m at the margins and adjoining landward field. Of the 54 sampled sand bodies, a total of 7 were designated as fossil channels.

Karst Depression: Karst depressions are similar to fossil channels in that they are likely the result of subaerial exposure causing a sinkhole style karst incision. They differ from fossil channels in that they occupy smaller areas, have no dominant orientation, and do not serve as a connection between sand fields. Karst depressions have steep boundaries, generally dropping 1-3 m below the carbonate platform thus distinguishing them from sand fields. Of the 54 sampled sand bodies, a total of 34 were designated as karst depressions.

***Thickness Measurements*:** Sediment thickness measurements were obtained with a jet probe (Figure 5) deployed from a small boat, and operated by a researcher on SCUBA. The jet probe is built from a small diameter pipe connected to a shipboard water pump via fire hose. High-pressure water is pumped out of the pipe in order to displace sediment as the SCUBA diver pushes it into sandy substrate. The probe stops penetrating when it contacts a boundary with bedrock or an impenetrable layer of consolidated sediment. The depth of penetration provides a measure of unconsolidated sediment thickness. The probe length is 3.0 m. If the sand

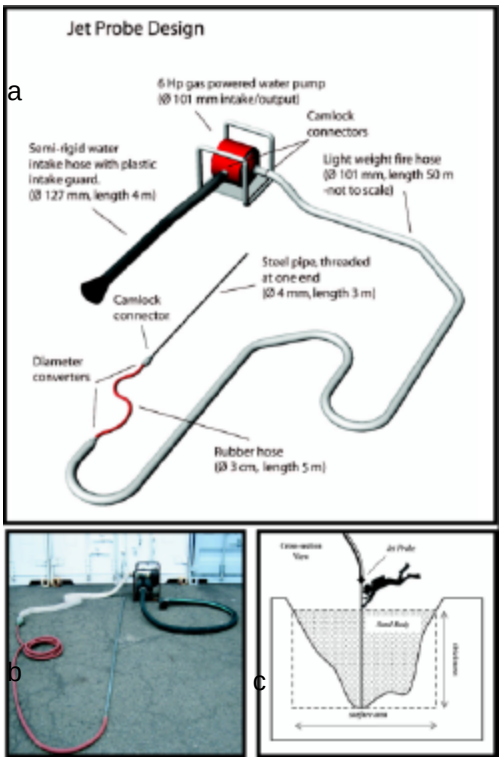

Figure 5. a) Jet probe schematic. b) Jet Probe. c) The jet probe is inserted into sand bodies until it ceases to penetrate. Thickness is measured in 10 cm increments off the probe.

body thickness exceeds 3.0 m, the value of 3.1 m is recorded. Appendix B contains tabulated jet probing results.

Sampling Locations: Using the jet probe, a total of 205 thickness measurements were obtained from 54 distinct sand bodies on the Kailua, Lanikai, and Waimanalo reef platforms. At each sample location 3 thickness measurements were taken within a 20 m radius of the anchored boat and the average thickness recorded for that site. Water depth at sample locations was recorded from a hull-mounted fathometer at an accuracy of +/- 0.5 m. Water depth varied from 1.5 m to 16.8 m, with an average of 5.2 m. General sediment characteristics were noted at each site. The probe was completely removed and inserted multiple times with each measurement to insure repeatable results. All sample locations were predetermined by examining aerial photos and bathymetry in conjunction with NOAA benthic habitat maps (Coyne et *al.*, 2002) and previous substrate studies in the region (Sea Engineering, 1997; Conger et *al.*, 2006). Survey points were located with a GPS receiver at an accuracy of +/- 5 m. Once anchored, drift of the boat was adjusted to match sample location so a diver could use the boat as a reference point for placing the jet probe. Figure 3 illustrates jet probe sample locations and sand body delineation.

Volume Calculations: Estimates of sand volume were obtained for each sand field by using one of two methodologies: 1) a Kriging method or 2) a Voronoi method with a volume correction factor. The selection of either methodology was based on the spatial density of available thickness measurements as well as the size and complexity of the given sand body. In instances of good data coverage a Kriging method was used. The Voronoi method was used for sand bodies with sparse coverage, where a single measurement must be representative of a large area, as it does not require a high data density. A total of 54 sand bodies are analyzed; Kriging was applied to a 9 sand bodies while the Voronoi model was applied the remaining 45 bodies. Table 2 summarizes sand body morphologies as applied to each methodology. Appendix C contains details on all volume estimations.

	MORHOLOGY			
D	Channel	Field	Karst	Total

Kriging	1	5	4	9
Voronoi	6	8	30	45
Total	7	13	34	54

Table 2. Summary of interpolation methods (column) applied to sand body morphologies classes.

Reporting of Volumes: In order to make volume estimates a more useful product, volume is not reported over the entire surface of every sand body sampled. In areas were the Kriging method could be used, volume was only calculated for the areas of greatest thickness (> 0.50 m). Similarly, volume results are given in a section-by-section basis for sand bodies using the Voronoi method. In many cases a single sand body, identified by a Sand Body ID, is broken into multiple sections, each reported as an Area ID. Volumes are reported for each Area ID individually. Table 3 summarizes volume estimations by region and Table 4 summarizes measured area of sand bodies. A series of maps and tables detailing thickness and volume estimations are included in Appendix A.

VOLUME (m^3)	Channel	Error	Karst	Error	Field	Error	Total	Error
Kailua Bay	825,115	75,056	150,715	15,244	0	0	975,830	90,300
Lanikai	23,616	5,432	43,703	9,719	129,987	3,089	197,306	18,240
Waimanalo Bay	0	0	504,396	47,999	20,136	1,660	524,532	49,659
Total	848,731	80,488	698,814	72,962	150,123	4,749	1,697,668	158,199

Table 3. Volume estimates with error in cubic meters presented as morphology class (column) and region (row).

AREA (m^2)	Fossil Channel	Karst Depression	Sand Field	Total
Kailua Bay	668,701	290,399	0	959,100
Lanikai	67,923	169,469	1,148,858	1,386,251
Waimanalo Bay	0	653,341	235,144	888,485
Total	736,624	1,113,209	1,384,002	3,233,836

Table 4. Sand body surface area presented as morphology class (column) and region (row).

***Kriging Method*:** The Kriging approach is a more statically robust method of estimation than the Voronoi method and was preferentially used whenever data density was suitable. Boundaries of sand bodies are assumed to be zero thickness and were represented by

points of zero thickness generated at 1 m spacing around each sand body. Modeling the variation between measurement points and the edges was accomplished with a semi-variogram. A semi-variogram model quantifies the relationship between variability of a native dataset and spatial location as an equation for a line. The equation for each semi-variogram model is used to model the rate of change between points where thickness is known, i.e. jet probe thickness measurements and edges (Webster and Oliver, 2001). In this usage, the changing slope of the semi-variogram line is analogous to the changing slope of the reef-top depression.

A separate variogram equation was produced for each sand body so that the thickness model would be individualized to the unique characteristics of each body. A spherical semi-variogram model was used in all cases. Points of zero thickness along the edge were included when producing semi-variogram. Rasterized thickness estimation maps were created at a resolution of 1 m. Volume calculations were made for areas of sediments estimated to be >0.50 m thick, each reported as a separate Area ID. Thickness and volume calculation results are presented in Appendix A.

Voronoi Method: The Voronoi method assumes that sand body thickness is perfectly uniform up to the edge of the sand body. See Figure 5 for an illustration of the method. This method is used when thickness data is too sparse for a Kriging approach to be useful. Perimeters of each sand body and thickness measurements were mapped and entered into ArcGIS. An ArcGIS Voronoi function was used to subset each sand body into series of smaller adjoining polygons or sub-polygons; each sub-polygon formed around a single thickness measurement. The Voronoi function draws sub-polygon boundaries so that any location within a given sub-polygon is closer to its associated measurement point than to the measurement point of any other sub-polygon (Webster and Oliver, 2001).

The sediment thickness within each sub-polygon is assumed to be the same as the thickness measurement it contains. Volume of sediment is calculated for each sub-polygon as the product of the area and thickness. The volumes for all sub-polygons within a single sand body are summed to calculate a total sediment volume for the entire sand field (see Appendix C). Afterwards, a correction is applied to account for over-

estimation of volume. Sub-polygons created by this process form the boundaries for the individual Area ID's.

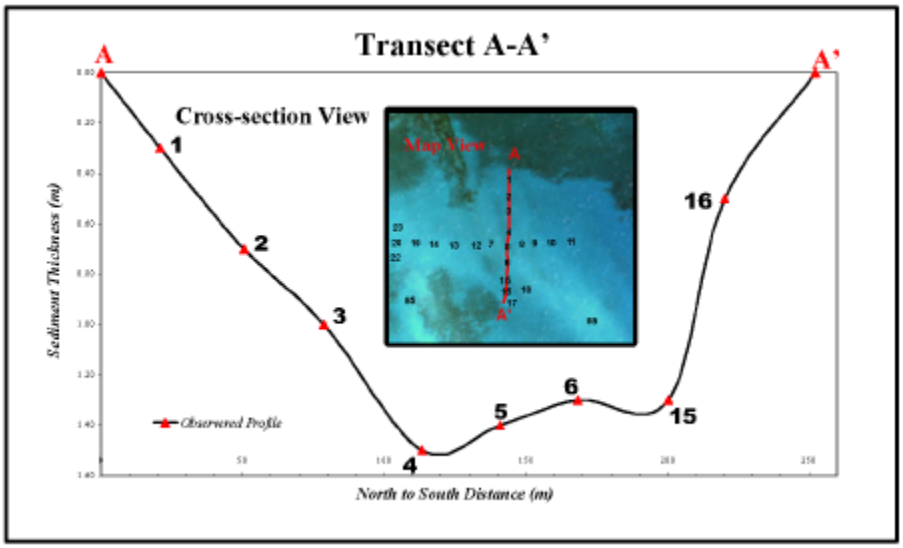

Figure 6. Kailua Bay. Thickness profile generated from a transect of point measurements. Note the thickness irregularity in sand bodies.

Voronoi Volume Correction: A major source of uncertainty with the Voronoi model is the assumption that the walls of reef top depressions are at right angles to the base of the depression. A transect of thickness measurements (transect A-A' in Figure 6) from Kailua Bay suggests that sand bodies are thickest in the center and gradually thin toward the edges.

Given the high range of variability in sand body thickness, failing to account for sand body morphology likely produces an over-estimate of sand volume. Correction of over-estimated sand volumes is accomplished by calculating an empirically derived reduction factor. Reduction factors are calculated as the average percent difference between Kriging and Voronoi estimations performed on the same set of sand bodies. Results from comparative volume estimations of 10 sand bodies are segregated by sand body morphology and averaged so as to calculate reduction factors that are morphology specific.

Of the 10 bodies used, 4 were classified as sand fields, while the remaining 6 were classified as karst fields. No bodies classified as channel morphology were used due to a lack of adequate examples, however the assumption is made that channel and karst morphologies share similar aspects of genesis, possess similar subsurface-

topography, and thus can utilize the same reduction factor. The reduction factor calculated for sand field morphologies is 88.25% ±8.25% (i.e. Voronoi estimations are reduced by 88.25% ±8.25%), while 64.67% ±23% is used for karst and channel morphologies. Uncertainty calculation is described below, in the section *Prediction Uncertainty.* These reduction factors cause dramatic decreases when applied to the Voronoi-based volume estimates, but provide a more informed and realistic estimate.

Prediction Uncertainty: Measurement uncertainties are ±5 cm vertical uncertainty associated with jet probe measurement and ±5 m of horizontal uncertainty associated with accuracy of the GPS receiver. These uncertainties are taken into account during the Kriging process as a nugget variable and thus are propagated through the interpolation process as a pixel-by-pixel error value. Therefore, every map of estimated volume created via Kriging also has a map of the pixel-by-pixel estimation uncertainty in meters. Areas defined for volume estimations are used with error maps to calculate the error in volume estimation for each area.

Percent difference between estimated volume and estimated error was calculated for each sand body. These percent differences were averaged simultaneously with values used for calculating the reduction factors, resulting in the uncertainty values reported for Voronoi estimates. The error results are presented as tables in the maps of estimated sediment volumes (Appendix A).

RESULTS AND DISCUSSION

Fossil Channel: Of the 54 sampled sand bodies, 8 were classified as fossil channels. Fossil channels are estimated to contain 848,731 +/-80,488 m^3 of sediment and cover an area of 736,624 m^2. The average volume-to-surface area ratio is 1.15 m^3/m^2, the highest ratio in the study area. Most sediment in this morphology class is contributed by the Kailua sand channel, of which only the shoreward section is being considered in this study. Previous jet probe studies in the deeper channel have shown sediment thickness to exceed 3.0 m. In southern Kailua, a group of smaller channels form the fragmented

remnants of what is most likely a channel closed by reef growth. Another smaller intact channel exists in Lanikai, but does not connect with a significant shoreward sand body.

Defining a specific morphology for the shoreward end of the Kailua sand channel is difficult as the channel widens landward, losses the high bounding topographic relief, and transitions into sand field type morphology. However, a linear trace of high thickness continues landward through the sand field along the central axis of the channel. This indicates that the shoreward portion of the channel has been filled and overtopped by sand, producing a sand body that qualifies as both a channel and a field. For the purpose of estimating sand volume the Kailua sand channel is considered a member of channel morphology class.

Sand deposits in fossil channels tend to be consistently thick and yellow to white coloration. Surface sediments in these channels appear medium- to coarse-grained, however subsurface sampling in the Kailua channel has shown significant amounts of fine-grained sediment (US Army Corps of Engineers, 1978). Channels likely serve as surge channels for waves breaking over the fringing reef. The focusing of wave energy through these channels would cause preferential grain sorting as grains transported, leaving a varied stratigraphy of fine and coarse sediments related to variations in transport energy.

Sand Field: Of the 54 sampled sand bodies, 12 were classified as sand fields. Sand fields are estimated to contain 150,123 +/-4,749 m^3 of sediment and cover an area of 1,384,002 m^2. The average volume-to-surface area ratio is 0.11 m^3/m^2, the lowest ratio in the study area.

Sediment thickness tends to grade from 0.5 m near to shore thickening to over 3.0 m near the seaward edge. Sediments are fine to medium sand with a mixture of sandy and gravelly substrata. Nearshore sand fields are generally connected to the adjacent beach where they potentially function as sediment storage and source locales participating is volume fluctuations on the beach.

Karst Depressions: Of the 54 sampled sand bodies, 34 are classified as karst depressions. Karst depressions are estimated to contain 695,814 +/-47,999 m^3 of sediment and cover

an area of 1,113,209 m^2. The average volume-to-surface area ratio is 0.63 m^3/m^2, the mid-range ratio in the study area.

Sediments in karst depressions are observed to contain one or both of two characteristic strata: 1) medium to coarse light-colored sand and 2) coral gravel varying between 5 cm fragments to hand-sized branches. Sediment bodies in karst depressions consist of either 1.0 – 2.0 m thick sand, 0.5 – 1.0 m sand overlaying coral rubble, or an absence of sand with coral rubble outcropping on the surface. Coral rubble deposits were not included in thickness and volume analysis. Sandy bodies without coral rubble tend to lie directly on fossilized reef platform.

Coral accretion on the perimeter of karst depressions suggests Holocene growth has shrunk the area of many depressions, possibly isolating one large depression into a number of smaller depressions. Sediment produced on the reef is thought to be transported to the beach in a series of steps between depressions (Moberly and Chamberlain, 1964) making karst depressions a potentially important component of shallow (3.0 – 5.0 m depth) sediment storage in the littoral system.

An expansive system of interconnected, sand-filled karst depressions dominates the topography of the central-south Waimanalo area. This feature resembles a sandy lagoon in that it runs shore-parallel between a fringing reef and outcropping back reef in 4-7 m of water. Sediment thickness is greatest in two isolated semi-circular areas. The lack of any linear zones of thickness exclude this feature from consideration as a channel feature.

CONCLUSIONS

Jet probing of shallow sand bodies allows volume estimates to be made for a total of 54 sand bodies. Sand channels appear to have the greatest overall volume-to surface area ratio (1.15 m^3/m^2), however if data from the Kailua sand channel is excluded, the ratio drops to 0.29 m^3/m^2, indicating that the volume of sediment infilling channels in the study area varies greatly. Most sand channels in the study area lack the size, continuality, and terminal sand fields of the Kailua sand channel. Absence of a major terminal sand body attached to either end of the smaller channels most likely indicates a lack of active transport, which could account for low volume relative to the larger Kailua sand channel.

Karst depressions have a volume-to surface area ratio of 0.63 m^3/m^2 and lack major anomalies such as the Kailua sand channel. The relative abundance of karst depressions in the study area suggests that karst depressions play a major role in reef-top sand storage. Sand fields have the lowest volume-to-surface area ratio (0.11 m^3/m^2). Given that a lack of significant confining topographic relief is the differentiating feature for sand fields, it is likely that topography is the foremost control in reef-top sand storage.

APPENDICES

A. Maps of Sediment Thickness and Volume Estimates

B. Tabulated Jet Probing Results

C. Tabulated Sediment Thickness and Volume Estimates

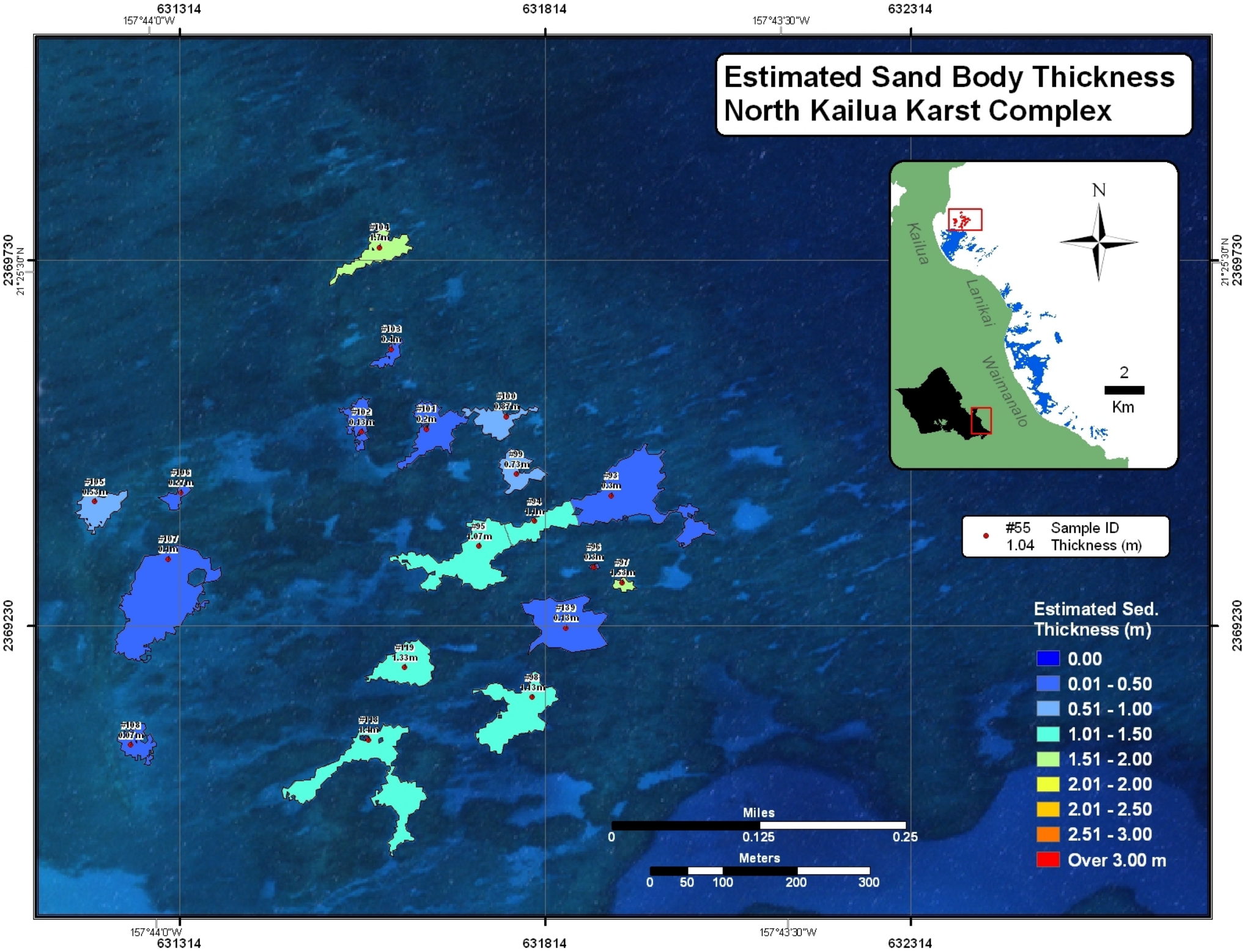
Estimated Sand Body Thickness
North Kailua Karst Complex
631314
631814
632314
157°44'0"W
157°43'30"W
2369730
2369230
21°25'30"N
#104
0.7m
#103
0.4m
#102
0.13m
#101
0.2m
#100
0.87m
#99
0.73m
#93
0.8m
#94
1.1m
#95
1.07m
#96
0.8m
#97
1.23m
#105
0.55m
#106
0.27m
#107
0.4m
#89
0.43m
#119
1.33m
#98
1.43m
#108
0.07m
#118
1.4m
N
Kailua
Lanikai
Waimanalo
2
Km
#55 Sample ID
1.04 Thickness (m)
Estimated Sed. Thickness (m)
0.00
0.01 - 0.50
0.51 - 1.00
1.01 - 1.50
1.51 - 2.00
2.01 - 2.00
2.01 - 2.50
2.51 - 3.00
Over 3.00 m
Miles
0
0.125
0.25
Meters
0
50
100
200
300

Estimated Sediment Volume
North Kailua Karst Complex

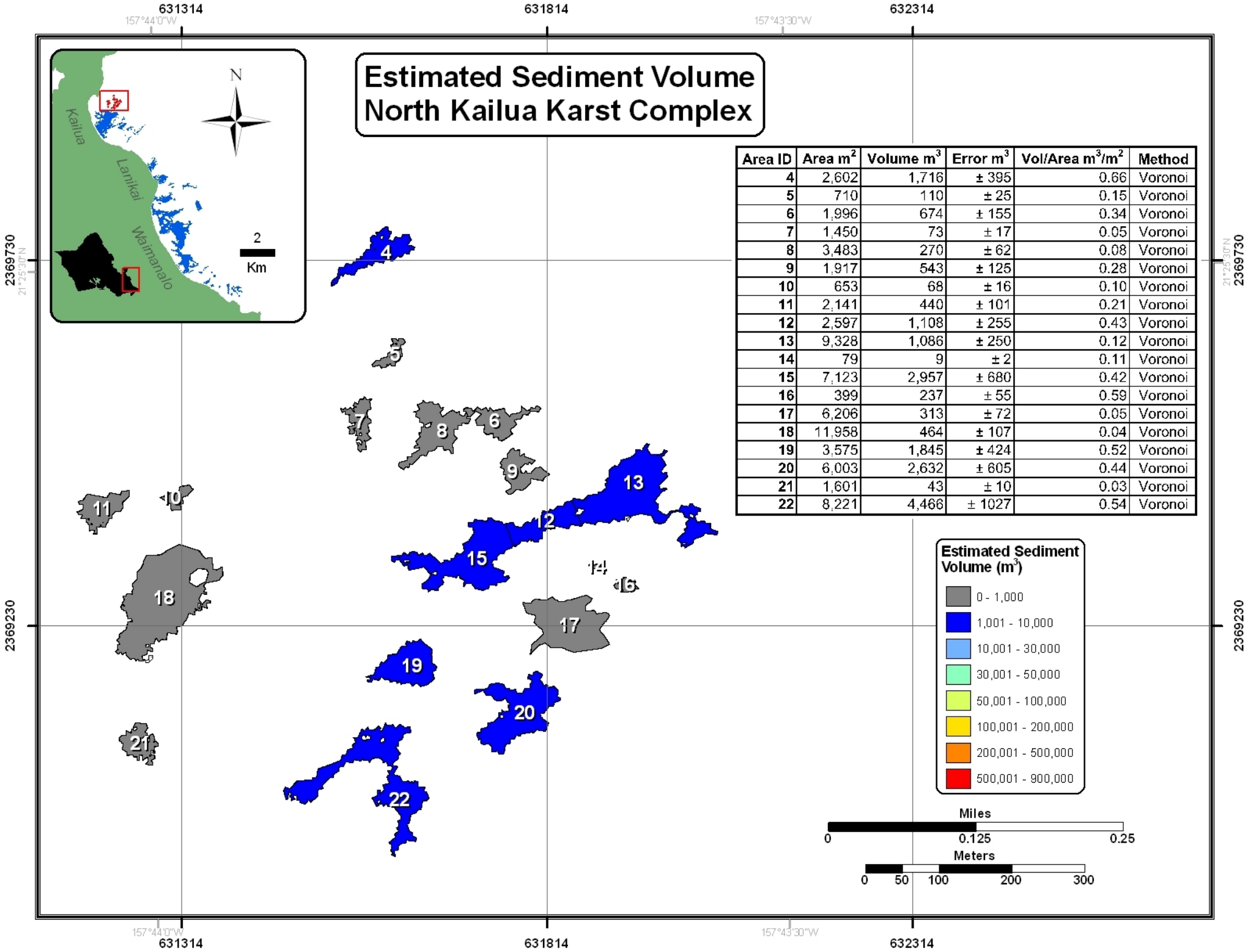

Area ID	Area m^2	Volume m^3	Error m^3	Vol/Area m^3/m^2	Method
4	2,602	1,716	± 395	0.66	Voronoi
5	710	110	± 25	0.15	Voronoi
6	1,996	674	± 155	0.34	Voronoi
7	1,450	73	± 17	0.05	Voronoi
8	3,483	270	± 62	0.08	Voronoi
9	1,917	543	± 125	0.28	Voronoi
10	653	68	± 16	0.10	Voronoi
11	2,141	440	± 101	0.21	Voronoi
12	2,597	1,108	± 255	0.43	Voronoi
13	9,328	1,086	± 250	0.12	Voronoi
14	79	9	± 2	0.11	Voronoi
15	7,123	2,957	± 680	0.42	Voronoi
16	399	237	± 55	0.59	Voronoi
17	6,206	313	± 72	0.05	Voronoi
18	11,958	464	± 107	0.04	Voronoi
19	3,575	1,845	± 424	0.52	Voronoi
20	6,003	2,632	± 605	0.44	Voronoi
21	1,601	43	± 10	0.03	Voronoi
22	8,221	4,466	± 1027	0.54	Voronoi

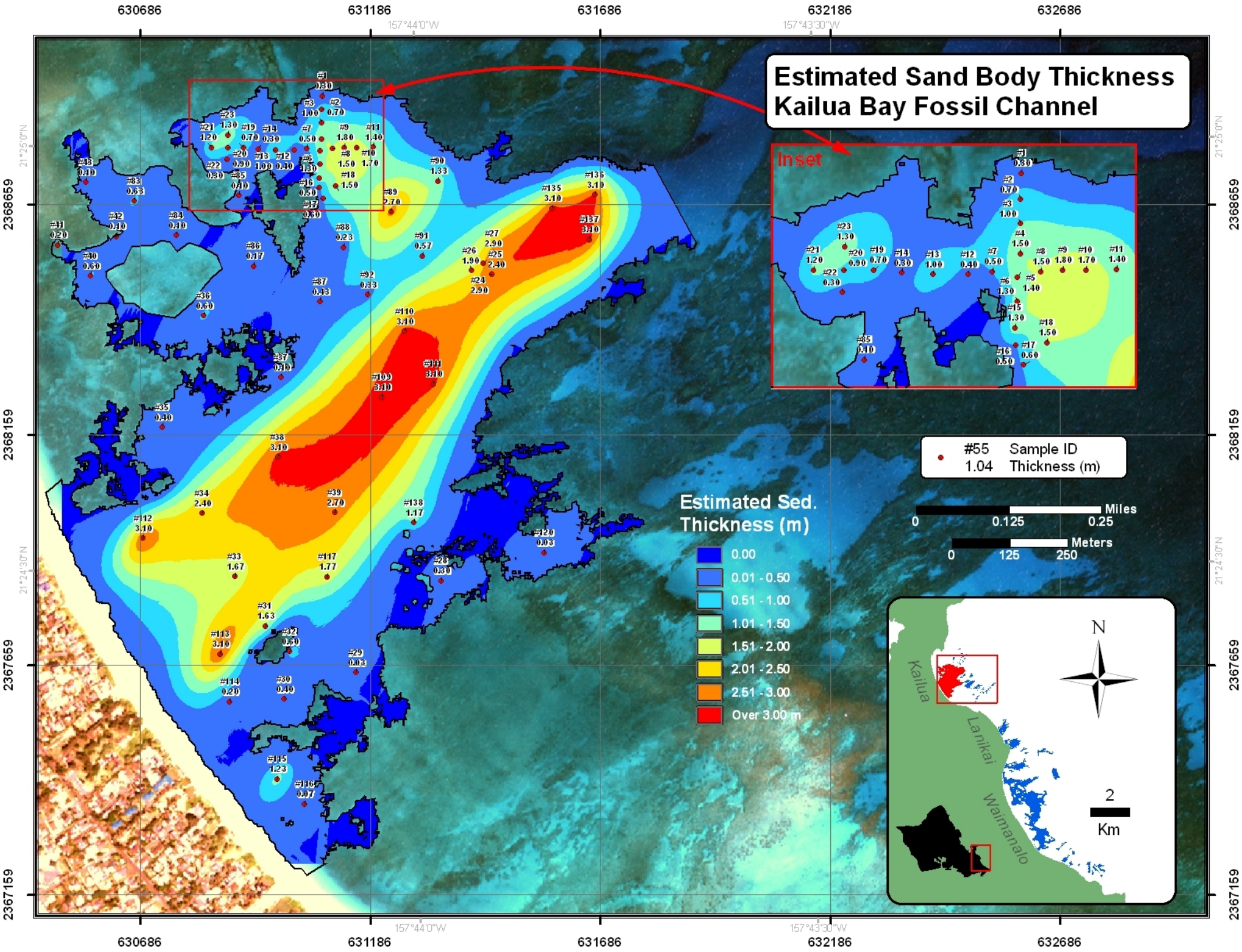
Estimated Sand Body Thickness
Kailua Bay Fossil Channel
Inset
Estimated Sed. Thickness (m)
0.00
0.01 - 0.50
0.51 - 1.00
1.01 - 1.50
1.51 - 2.00
2.01 - 2.50
2.51 - 3.00
Over 3.00 m
#55 Sample ID
1.04 Thickness (m)
Miles
0 0.125 0.25
Meters
0 125 250
N
Kailua
Lanikai
Waimanalo
2
Km
630686
631186
631686
632186
632686
2368659
2368159
2367659
2367159
157°44'0"W
157°43'30"W
21°25'0"N
21°24'30"N

Estimated Sediment Volume
Kailua Bay Fossil Channel

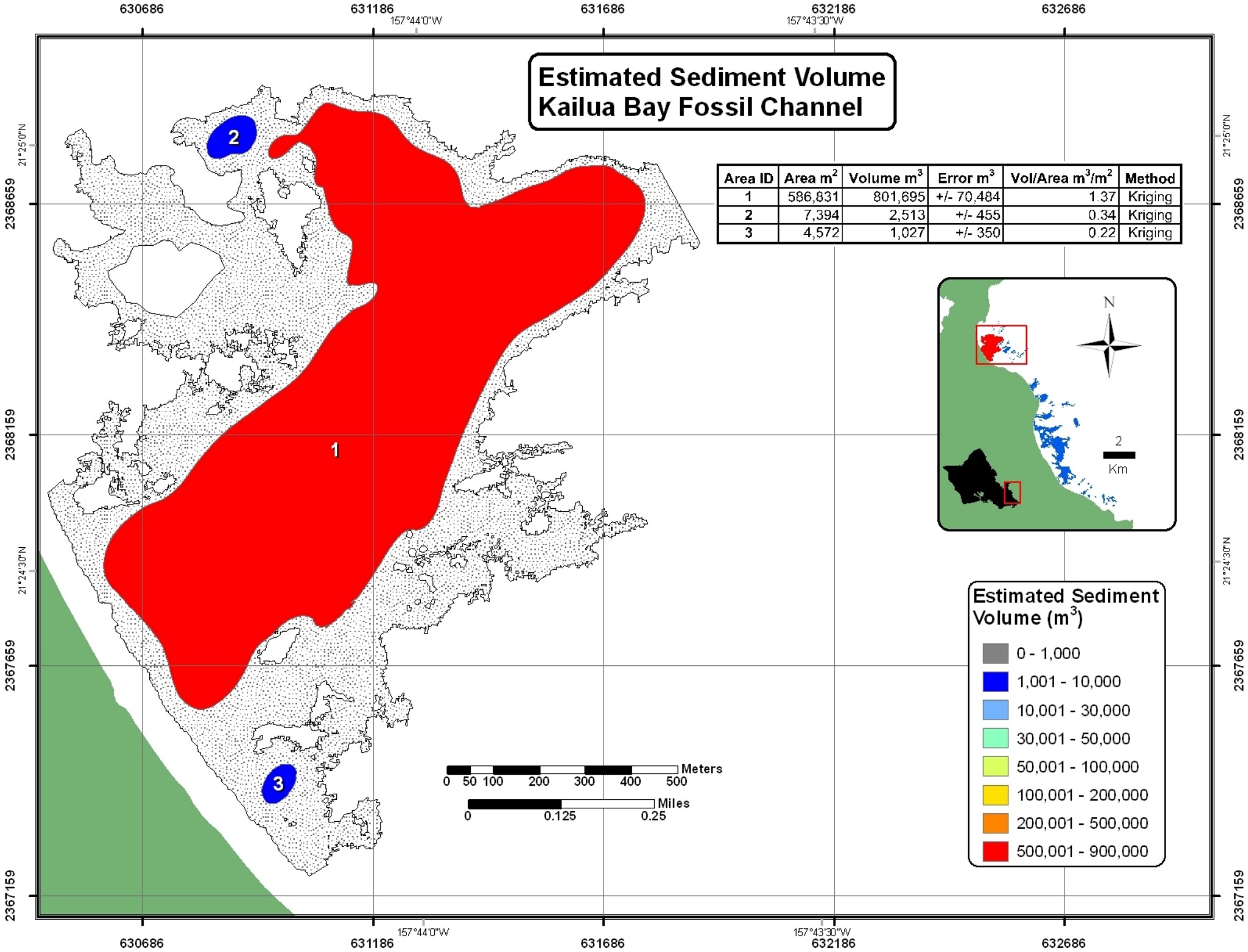

Area ID	Area m^2	Volume m^3	Error m^3	Vol/Area m^3/m^2	Method
1	586,831	801,695	+/- 70,484	1.37	Kriging
2	7,394	2,513	+/- 455	0.34	Kriging
3	4,572	1,027	+/- 350	0.22	Kriging

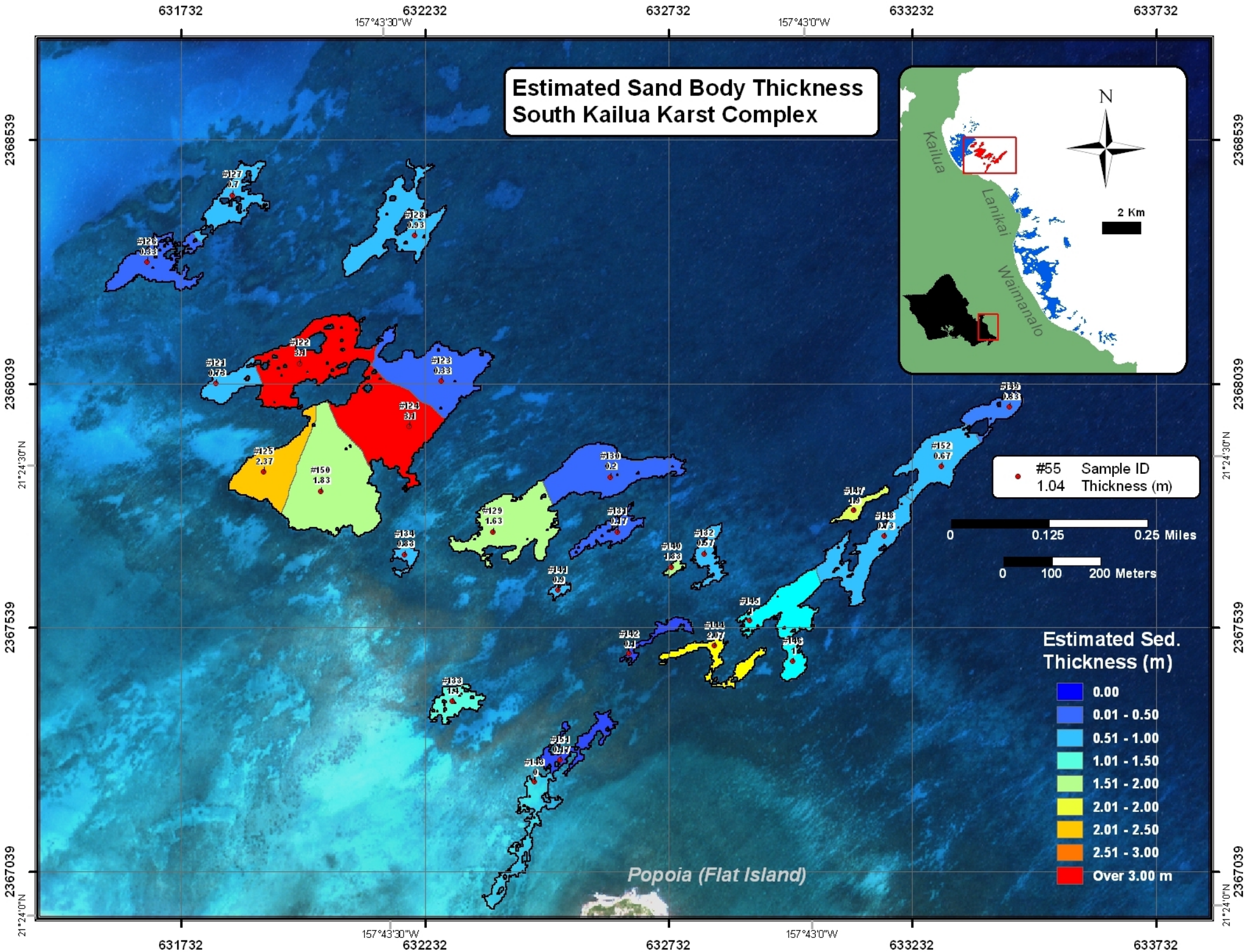
Estimated Sand Body Thickness
South Kailua Karst Complex
631732
632232
632732
633232
633732
157°43'30"W
157°43'0"W
2368539
2368039
2367539
2367039
21°24'30"N
21°24'0"N
N
Kailua
Lanikai
Waimanalo
2 Km
#55 Sample ID
1.04 Thickness (m)
0
0.125
0.25 Miles
0
100
200 Meters
Estimated Sed. Thickness (m)
0.00
0.01 - 0.50
0.51 - 1.00
1.01 - 1.50
1.51 - 2.00
2.01 - 2.00
2.01 - 2.50
2.51 - 3.00
Over 3.00 m
Popoia (Flat Island)

Estimated Sediment Volume South Kailua Karst Complex

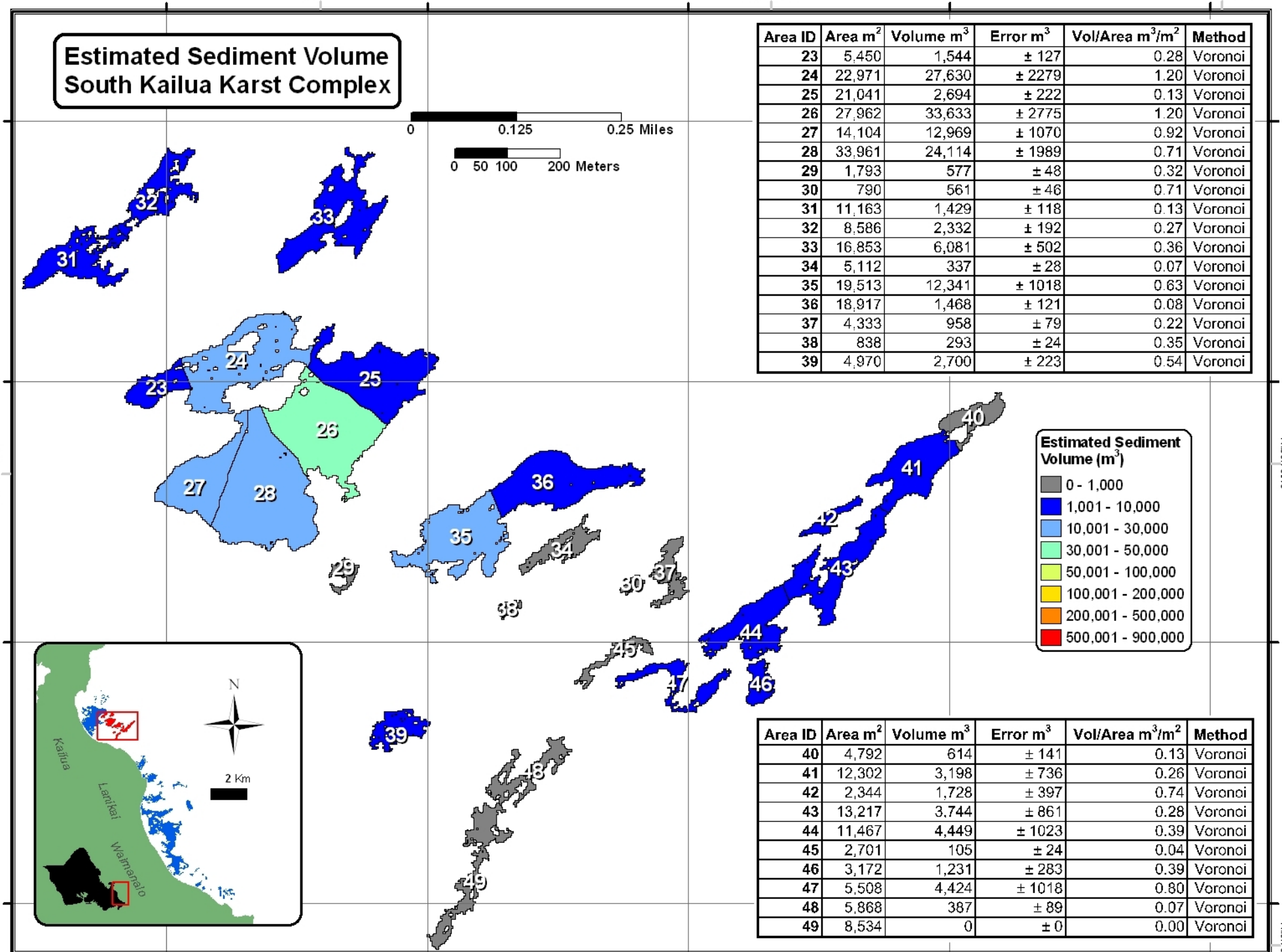

Area ID	Area m^2	Volume m^3	Error m^3	Vol/Area m^3/m^2	Method
23	5,450	1,544	± 127	0.28	Voronoi
24	22,971	27,630	± 2279	1.20	Voronoi
25	21,041	2,694	± 222	0.13	Voronoi
26	27,962	33,633	± 2775	1.20	Voronoi
27	14,104	12,969	± 1070	0.92	Voronoi
28	33,961	24,114	± 1989	0.71	Voronoi
29	1,793	577	± 48	0.32	Voronoi
30	790	561	± 46	0.71	Voronoi
31	11,163	1,429	± 118	0.13	Voronoi
32	8,586	2,332	± 192	0.27	Voronoi
33	16,853	6,081	± 502	0.36	Voronoi
34	5,112	337	± 28	0.07	Voronoi
35	19,513	12,341	± 1018	0.63	Voronoi
36	18,917	1,468	± 121	0.08	Voronoi
37	4,333	958	± 79	0.22	Voronoi
38	838	293	± 24	0.35	Voronoi
39	4,970	2,700	± 223	0.54	Voronoi

Area ID	Area m^2	Volume m^3	Error m^3	Vol/Area m^3/m^2	Method
40	4,792	614	± 141	0.13	Voronoi
41	12,302	3,198	± 736	0.26	Voronoi
42	2,344	1,728	± 397	0.74	Voronoi
43	13,217	3,744	± 861	0.28	Voronoi
44	11,467	4,449	± 1023	0.39	Voronoi
45	2,701	105	± 24	0.04	Voronoi
46	3,172	1,231	± 283	0.39	Voronoi
47	5,508	4,424	± 1018	0.80	Voronoi
48	5,868	387	± 89	0.07	Voronoi
49	8,534	0	± 0	0.00	Voronoi

Estimated Sediment Volume
Lanikai Sand Fields and Karst Depressions

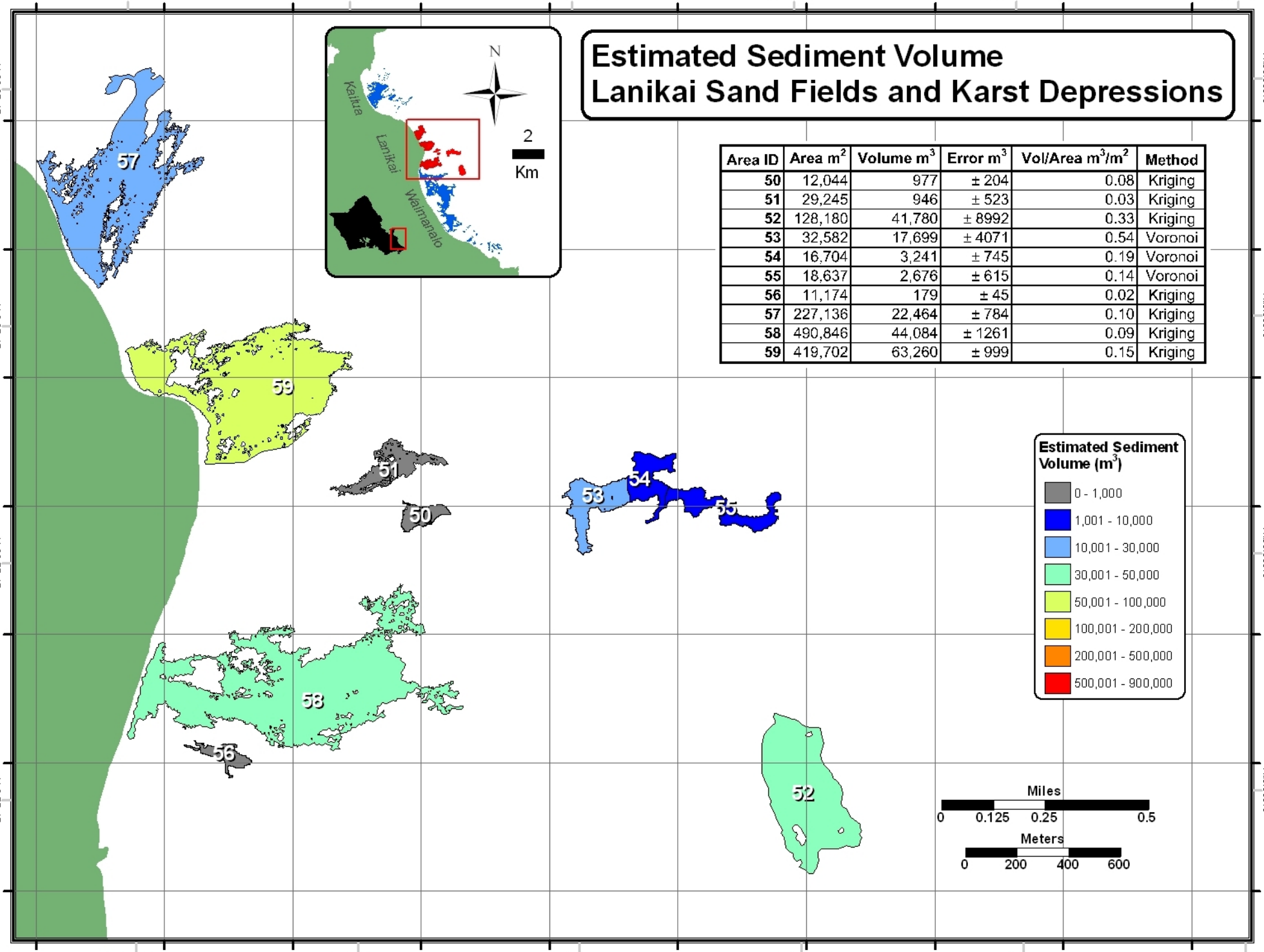

Area ID	Area m^2	Volume m^3	Error m^3	Vol/Area m^3/m^2	Method
50	12,044	977	± 204	0.08	Kriging
51	29,245	946	± 523	0.03	Kriging
52	128,180	41,780	± 8992	0.33	Kriging
53	32,582	17,699	± 4071	0.54	Voronoi
54	16,704	3,241	± 745	0.19	Voronoi
55	18,637	2,676	± 615	0.14	Voronoi
56	11,174	179	± 45	0.02	Kriging
57	227,136	22,464	± 784	0.10	Kriging
58	490,846	44,084	± 1261	0.09	Kriging
59	419,702	63,260	± 999	0.15	Kriging

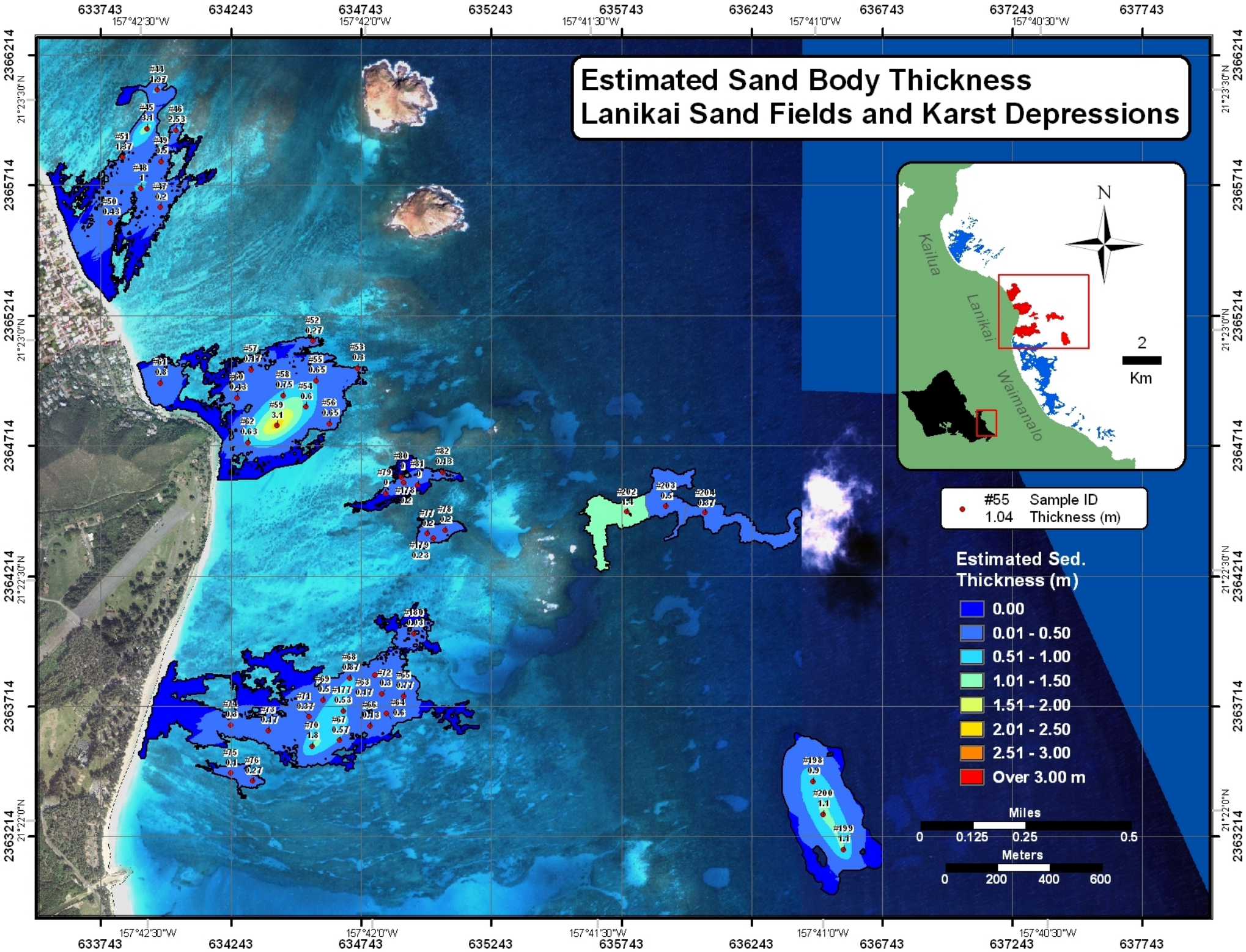
Estimated Sand Body Thickness
Lanikai Sand Fields and Karst Depressions
633743
634243
634743
635243
635743
636243
636743
637243
637743
157°42'30"W
157°42'0"W
157°41'30"W
157°41'0"W
157°40'30"W
2366214
2365714
2365214
2364714
2364214
2363714
2363214
21°23'30"N
21°23'0"N
21°22'30"N
21°22'0"N
N
Kailua
Lanikai
Waimanalo
2
Km
#55 Sample ID
1.04 Thickness (m)
Estimated Sed. Thickness (m)
0.00
0.01 - 0.50
0.51 - 1.00
1.01 - 1.50
1.51 - 2.00
2.01 - 2.50
2.51 - 3.00
Over 3.00 m
Miles
0
0.125
0.25
0.5
Meters
0
200
400
600

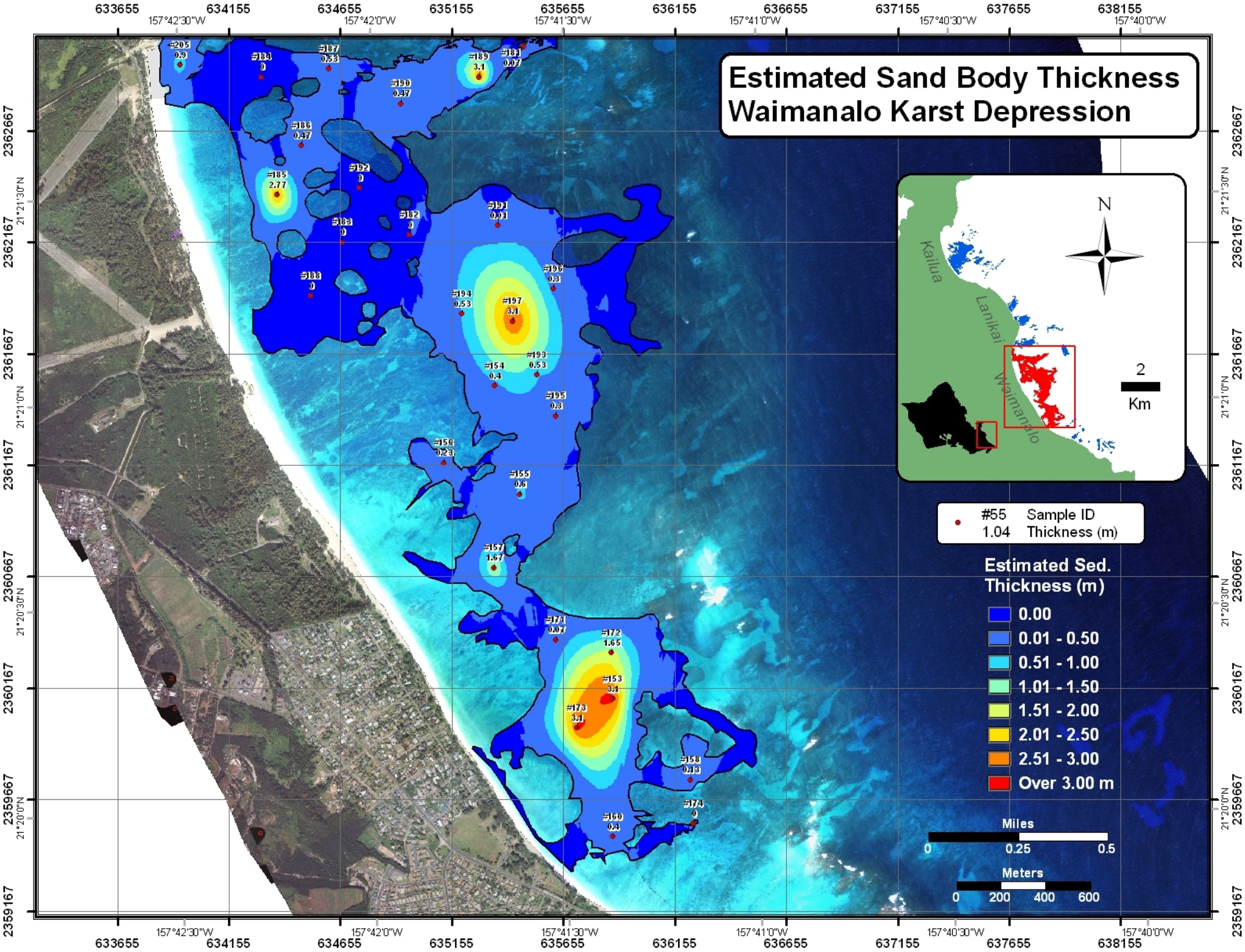
Estimated Sand Body Thickness
Waimanalo Karst Depression
633655
634155
634655
635155
635655
636155
636655
637155
637655
638155
157°42'30"W
157°42'0"W
157°41'30"W
157°41'0"W
157°40'30"W
157°40'0"W
2362667
2362167
2361667
2361167
2360667
2360167
2359667
2359167
21°21'30"N
21°21'0"N
21°20'30"N
21°20'0"N
#205 0.9
#184 0
#187 0.53
#189 3.1
#181 0.07
#190 0.47
#186 0.47
#185 2.77
#192 0
#191 0.01
#183 0
#182 0
#188 0
#196 0.3
#194 0.53
#197 3.1
#193 0.53
#154 0.4
#195 0.3
#156 0.23
#155 0.6
#157 1.67
#171 0.07
#172 1.65
#153 3.1
#173 3.1
#158 0.43
#174 0
#160 0.4
N
Kailua
Lanikai
Waimanalo
2
Km
#55 Sample ID
1.04 Thickness (m)
Estimated Sed. Thickness (m)
0.00
0.01 - 0.50
0.51 - 1.00
1.01 - 1.50
1.51 - 2.00
2.01 - 2.50
2.51 - 3.00
Over 3.00 m
Miles
0
0.25
0.5
Meters
0
200
400
600

Estimated Sediment Volume
Waimanalo Karst Depression

Area ID	Area m^2	Volume m^3	Error m^2	Vol/Area m^3/m^2	Method
73	221,114	243,220	± 15266	1.10	Kriging
74	17,195	5,860	± 802	0.34	Kriging
75	240,583	173,502	± 18808	0.72	Kriging
76	37,555	23,946	± 1957	0.64	Kriging
77	21,496	13,672	± 1000	0.64	Kriging

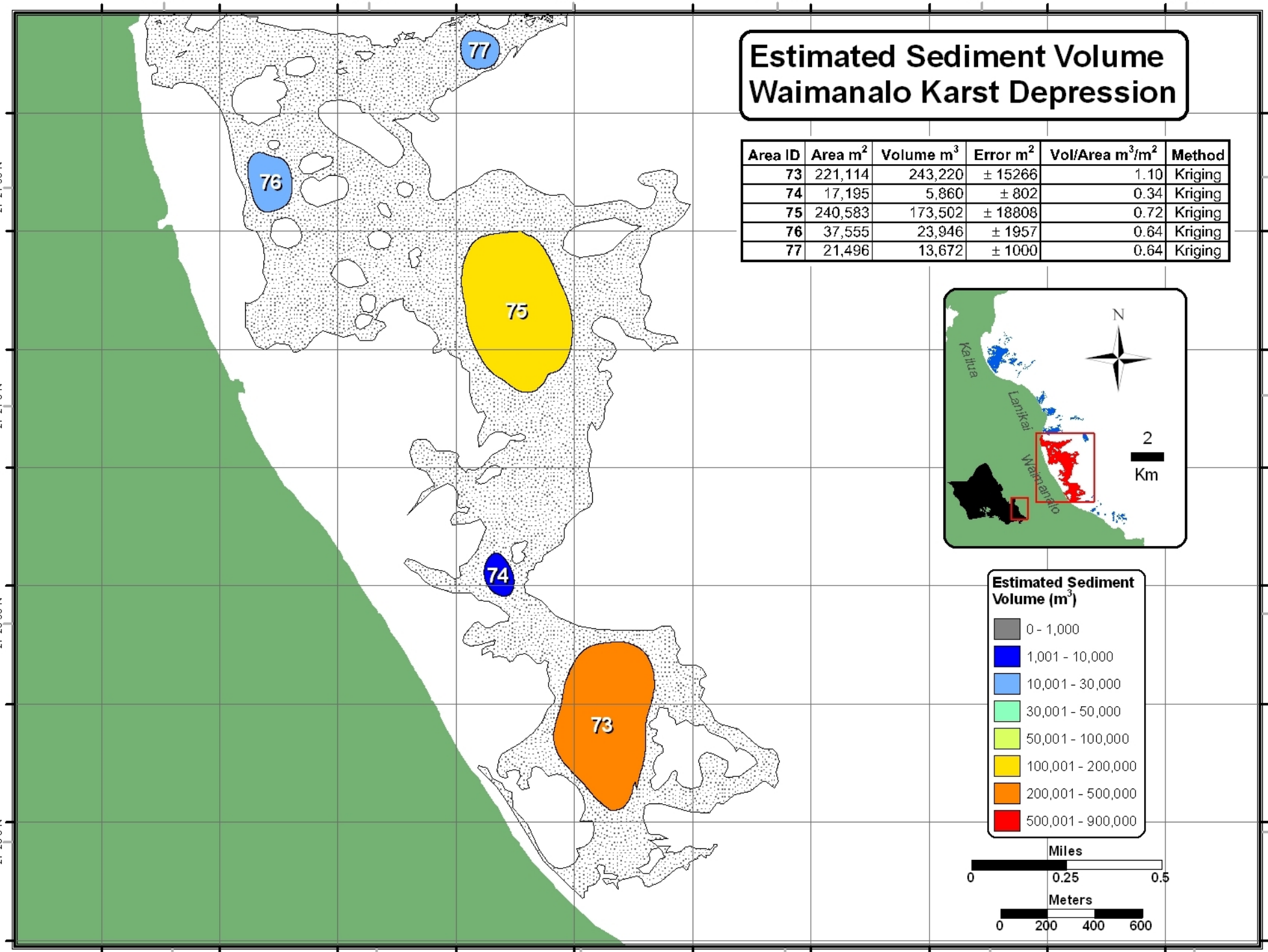

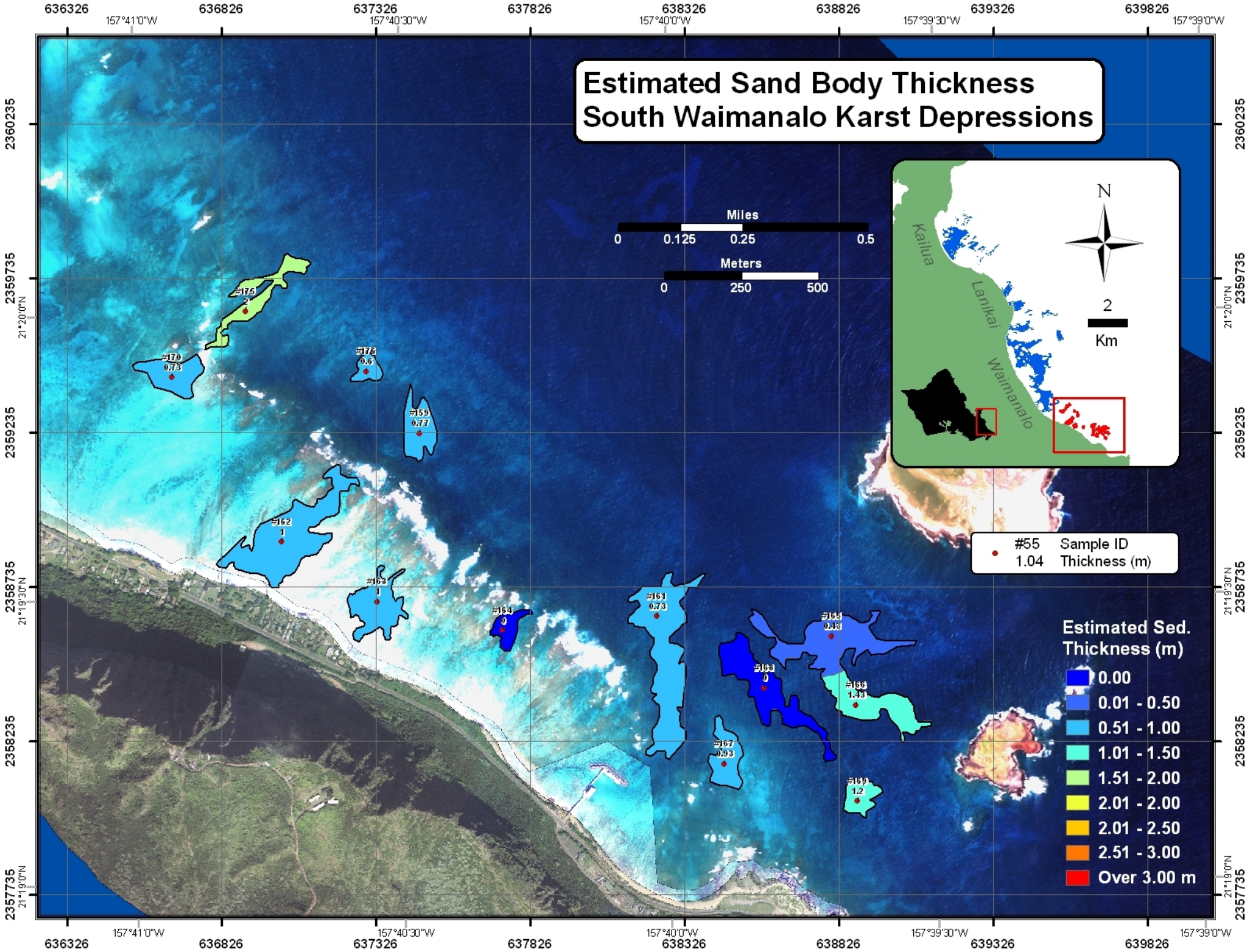
Estimated Sand Body Thickness
South Waimanalo Karst Depressions
Miles
0
0.125
0.25
0.5
Meters
0
250
500
N
2
Km
Kailua
Lanikai
Waimanalo
#55 Sample ID
1.04 Thickness (m)
Estimated Sed. Thickness (m)
0.00
0.01 - 0.50
0.51 - 1.00
1.01 - 1.50
1.51 - 2.00
2.01 - 2.00
2.01 - 2.50
2.51 - 3.00
Over 3.00 m
#175 2
#170 0.73
#176 0.6
#159 0.77
#162 1
#163 1
#164 0
#161 0.73
#165 0.43
#168 0
#166 1.43
#167 0.93
#169 1.2
636326
636826
637326
637826
638326
638826
639326
639826
157°41'0"W
157°40'30"W
157°40'0"W
157°39'30"W
157°39'0"W
2360235
2359735
2359235
2358735
2358235
2357735
21°20'0"N
21°19'30"N
21°19'0"N

Estimated Sediment Volume
South Waimanalo Karst Depressions

Area ID	Area m^2	Volume m^3	Error m^3	Vol/Area m^3/m^2	Method
60	20,294	15,748	± 3622	0.78	Voronoi
61	61,886	17,529	± 4032	0.28	Voronoi
62	8,243	0	± 0	0.00	Voronoi
63	36,575	0	± 0	0.00	Voronoi
64	9,644	1,360	± 112	0.14	Voronoi
65	45,198	2,284	± 188	0.05	Voronoi
66	28,411	4,774	± 394	0.17	Voronoi
67	17,823	1,529	± 126	0.09	Voronoi
68	17,195	5,137	± 1182	0.30	Voronoi
69	6,337	447	± 37	0.07	Voronoi
70	16,024	5,782	± 1330	0.36	Voronoi
71	58,130	6,830	± 563	0.12	Voronoi
72	24,783	2,912	± 240	0.12	Voronoi

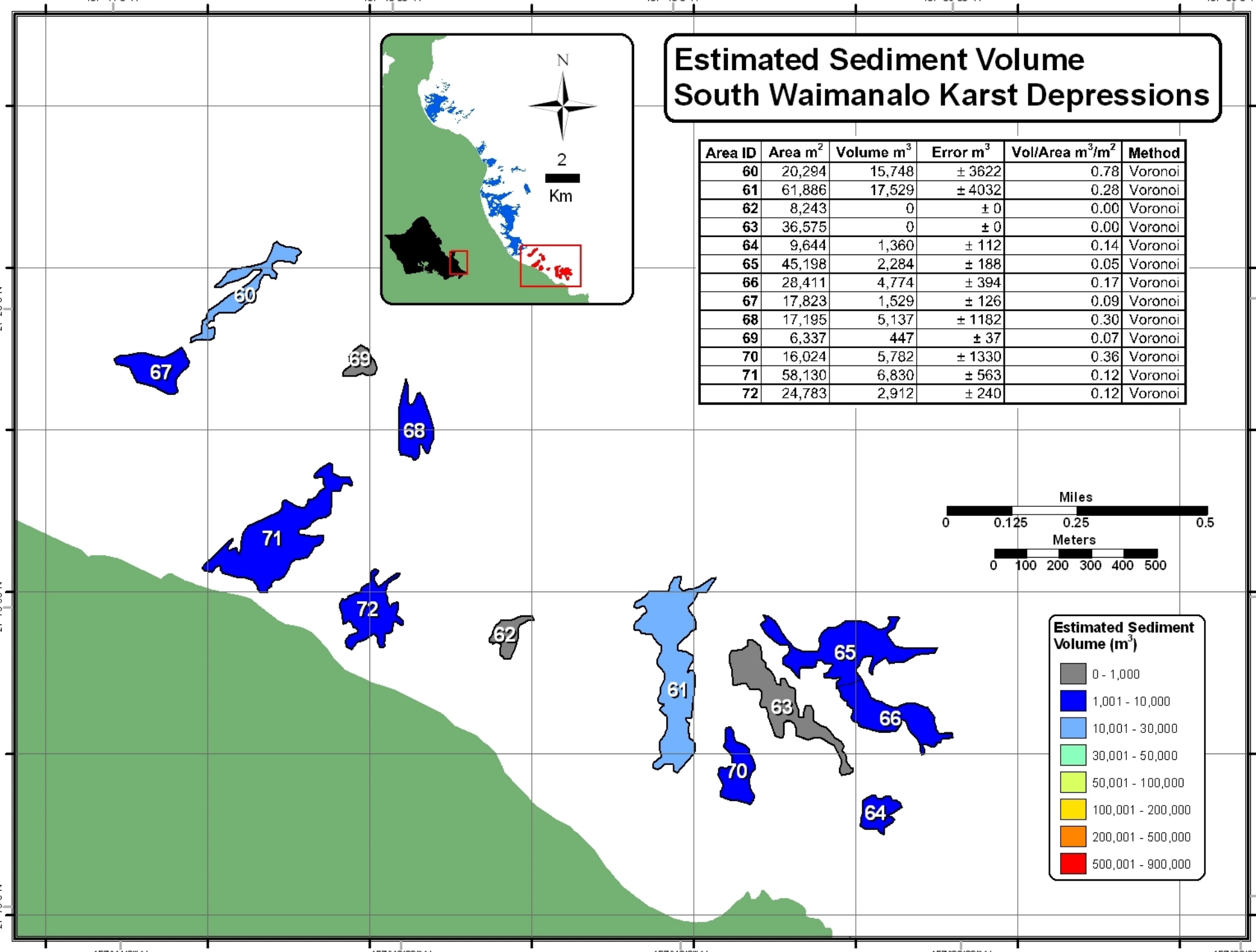

Appendix B
Thickness
Measurement Data

POINT LOCATION *MORPHOLOGY*	MEASUREMENT POINT ID	WATER DEPTH (m, MSL)	SEDIMENT THICKNESS (m)	OBSERVATIONS
Kailua Bay				
Fossil Channel				
	1	-5.5	0.30	Sand overlaying hardbottom
	2	-5.0	0.70	Sand overlaying hardbottom
	3	-5.0	1.00	Sand overlaying hardbottom
	4	-4.5	1.50	Sand overlaying hardbottom
	5	-4.0	1.40	Sand overlaying hardbottom
	6	-3.6	1.30	Sand overlaying hardbottom
	7	-4.0	0.50	Sand overlaying hardbottom
	8	-4.5	1.50	Sand overlaying hardbottom
	9	-4.5	1.80	Sand overlaying hardbottom
	10	-5.0	1.70	Sand overlaying hardbottom
	11	-5.7	1.40	Sand overlaying hardbottom
	12	-3.6	0.40	Sand overlaying hardbottom
	13	-3.8	1.00	Sand overlaying hardbottom
	14	-3.7	0.30	Sand overlaying hardbottom
	15	-3.6	1.30	Sand overlaying hardbottom
	16	-3.2	0.50	Sand overlaying hardbottom
	17	-3.0	0.60	Sand overlaying hardbottom
	18	-3.5	1.50	Sand overlaying hardbottom
	19	-3.6	0.70	Sand overlaying hardbottom
	20	-3.7	0.90	Sand overlaying hardbottom
	21	-3.8	1.20	Sand overlaying hardbottom
	22	-3.6	0.30	Sand overlaying hardbottom
	23	-4.0	1.30	Sand overlaying hardbottom
	24	-4.6	2.90	Sand overlaying hardbottom
	25	-4.6	2.40	Sand overlaying hardbottom
	26	-4.3	1.90	Sand overlaying hardbottom
	27	-5.1	2.90	Sand overlaying hardbottom
	28	-4.0	0.30	Sand overlaying hardbottom
	29	-3.7	0.03	Limestone outcroping in thin sand
	30	-3.8	0.40	Sand overlaying hardbottom
	31	-4.0	1.63	Sand overlaying hardbottom
	32	-4.1	0.60	Sand overlaying hardbottom
	33	-4.1	1.67	Sand overlaying hardbottom
	34	-3.7	2.40	Sand overlaying hardbottom
	35	-3.5	0.40	Sand overlaying hardbottom
	36	-3.4	0.60	Sand overlaying hardbottom
	37	-3.0	0.10	Limestone outcroping in thin sand
	38	-3.5	3.10	Sand beyond probing thickness (>3.0 m)

Appendix B

LOCATION *MORPHOLOGY*	MEASUREMENT POINT ID	WATER DEPTH (m, MSL)	SEDIMENT THICKNESS (m)	OBSERVATIONS
Kailua Bay				
Fossil Channel				
	43	-3.2	0.10	Limestone outcroping in thin sand supporting algea
	83	-2.7	0.63	Sand overlaying hardbottom
	84	-3.7	0.10	Limestone outcroping in thin sand
	85	-3.0	0.10	Limestone outcroping in thin sand supporting algea
	86	-3.7	0.17	Limestone outcroping in thin sand
	87	-3.7	0.43	Sand overlaying hardbottom
	88	-3.7	0.23	Sand overlaying hardbottom
	89	-3.0	2.70	Sand overlaying hardbottom
	90	-5.5	1.33	Sand overlaying hardbottom
	91	-4.0	0.57	Sand overlaying hardbottom
	92	-3.7	0.33	Sand overlaying hardbottom
	109	-4.3	3.10	Sand beyond probing thickness (>3.0 m)
	110	-3.7	3.10	Sand beyond probing thickness (>3.0 m)
	111	-4.3	3.10	Sand beyond probing thickness (>3.0 m)
	112	-3.7	3.10	Sand beyond probing thickness (>3.0 m)
	113	-3.7	3.10	Sand beyond probing thickness (>3.0 m)
	114	-3.7	0.20	Sand overlaying hardbottom
	115	-2.7	1.23	Sand overlaying hardbottom
	116	-3.0	0.07	Limestone outcroping in thin sand supporting algea
	117	-3.4	1.77	Sand overlaying hardbottom
	120	-4.6	0.03	Limestone outcroping in thin sand
	135	-5.5	3.10	Sand gravel mixture beyond probing thickness (>3.0 m)
	136	-8.2	3.10	Sand gravel mixture beyond probing thickness (>3.0 m)
	137	-7.0	3.10	Sand gravel mixture beyond probing thickness (>3.0 m)
	138	-4.9	1.17	Sand overlaying limestone, grey sands observed
	142	-6.1	0.10	Gravel and rubble with little sand
	143	-3.0	0.00	Gravel and rubble
	144	-5.5	2.07	Sand overlaying hardbottom
	145	-6.4	1.00	1.0 m of sand overlaying resistant layer of shell and coral rubble
	146	-7.3	1.00	1.0 m of sand overlaying resistant layer of coral rubble
	147	-10.4	1.90	Sand overlaying hardbottom
	148	-10.4	0.73	0.73 m sand overlaying resistant layer of coral rubble
	149	-13.7	0.33	Sand overlaying hardbottom
	151	-3.0	0.17	Gravel and rubble with little sand
	152	-12.2	0.67	Sand overlaying hardbottom

Appendix B

LOCATION *MORPHOLOGY*	MEASUREMENT POINT ID	WATER DEPTH (m, MSL)	SEDIMENT THICKNESS (m)	OBSERVATIONS
Kailua Bay				
Karst Depression				
	95	-7.3	1.07	Sand overlaying hardbottom
	96	-5.2	0.30	Sand overlaying hardbottom
	97	-6.7	1.53	Sand with a thin resistive layer at -1.0 m
	98	-9.1	1.13	Sand and carbonate discs 5 - 40 cm in diameter
	99	-7.6	0.73	Sand overlaying hardbottom
	100	-6.1	0.87	Sand overlaying hardbottom
	101	-7.6	0.20	Sand overlaying hardbottom
	102	-7.9	0.13	Sand overlaying hardbottom
	103	-6.4	0.40	Sand overlaying hardbottom
	104	-7.3	1.70	Sand overlaying hardbottom
	105	-6.4	0.53	Sand overlaying hardbottom
	106	-6.4	0.27	Sand overlaying hardbottom
	107	-7.6	0.10	Gravel and rubble with little sand
	108	-6.7	0.07	Limestone outcroping in thin sand
	118	-7.9	1.40	Sand overlaying hardbottom
	119	-8.5	1.33	1.33 m of sand overlaying resistant layer of shell and coral rubble
	139	-8.2	0.13	Gravel and rubble with little sand
	121	-6.7	0.73	Sand overlaying hardbottom
	122	-6.1	3.10	Sand beyond probing thickness (>3.0 m), resistive layer at -0.3 m
	123	-8.2	0.33	0.4 m of sand overlaying resistant layer of shell and coral rubble
	124	-6.1	3.10	Sand beyond probing thickness (>3.0 m), resistive layer at -0.6 m
	125	-3.0	2.37	Sand overlaying hardbottom
	126	-6.1	0.33	Limestone outcroping in thin sand
	127	-7.6	0.70	Sand overlaying hardbottom
	128	-7.6	0.93	Sand overlaying hardbottom
	129	-4.9	1.63	Sand overlaying hardbottom
	130	-7.6	0.20	Sand overlaying hardbottom
	131	-6.1	0.17	Limestone outcroping in thin sand
	132	-4.6	0.57	Sand overlaying hardbottom
	133	-5.5	1.40	Very fine sand overlaying hardbottom
	134	-4.9	0.83	Sand overlaying hardbottom
	140	-6.1	1.83	Sand overlaying hardbottom
	141	-4.3	0.90	Sand overlaying hardbottom
	150	-2.4	1.83	Sand overlaying hardbottom
	63	-3.1	0.17	Thin sand over hard bottom
	64	-3.3	0.60	Sand over hard bottom
	65	-3.1	0.77	Sand over hard bottom
	66	-3.8	0.13	Limestone outcroping in thin sand
	67	-3.8	0.57	Sand overlaying hardbottom
	68	-3.7	0.87	0.87 m of sand overlaying resistant layer of shell and coral rubble

Appendix B

LOCATION *MORPHOLOGY*	MEASUREMENT POINT ID	WATER DEPTH (m, MSL)	SEDIMENT THICKNESS (m)	OBSERVATIONS
Kailua Bay				
Karst Depression				
	73	-3.5	0.17	Limestone outcroping in thin sand
	74	-3.0	0.30	Limestone outcroping in thin sand
	75	-3.9	0.10	Limestone outcroping in thin sand
	76	-4.5	0.27	Limestone outcroping in thin sand
	177	-3.4	0.53	0.53 m of sand overlaying resistant layer of shell and coral rubble
	180	-3.7	0.03	Thin sand over hard bottom
	202	-9.1	1.40	Sand overlaying hardbottom
	203	-10.7	0.50	Sand overlaying hardbottom
	204	-11.3	0.37	Sand overlaying hardbottom
Lanikai				
Sand Field				
	44	-2.4	1.97	0.5 m of sand overlaying resistant layer of shell and coral rubble
	45	-2.4	3.10	Sand beyond probing thickness (>3.0 m)
	46	-2.4	2.53	2.53 m of sand overlaying resistant layer of shell and coral rubble
	47	-2.4	0.20	Sand overlaying hardbottom
	48	-2.4	1.00	Sand overlaying hardbottom
	49	-2.1	0.50	0.5 m of sand overlaying resistant layer of shell and coral rubble
	50	-2.1	0.43	Sand overlaying hardbottom
	51	-2.4	1.37	0.5 m of sand overlaying resistant layer of shell and coral rubble
	52	-4.0	0.27	0.27 m of sand overlaying resistant layer of shell and coral rubble
	53	-4.6	0.30	Sand overlaying hardbottom
	54	-3.4	0.60	0.6 m of sand overlaying resistant layer of shell and coral rubble
	55	-4.0	0.65	0.65 m of sand overlaying resistant layer of shell and coral rubble
	56	-3.7	0.65	0.65 m of sand overlaying resistant layer of shell and coral rubble
	57	-3.7	0.17	Thin sand overlaying hardbottom
	58	-3.4	0.75	0.75 m of sand overlaying resistant layer of shell and coral rubble
	59	-3.4	3.10	Sand beyond probing thickness (>3.0 m)
	60	-3.4	0.43	Sand overlaying hardbottom
	61	-2.4	0.80	Sand overlaying hardbottom
	62	-3.4	0.63	0.63 m of sand overlaying resistant layer of shell and coral rubble

Appendix B

LOCATION *MORPHOLOGY*	MEASUREMENT POINT ID	WATER DEPTH (m, MSL)	SEDIMENT THICKNESS (m)	OBSERVATIONS
Lanikai				
Karst Depression				
	77	-4.9	0.20	0.20 m of sand overlaying resistant layer of shell and coral rubble
	78	-4.6	0.20	0.20 m of sand overlaying resistant layer of shell and coral rubble
	79	-3.7	0.00	Gravel and rubble with little fine sand
	80	-3.4	0.00	Gravel and rubble with little fine sand
	81	-4.0	0.00	Gravel and rubble with little fine sand
	82	-4.3	0.13	Gravel and rubble with little sand
	178	-3.4	0.20	Sand overlaying hardbottom
	179	-4.3	0.23	Sand overlaying hardbottom
	198	-16.8	0.90	Coarse sand with sparse carbonate rubble throughout
	199	-16.8	1.10	Coarse sand with sparse carbonate rubble throughout
	200	-16.8	1.10	Coarse sand with sparse carbonate rubble throughout
Waimanalo Bay				
Fossil Channel				
	181	-7.3	0.07	Gravel and rubble with little sand
	184	-6.4	0.00	Halimeda rich gravel with partially hardened surface
	187	-6.4	0.53	Sand overlaying hardbottom
	189	-5.5	3.10	Sand beyond probing thickness (>3.0 m)
	190	-6.4	0.47	Sand overlaying hardbottom
	201	-4.3	0.90	0.9 m of fine sand overlaying halimeda rich gravel
	205	-4.6	0.90	0.9 m of fine sand overlaying halimeda rich gravel
Waimanalo Bay				
Sand Field				
	162	-1.5	1.00	Sand overlaying hardbottom
	163	-1.5	1.00	Sand overlaying hardbottom
	164	-3.4	0.00	Gravel and rubble
	170	-1.5	0.73	Sand overlaying hardbottom
Waimanalo Bay				
Karst Depression				
	153	-5.5	3.10	Coarse gravely sand beyond probing thickness (>3.0 m)
	154	-7.9	0.40	Reddish sand overlaying hardbottom
	155	-7.6	0.60	0.6 m of fine sand overlaying halimeda rich gravel
	156	-6.1	0.23	0.23 m of fine sand overlaying halimeda rich gravel
	157	-4.9	1.67	Sand overlaying hardbottom
	160	-4.6	0.40	Fine sand overlaying hardbottom
	171	-3.4	0.07	Limestone outcroping in thin sand
	172	-3.7	1.65	Gravely sand overlaying hardbottom
	173	-7.0	3.10	Coarse sand beyond probing thickness (>3.0 m)

Appendix B

LOCATION *MORPHOLOGY*	MEASUREMENT POINT ID	WATER DEPTH (m, MSL)	SEDIMENT THICKNESS (m)	OBSERVATIONS
Waimanalo Bay				
Karst Depression				
	188	-6.4	0.00	Gravel and rubble
	191	-9.1	0.01	thin sand overlaying halimeda rich gravel
	192	-6.7	0.00	Halimeda rich gravel
	193	-9.1	0.53	0.53 m of fine sand overlaying halimeda rich gravel
	194	-7.9	0.53	Sand overlaying hardbottom
	195	-9.1	0.30	0.30 m of sand overlaying halimeda/coral gravel
	196	-9.8	0.30	0.30 m of sand overlaying halimeda/coral gravel
	197	-8.8	3.10	Sand beyond probing thickness (>3.0 m)
	158	-4.6	0.13	Limestone outcroping in thin sand
	159	-6.7	0.77	Sand overlaying hardbottom
	161	-7.9	0.73	Very fine sand overlaying hardbottom
	165	-8.2	0.43	Sand with fossil reef and coral rubble outcroping
	166	-8.8	1.43	Gravely sand with fossil reef outcroping
	167	-3.4	0.93	Coarse sand overlaying hard bottom
	168	-7.6	0.00	Limestone supporting algea
	169	-7.9	1.20	1.20 m of sand overlaying coral gravel
	174	-3.4	0.00	Limestone surface with no sand
	175	-4.6	2.00	Sand overlaying hardbottom
	176	-5.2	0.60	Spur and groove reef with sand infill

Appendix C
Volume Estimates

LOCATION *MORPHOLOGY*	SAND BODY ID	AREA ID	AREA (m^2)	VOLUME (m^3)	ERROR (m^3)	VOL/AREA (m^3/m^2)	METHOD
Kailua Bay							
Fossil Channel							
	26	1	586,831	801,695	± 70,484	1.37	Kriging
	26	2	7,394	2,513	± 455	0.34	Kriging
	26	3	4,572	1,027	± 350	0.22	Kriging
	46	40	4,792	614	± 141	0.13	Voronoi
	46	41	12,302	3,198	± 736	0.26	Voronoi
	53	42	2,344	1,728	± 397	0.74	Voronoi
	46	43	13,217	3,744	± 861	0.28	Voronoi
	46	44	11,467	4,449	± 1023	0.39	Voronoi
	54	45	2,701	105	± 24	0.04	Voronoi
	15	46	3,172	1,231	± 283	0.39	Voronoi
	47	47	5,508	4,424	± 1018	0.80	Voronoi
	25	48	5,868	387	± 89	0.07	Voronoi
	25	49	8,534	0	± 0	0.00	Voronoi
Karst Depression							
	1	23	5,450	1,544	± 127	0.28	Voronoi
	1	24	22,971	27,630	± 2279	1.20	Voronoi
	1	25	21,041	2,694	± 222	0.13	Voronoi
	1	26	27,962	33,633	± 2775	1.20	Voronoi
	1	27	14,104	12,969	± 1070	0.92	Voronoi
	1	28	33,961	24,114	± 1989	0.71	Voronoi
	13	29	1,793	577	± 48	0.32	Voronoi
	14	30	790	561	± 46	0.71	Voronoi
	24	31	11,163	1,429	± 118	0.13	Voronoi
	24	32	8,586	2,332	± 192	0.27	Voronoi
	41	33	16,853	6,081	± 502	0.36	Voronoi
	42	34	5,112	337	± 28	0.07	Voronoi
	43	35	19,513	12,341	± 1018	0.63	Voronoi
	43	36	18,917	1,468	± 121	0.08	Voronoi
	44	37	4,333	958	± 79	0.22	Voronoi
	45	38	838	293	± 24	0.35	Voronoi
	48	39	4,970	2,700	± 223	0.54	Voronoi
	3	4	2,602	1,716	± 395	0.66	Voronoi
	4	5	710	110	± 25	0.15	Voronoi
	38	6	1,996	674	± 155	0.34	Voronoi
	5	7	1,450	73	± 17	0.05	Voronoi
	38	8	3,483	270	± 62	0.08	Voronoi
	6	9	1,917	543	± 125	0.28	Voronoi
	7	10	653	68	± 16	0.10	Voronoi
	8	11	2,141	440	± 101	0.21	Voronoi

Appendix C

LOCATION *MORPHOLOGY*	SAND BODY ID	AREA ID	AREA (m^2)	VOLUME (m^3)	ERROR (m^3)	VOL/AREA (m^3/m^2)	METHOD
Kailua Bay							
Karst Depression							
	10	17	6,206	313	± 72	0.05	Voronoi
	51	18	11,958	464	± 107	0.04	Voronoi
	11	19	3,575	1,845	± 424	0.52	Voronoi
	39	20	6,003	2,632	± 605	0.44	Voronoi
	12	21	1,601	43	± 10	0.03	Voronoi
	40	22	8,221	4,466	± 1027	0.54	Voronoi
Lanikai							
Karst Depression							
	49	50	12,044	977	± 204	0.08	Kriging
	28	51	29,245	946	± 523	0.03	Kriging
	37	52	128,180	41,780	± 8992	0.33	Kriging
Fossil Channel							
	29	53	32,582	17,699	± 4071	0.54	Voronoi
	29	54	16,704	3,241	± 745	0.19	Voronoi
	29	55	18,637	2,676	± 615	0.14	Voronoi
Sand Field							
	50	56	11,174	179	± 45	0.02	Kriging
	27	57	227,136	22,464	± 784	0.10	Kriging
	29	58	490,846	44,084	± 1261	0.09	Kriging
	28	59	419,702	63,260	± 999	0.15	Kriging
Waimanalo Bay							
Karst Depression							
	2	60	20,294	15,748	± 3622	0.78	Voronoi
	20	61	61,886	17,529	± 4032	0.28	Voronoi
	34	68	17,195	5,137	± 1182	0.30	Voronoi
	36	70	16,024	5,782	± 1330	0.36	Voronoi
Sand Field							
	22	62	8,243	0	± 0	0.00	Voronoi
	30	63	36,575	0	± 0	0.00	Voronoi
	31	64	9,644	1,360	± 112	0.14	Voronoi
	32	65	45,198	2,284	± 188	0.05	Voronoi
	32	66	28,411	4,774	± 394	0.17	Voronoi
	33	67	17,823	1,529	± 126	0.09	Voronoi
	35	69	6,337	447	± 37	0.07	Voronoi
	21	71	58,130	6,830	± 563	0.12	Voronoi
	17	72	24,783	2,912	± 240	0.12	Voronoi

BIBLIOGRAPHY

Athens, J. S., and Ward, J. V., 1991, Paleoenvironmental and Archaeological Investigations, Kawainui Marsh Flood Control Project, Oahu Island, Hawaii.: International Archaeological research Institute, Inc. Honolulu Hawaii Prepared for U.S. Army Engineering Division, Pacific Ocean. Contract No. DACW83-90-C-0050.

Barry, J., Schock, S., and Ericksen, M., 1997, A New Broad Band Frequency Modulated Subbottom Profiling Developed for Hawaii: Seventh Annual International Offshore and Polar Engineering Conference p. 120-128.

Bodge, K., and Sullivan, S., 1999, Hawaii Pilot Beach Restoration Project: Coastal Engineering Investigaton: State of Hawaii Department of Land and Natural Resources, Honolulu.

Cacchione, D., and Tate, G., 1998, Bottom Currents, Waves and Sand Transport in Reef Channel off Kailua, Hawaii: Proc. Sea grant Coastal Erosion Mgmt, Conf., Maui, Hawaii.

Casciano, F., and Palmer, R., 1969, Potential of Offshore Sand as an Exploitable Resource in Hawaii: Sea Grant Program: Univ. of Hawaii: #69-4.

Conger, C. L., Fletcher, C., Hochberg, E., Frazer, N., and Rooney, J., In Review, Patterns of Sand Distribution Across the Insular Shelf, Oahu, Hawaii.

Conger, C. L., Hochberg, E., Fletcher, C. H., and Atkinson, M., 2006, Decorrelating Remote Sensing Color Bands From Bathymetry in Optically Shallow Waters: IEEE Transactions on Geoscience and Remote Sensing, v. 44.

Conger, C. L. F., C.H., and Barbee, M., 2005, Artificial neural network classification of sand in all visible submarine and subaerail regions of a digital image: Journal of Coastal Research, v. 21, p. 1173-1177.

Coulbourn, W., Campbell, J., Anderson, M., Daugherty, V., Greenberb, S., Izuka, R., Lauritzen, B., Tsutsui, B., and Yan, C., 1988, Sand deposits offshore Oahu, Hawaii: Pacific Science, v. 42, p. 267-299.

Cox, D., 1978, Notes on Hawaiian Sand Beach Management, Hawaii Coastal Zone Management Program, Honolulu, University of Hawaii.

Coyne, M., Battista, T., Anderson, M., Waddell, J., Smith, W., Jokiel, P., Kendall, M., and Monaco, M., 2003, Benthic Habitats of the Main Hawaiian Islands: NOAA Technical Memorandum NOS NCCOS CCMA 152, URL: http://biogeo.nos.noaa.gov/projects/mapping/pacific.

Dollar, S., 1979, Sand Mining in Hawaii: Research, Restrictions, and Choices for the Future: UNIHI-SEAGRANT-TP-79-01. Seagrant College Program, Univ. of Hawaii.

Fletcher, C. H., Grossman, E., Richmond, B. M., and Gibbs, A., 2002, Atlas of Natural of Natural Hazards on the Hawaiian Coasts: Denver, CO, U.S. Geological Survey, Geologic Investigations Series I-2761, 182 p.

Fletcher, C. H., Murrat-Wallace, C. G., C., Popp, B., and Sherman, C. E., 2005, Age and Origin of Late Quaternary Eolinanite, Kaiehu Point (Moomomi), Hawaii: Journal of Coastal Research, v. SI 42, p. 92-112.

Grossman, E., and Fletcher, C., 1998, Sea level higher than present 3500 years ago on the northern main Hawaiian Islands: Geology, v. 26.

—, 2004, Holocene Reef Development Where Wave Energy Reduces Accmmodation Space. Kailua Bay, Winward Oahu, Hawaii, USA: Journal of Sedimentary Research, v. 74, p. 49-63.

Grossman, E. E., 2001, Holocene sea-level history and reef development in Hawaii and the central Pacific Ocean, University of Hawaii, Manoa 257 p.

Hampton, M. A., Blay, C. T., and Murray, C., 2004, Carbonate Sediment Depositis on the Reef Front Around Oahu, Hawaii: Marine Georesources and Geotechnology, v. 22, p. 65-102.

Hampton, M. A., Blay, C. T., Murray, C., Torresan, L., Frazee, C., Richmond, B. M., and Fletcher, C., 2003, Data Report, Geology of Reef-Front Carbonate Sediment Deposits Around Oahu, Hawaii: U.S. Geological Survey Open-File Report 03-441.

Harney, J. N., and Fletcher, C. H., 2003, A budget of Caronate Framework and Sediment Production, Kailua Bay, Oahu, Hawaii: Journal of Sedimentary Research, v. 73, p. 856-868.

Harney, J. N., Grossman, E. E., Richmond, B. R., and Fletcher, C. H., 2000, Age and composition of carbonate shoreface sediments, Kailua Bay, Oahu, Hawaii: Coral Reefs, v. 19, p. 141-154.

Kraft, J., 1982, Terrigenous and Carbonate Clastic Facies in a Transgressive Sequence Over Volcanic Terrain: American Association of Petroleum Geologists Bulletin, v. 66, p. 589.

—, 1984, Local relative sea level changes and the evolution of coastal environments, windward Oahu, Hawaii: IGCP Proj. No. 061. Sea-Level 5:5-6.

Maragos, J., Roach, J., Bowers, R., Hemmes, D., Self, F., Macneil, J., Ells, K., Omeara, P., Vansant, J., Sato, A., Jones, J., and Kam, D., 1977, Enviromental Surveys Before, During, after Offshore Marine Sand Mining Operatations at Keauhou Bay, Hawaii: Sea Grant Program: Univ. of Hawaii, v. Working Paper No. 28.

Moberly, R., Campbell, J., and Coulbourn, W., 1975, Offshore and Other Sand resources for Oahu, Hawaii.

Moberly, R., and Chamberlain, T., 1964, Hawaiian Beach Systems: Univ. of Hawaii. Prepared for Habors Divions, Hawaii DOT. Contract 6496.

Ocean Innovators Inc, 1977a, Offshore Sand Deposit Data Collection, Kualoa regional Park Beach Erosion Project, Kaneohe Bay, Oahu.: Prepared for U.S. Army Engineer Div., Pacific Ocean.

—, 1977b, Offshore Sand Sample Data, South and West Shores, Oahu.: Prepared for Marine Affairs Coordinator, Task Order No. 120.

—, 1977c, Sand Deposit Investigation Offshore of Nanakuli, Oahu.: Prepared for the U.S. Army Engineer Div., Pacific Ocean.

—, 1978a, Kailua Bay Offshore Sand Survey: Prepared for U.S. Army Engineer Div., Pacific Ocean.

—, 1978b, North Kaneohe bay offshore Sand Reconnaissance and Sampling: Prepared for the U.S. Army Engineer Div., Pacific Ocean.

—, 1979, Offshore Sand Sampling North and Winward Shores, Oahu.: Under contract to Marine Affairs Coordinator, Office of Governer, State of Hawaii, Order No. 163.

Richmond, B. M., Cacchione, D., Howd, P., and D'Orio, M., 2002, Sand transport within a reef channel off Kailua, Oahu, Hawaii: Ocean Science meeting, American Geopyhical Union.

Rooney, J., Fletcher, C., Grossman, E., Engels, M., and Field, M., 2004, El Nino Influence on Holocene Reef Accretion in Hawaii: Pacific Science, v. 58, p. 305-324.

Sea Engineering Inc, 1993, Beach Nourishment Viablity Study: Prepared for Hawaii Coastal Zone Management Program

Sherman, C. E., Fletcher, C. H., and Rubin, K. H., 1999, Marine and Meteoric Diagenesis of Pleistocene Carbonates from a Nearshore Submarine Terrace, Oahu, Hawaii: Journal of Sedimentary Research, v. 69.

U.S. Army Engineer District, 1978, Detailed Project report and Final Environmental Statement, Kailua Beach Park Erosion Control, Kailua, Oahu, Hawaii.

Webster, R., and Oliver, M., 2001, Geostatistics for Environmental Scientists: Statistic in Pratice: West Sussex, Wiley &Sons.

APPENDIX G

CMB REPORT 06-014: RESULTS OF OFFSHORE SAND INVESTIGATION FOR THE SOUTHEAST OAHU REGIONAL SEDIMENT MANAGEMENT DEMONSTRATION PROJECT, HAWAII, HONOLULU DISTRICT

GEOTECHNICAL AND STRUCTURES LABORATORY
ENGINEER RESEARCH AND DEVELOPMENT CENTER
US ARMY CORPS OF ENGINEERS

Geotechnical and Structures Laboratory

US Army Corps of Engineers®
Engineer Research and Development Center

Concrete and Materials Branch
Testing and Evaluation Program

CMB Report 06-014: Results of Offshore Sand Investigation for the Southeast Oahu Regional Sediment Management Demonstration Project, Hawaii, Honolulu District

Joe G. Tom and Judy C. Tom

September 2006

Concrete and Materials Branch
Testing and Evaluation Program

September 2006

CMB Report 06-014: Results of Offshore Sand Investigation for the Southeast Oahu Regional Sediment Management Demonstration Project, Hawaii, Honolulu District

Prepared For

US Army Engineer District, Honolulu

By Joe G. Tom and Judy C. Tom

US Army Engineer Research and Development Center
3909 Halls Ferry Road
Vicksburg, MS 39180-6199

Contents

Preface iv

1—Introduction 1

Background 1
Authorization 2
Objective 2
Samples 2
Tests 3

2—Evaluation 4

Sand Samples 4

3—Conclusions and Recommendations 6

Sand Samples 6

Appendix A: Maps of Sand Sample Locations

Appendix B: Sand Sample Identification and Masses

Appendix C: Sand Sample Graphic Results

Appendix D: Sand Sample Numerical Results

Preface

The work described in this report was authorized by the US Army Engineer District, Honolulu, (POH) for the Southeast Oahu Regional Sediment Management (SEO/RSM) Demonstration Project. The work was performed under MIPR No. W81HEM50275957, managed at the US Army Engineer Research and Development Center (ERDC), Vicksburg, MS. Mr. Joe G. Tom, ERDC, Geotechnical and Structures Laboratory (GSL), was the Principal Investigator. Mr. Tom and Ms. Judy C. Tom prepared this report. Drs. Philip G. Malone and Charles A. Weiss, Jr., GSL, consulted on the investigation.

Dr. W. Allen Roberson, Chief, Concrete and Materials Branch (CMB), monitored the investigation at ERDC, GSL, under the general supervision of Dr. Albert J. Bush, Chief, Engineering Systems and Materials Division, and Dr. David W. Pittman, Director, GSL.

1 Introduction

Background

The US Army Engineer Research and Development Center (ERDC) have the responsibility of quality assurance for construction materials on US Army Corps of Engineers projects. That responsibility includes the assurance that all construction materials meet the minimum requirements of the project specifications. The ERDC performs this function for the Districts through its Laboratories. The quality assurance responsibility also includes preliminary investigations of construction materials in preparation of the Materials Design Memorandum for the Districts. Construction materials include portland-cement concretes, asphalt concrete, soils, stones, joint materials, steel reinforcements, and other materials as requested.

This investigation is being conducted to determine the general movement of sediment offshore of Wailea Point (which is located in the central portion of the region).

Analysis of sediment grain size trends; Benthic sand samples will be collected around target SEO/RSM areas for grain size determination. Analysis of the resulting grain size distributions will reveal trends (i.e., coarse vs. fine) of long-term sediment erosion and deposition within adjacent areas of the sample regions. Sediment sampling will be carried out in two locations: (1) ~2.0 km^2 vicinity of Wailea Point. (250 samples) and (2) a smaller study on the shoreward opening of the Kailua sand channel (100 samples).

Sample spacing will be denser in areas of more specific interest, such as a 37.5 m spacing applied in the immediate vicinity of Wailea Point. changing to 75 m spacing in the off shore sand fields and 150 m spacing in the regions between sand fields. The resulting sediment transport vectors will have resolutions varying with sample spacing, such that vectors near shore will be plotted every 75 m and vectors in offshore sand fields will be plotted every 150 m. A final report containing all data, procedures, results, and interpretations from the grain size trend analysis will be

delivered. The approach and theory behind grain size trend analysis is published in McLaren and Bowles (1985), Goa and Collins (1992), Le Roux (1994), Hughes (2005).

Authorization

This work is authorized under US Army Engineer District, Honolulu, MIPR No. W81HEM50275957. Mr. Thomas D. Smith, CEPOH-EC-T, made the request for the offshore sediment sampling investigations.

Objective

The objective of this report is to provide specific results of tests and evaluations performed on the sand samples that are to be used in the sediment trend analysis.

Samples

The Concrete and Materials Branch (CMB) of the Geotechnical and Structures Laboratory, ERDC, received 224 samples of various beach sands taken from offshore of Wailea Point as shown on the maps in Appendix A. The samples were assigned CMB Serial Number 060166 supplemented with the POH sample number as shown in Appendix B, Table B1. The sand samples were collected by students from the University of Hawaii at Manoa under the direction of Mr. Christopher Bochiccho, Department of Geology and Geophysics, and Mr. Thomas D. Smith, CEPOH-EC-T, and sent to ERDC. Appendix B, Table B1 lists the initial mass determinations from the University of Hawaii and also the results determined from the as-received mass in their original bags and the oven-dry mass of each sample. Numerically, the samples are listed as 0 to 295, with many samples not sent to ERDC for analysis; those are indicated with a zero reading rather than a blank or deleted listing. Two samples, No. 76 and No. 144, were indicated as having been sent for analysis, however the samples were not found in the shipping containers. Another sample, No. 293, was indicated as having no sample sent for analysis; however, the sample numbered as 293 was found in the shipping containers and evaluated with the other samples.

Tests

The sand samples were tested and evaluated for particle size distribution with the current version of the following test methods or specifications:

a. ASTM C 136, “Standard Test Method for Sieve Analysis of Fine and Coarse Aggregates.”

b. ASTM C 702, “Standard Practice for Reducing Samples of Aggregate to Testing Size.”

2 Evaluation

Sand Samples

The 224 samples of various beach sands (CMB Serial No. 060166) were evaluated in accordance with the standard test method, ASTM C 136. Each sample was removed from the zip-lock bag and surface-dried in a 100-degree F environmental room for approximately 24 hours to allow the wet dust material adhering to the interior of the bag to dry so that it could be easily removed without lost. The dry dust material was added back to the original sample and the entire sample was oven-dried to a constant mass. The larger samples of beach sand were reduced to testing size using a mechanical splitter in accordance with ASTM C 702.

The standard method requires the use of sieves designated in SI units and listed in units of millimeters and microns with an alternate listing in US inches. The SI sieves were converted to Phi, Φ, units as required by the Honolulu District personnel. The conversion on the sieve sizes are listed in Table 1 below. The nest of sieves started with -2.0-Phi down to 5.0-Phi sieve size in 0.5-Phi intervals. The nest of sieves included 15 individual sieves plus a collecting pan. Due to the large number of sieves, the analysis was divided into two operations, one set of sieves from -2.0-Phi to 2.0-Phi, and another set of sieves from 2.5-Phi to 5.0-Phi. Therefore, each sample or split portion was sieved twice, once in the larger sieves and then the material remaining in the collecting pan was placed in the second set of sieves and tested.

The material retained on each individual sieve was weighed and final mass recorded. The results were calculated as a percentage of the total sample sieved. All of the material from each sample was returned to the original bag and will be shipped back to Mr. Thomas D. Smith, CEPOH-EC-T, in Honolulu, Hawaii, upon completion of this investigation.

Table 1. Phi units with conversions to SI units and US equivalent units

Phi Units	Conversion to SI units	Standard Sieve Designation	Alternative US Designation
Φ	mm	mm / μm	No.
-2.0	4.00	4.00	No. 5
-1.5	2.83	2.80	No. 7
-1.0	2.00	2.00	No. 10
-0.5	1.41	1.40	No. 14
0.0	1.00	1.00	No. 18
0.5	0.707	710	No. 25
1.0	0.500	500	No. 35
1.5	0.354	355	No. 45
2.0	0.250	250	No. 60
2.5	0.177	180	No. 80
3.0	0.125	125	No. 120
3.5	0.088	90	No. 170
4.0	0.063	63	No. 230
4.5	0.044	45	No. 325
5.0	0.031	32	No. 450

3 Conclusions and Recommendations

Sand Samples

The 224 samples of beach sand (CMB Serial No. 060166) were tested and evaluated for particle size distribution in accordance with the project requirements. The sample results are provided as the results of the percentage of the total amount sieved per sieve size. The results are shown in graphic format to display the distribution of the particles sizes throughout the range of the sample as presented in Appendix C. The numerical results are provided in Appendix D.

POH personnel indicated 225 samples were sent; however, only 224 samples were received. Sample numbers 76 and 144 were not received with the other samples. Sample number 293 was not listed as being sent; however, a sample identified as number 293 was received and analyzed. A total of 224 samples were received and analyzed for particle size distribution.

Appendix A

Maps of Sand Sample Locations (not included)

Appendix B

Sand Sample Identification and Masses (excerpt)

Table 2 (excerpt). Sand Samples, CMB Serial Number 060166				
CMB Serial Supplement No.	**Field Identification**	**POH Mass, g**	**As-Received Mass in Bag, g**	**Oven-Dry Mass, g**
0	0	615	586	432.0
1	1	538	511	376.10
2	2	630	626	450.2
3	3	452	441	309.40
4	4	604	583	423.4
5	5	650	606	452.2
6	6	568	545	435.5
7	7	716	617	501.9
8	8	705	646	489.1
9	9	625	562	381.90

Appendix C

Sand Sample Graphic Results (excerpt)

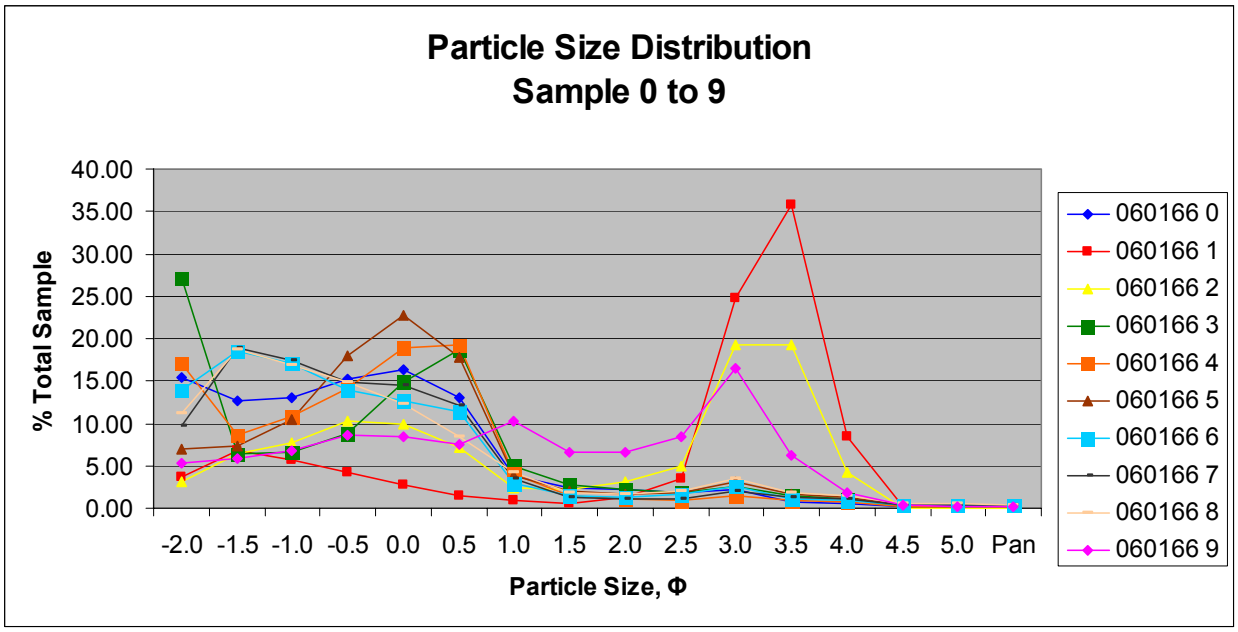
Particle Size Distribution
Sample 0 to 9
% Total Sample
40.00
35.00
30.00
25.00
20.00
15.00
10.00
5.00
0.00
-2.0
-1.5
-1.0
-0.5
0.0
0.5
1.0
1.5
2.0
2.5
3.0
3.5
4.0
4.5
5.0
Pan
Particle Size, Φ
060166 0
060166 1
060166 2
060166 3
060166 4
060166 5
060166 6
060166 7
060166 8
060166 9

Appendix D

Sand Sample Numerical Results (excerpt)

Table C1 (excerpt). Numerical Results of Particle Size Distribution for Samples 0 to 9

Particle Size, Φ	060166 0	060166 1	060166 2	060166 3	060166 4	060166 5	060166 6	060166 7	060166 8	060166 9
-2.0	15.41	3.65	3.16	27.07	17.02	7.02	13.94	9.68	11.14	5.41
-1.5	12.67	6.86	6.34	6.47	8.63	7.41	18.48	18.82	18.69	5.94
-1.0	12.96	5.72	7.76	6.62	10.82	10.45	17.00	17.39	16.85	6.76
-0.5	15.25	4.26	10.28	8.73	14.17	18.04	13.92	14.94	14.93	8.64
0.0	16.35	2.67	9.88	14.95	18.84	22.72	12.64	14.50	12.25	8.41
0.5	12.94	1.49	7.12	18.68	19.34	17.87	11.29	12.19	8.44	7.61
1.0	3.86	0.86	2.40	4.94	3.97	3.80	2.85	3.50	4.27	10.20
1.5	2.46	0.64	2.12	2.73	1.46	2.01	1.39	1.29	1.81	6.61
2.0	2.24	1.30	3.06	2.24	1.12	1.71	1.33	1.04	1.56	6.68
2.5	1.91	3.42	4.95	1.75	0.97	1.91	1.59	1.17	1.93	8.42
3.0	2.17	24.74	19.18	2.57	1.48	3.16	2.58	2.08	3.43	16.49
3.5	0.72	35.74	19.32	1.53	0.96	1.61	1.19	1.21	1.80	6.20
4.0	0.56	8.42	4.25	1.02	0.70	1.26	0.93	1.10	1.47	1.85
4.5	0.16	0.13	0.07	0.26	0.20	0.39	0.30	0.39	0.50	0.33
5.0	0.16	0.05	0.04	0.23	0.16	0.34	0.28	0.37	0.50	0.24
Pan	0.18	0.05	0.07	0.21	0.16	0.30	0.29	0.33	0.43	0.21
	100.0	100.0	100.0	100.0	100.0	100.0	100.0	100.0	100.0	100.0

APPENDIX H

REGIONAL SEDIMENT MANAGEMENT BULLETIN
VOL 4, WNTER/SPRING 2006

Regional Sediment Management

Southeast Oahu Regional Sediment Management: Identifying Sediment Pathways in the Vicinity of Wailea Point

Improved Characterization and Estimates of Sediment Sources, Pathways, and Sinks under the System-Wide Water Resources Program (SWWRP)

New Program Manager

Volume 4

Winter/Spring 2006

Southeast Oahu Regional Sediment Management: Identifying Sediment Pathways in the Vicinity of Wailea Point

by Thomas D. Smith and Jessica R. Hays, U.S. Army Engineer District, Honolulu

Initial regional sediment management efforts in Hawaii have been focused along the southeast O'ahu (Hawaiian for the gathering place) coast. The Southeast O'ahu Regional Sediment Management (SEO/RSM) study area extends along approximately 12 miles of shoreline from Mokapu (taboo) Point to the north and Mokapu'u (hilltop) to the south. Towns within the region include Kailua (whole in the sea), Lanikai (sky and sea) and Waimanalo (sweet water). Military installations within the area are Marine Corps Base Hawaii and Bellow Air Force Station (AFS). The region experiences prevailing trade winds from the northeast, associated trade showers, and locally generated wind waves. A broad shallow nearshore reef extends along the length of the region. The reef is nominally 2,000 feet wide and has an average depth of about 4 feet. Small offshore islets such as Manana (buoyant), Kaohikaipu (hold back breaking waves), Na Mokulua (calmed, two adjacent islands), Popoi'a, and Mokolea (filled with water) Rock are scattered throughout the reef flat.

Generally, wide sand beaches are a rare sight in Hawaii, but within the SEO region there are a number of long stretches of pristine kahaone (sandy beach). These areas include numerous State of Hawaii-owned beach parks and portions of Bellow AFS. Beach sand in the region primarily comprises calcium carbonate grains derived from shells, corals, and other aquatic organisms. Basalt from the eroding island mountains can also be found in sand samples taken within the active beach profile. At the northern limit of the region, significant quantities of olivine are also present along the upper reaches of the beach.

This is not to say the region does not have erosion and sediment management issues. At Ka'elepulu (hollow and wet) stream mouth, sand from the adjacent shorelines accumulates and blocks the flow of water from Enchanted Lake upstream. The existing sediment management practice is to periodically excavate the sand from the mouth of the stream and place it along the adjacent streambanks. Not only does this practice take the material out of the active profile, strong trade winds blow the sand mauka (toward the mountain) and out of the system. On either side of Wailae (happy water) Point, coastal structures have been constructed such as seawalls, groins, revetments and jetties. Beaches in these areas (including portions of both Lanikai and Bellows AFS) are narrow to nonexistent. At the southern end of the region, the shoreline is eroding and currently within a few feet of Kalanianna'ole Highway along Kaupo (a variety of native banana) and Kaiona (sea mite) beaches. The highway is a major transit route and provides the only access to much of the windward O'ahu coastal margin. The scarcity

of beach quality sand and environmental concerns in Hawaii limit the opportunities for beach nourishment.

A major goal of the SEO/RSM study is to quantify the movement of sand offshore of Wailea (happy waters) Point. The point is located in the central portion of the region and divides the town of Lanikai to the north and Bellows AFS to the south. At the present, the portion of Lanikai beach located adjacent to Wailea Point is awash at high tide and a continuous series of seawalls has been built to protect oceanfront singe-family homes. Further to the north, the beach widens significantly until one reaches Alala (a variety of sweet potato) Point. Beyond Alala Point, the beaches of Kailua are from 100 feet to 200 feet wide and the oceanfront houses are set back up to 300 feet from the mean high water shoreline.

Similarly, south of the point the shoreline has been armored through construction of a revetment along approximately 2,000 feet of the Bellows AFS shoreline. A 50-foot-long groin has been constructed at the point which retains a small pocket beach in front of an officer's beach cottage rental unit. Jetties have also been constructed at the mouth of Waimanalo stream in an attempt to keep the mouth of the stream from being plugged by the influx of sand from adjacent beaches. In order to quantify sediment transport in the vicinity of Wailea Point, the SEO/RMS study strives to incorporate multiple assessment techniques to attain an understanding of the regional coastal processes at work, assess anthropogenic impacts to the system and develop a sediment budget for the area and ultimately the entire region.

In pursuit of a regional sediment budget for SEO, wave, current, and sediment data have been collected, a wave transformation model has been coupled to a water circulation model, and a historical shoreline change analysis is underway. Field data collection was conducted for a one month period in the fall of 2005. Data collection consisted of deployment of Acoustic Doppler Current Profilers (ADCP) and currents) and Acoustic Doppler Velocimeters (ADV) gauges and the tracking of drogues following their release at various locations within Kailua and Waimanalo bays. Instrument locations are shown in Figure 1. Deployment was on 9 Aug 2005 and retrieval was on 14 Sep 2005. Each gauge successfully collected a minimum of one month of time series data.

The ADCP gauges were RD Instruments 1,200 kilohertz Workhorse, bottom mounted facing upward with the sensor head approximately 0.4 meters off the bottom. Figure 2 shows the custom built

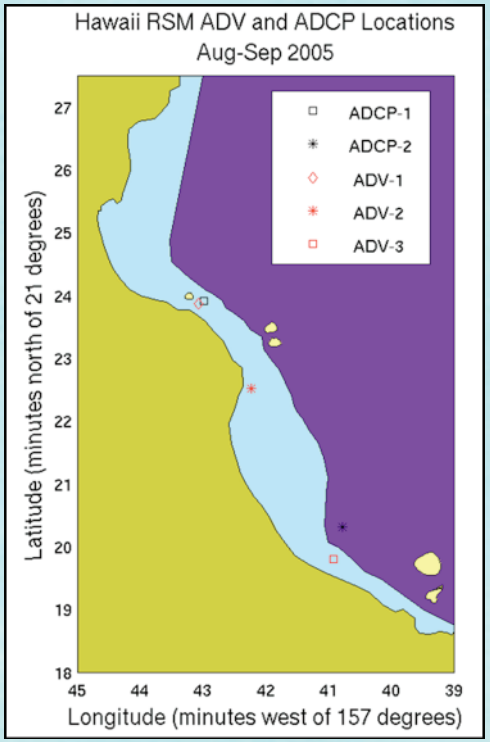

Figure 1. ADCP and ADV locations.

Figure 2. ADCP in frame (left) and close-up of transducer head with biofouling (right).

Figure 3. Hydra ADV in frame (left) and closer view of the biofouled sensor head (right).

mount that was held to the bottom with about 80 pounds of lead weight. These gauges have four acoustic transducers for measuring currents and a pressure sensor, from which horizontal and vertical current profiles were computed at 0.2-meter vertical spacing. These units sampled at 2 kilohertz for directional wave measurements. Each hourly wave burst was approximately 34 minutes long, starting at the top of each hour, and consisted of 4,096 points. There is a 0.44-meter blanking distance from the transducer head, and with a 0.2-meter bin width, this makes the first sample 0.72 meter past the transducer, or about 1.12 meters off the bottom. Current profiles were collected every 10 minutes from a 200-point average.

The three ADV gauges were the Sontek's Hydra model that sample a single point current velocity (U, V, and W) and contained an external pressure sensor. The instrument frame and ADV transducer are shown in Figure 3 (after gauge retrieval). The sample volume for the current measurement is approximately 1 to 2 centimeters in size and about 0.17 meters from the center transducer. This unit uses three beams to determine the three current components.

Four inexpensive current drogues (drifters) were designed and built at the USACE Coastal and Hydraulics Laboratory (CHL) Field Research Facility (FRF) that used Global Positioning System (GPS) tracking and radio telemetry for positioning. They were constructed with off-the-shelf plumbing supplies (PVC pipe, vertical risers, rubber unions, hose clamps), Garmin Geko GPS

Figure 4. GPC current drogue with traditional drifter (grapefruit) and Hawaiian drifter (coconut). Drifter floats just below the surface.

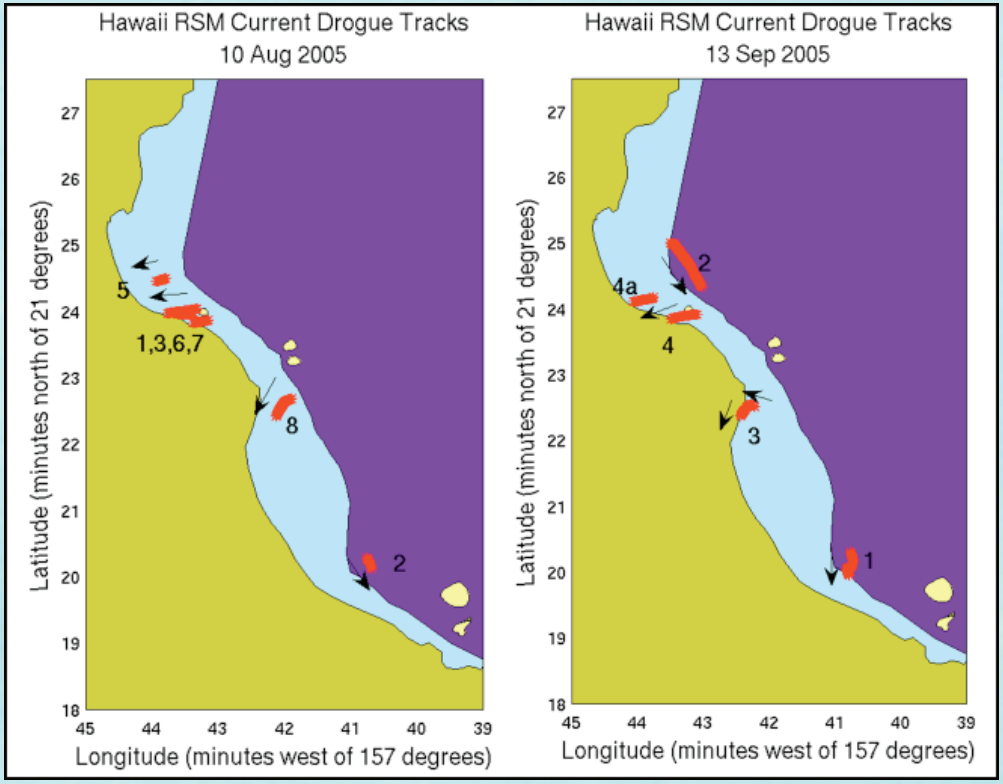

Figure 5. Drogue tracks with track number for 10 August (left) and 13 September (right).

receivers, and MaxStream (model XStream-PKG-R) radio modems (Figure 4). The sails had about a 1-meter cross section. The lower vertical PCV pipe (submerged) contained the modem and batteries, the upper horizontal pipe contained the GPS receiver and radio antennas. A National Electrical Manufactures Association (NEMA) GPS data string was transmitted once per second and the Garmin Fround Control Points (GCP) unit internally recorded positions every 30 seconds. These GPS units are Wide Area Augmentation System

(WAAS) enabled and have a horizontal accuracy of about 3 meters. The radio tracking required line of sight, and it was not possible to simultaneously receive drifters signals in the Kailua and Waimanalo bays.

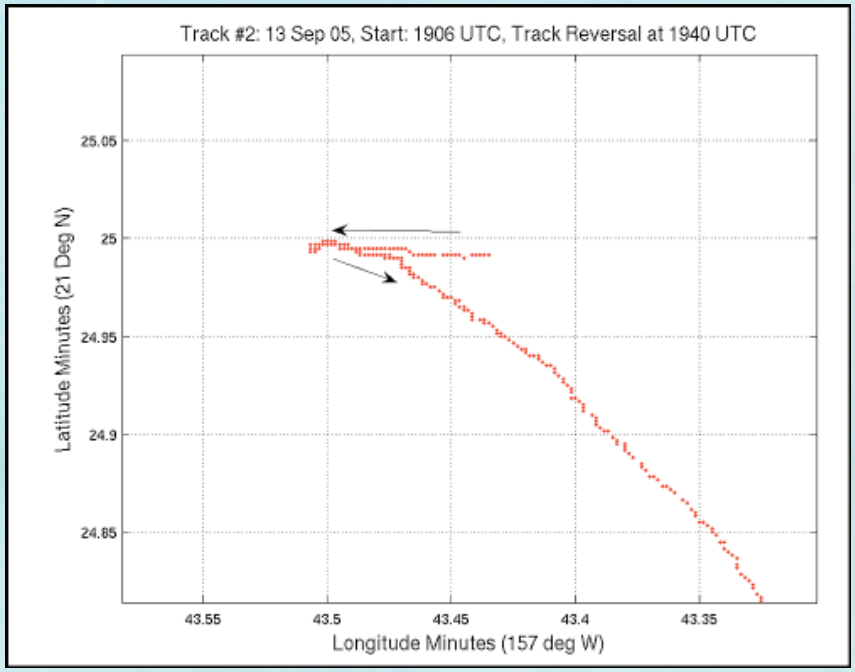

Figure 6. Drouge track reversal on 13 September.

Drogue tracks with track numbers are shown in Figure 5. Some drogues were deployed in the vicinity of the ADV and ADCP gauges for interomparison. An interesting reversal of drogue No. 2 was observed shortly after deployment on 13 Sep (Figure 6), starting off on a nearly due west tract and then turning back to a southeast trajectory.

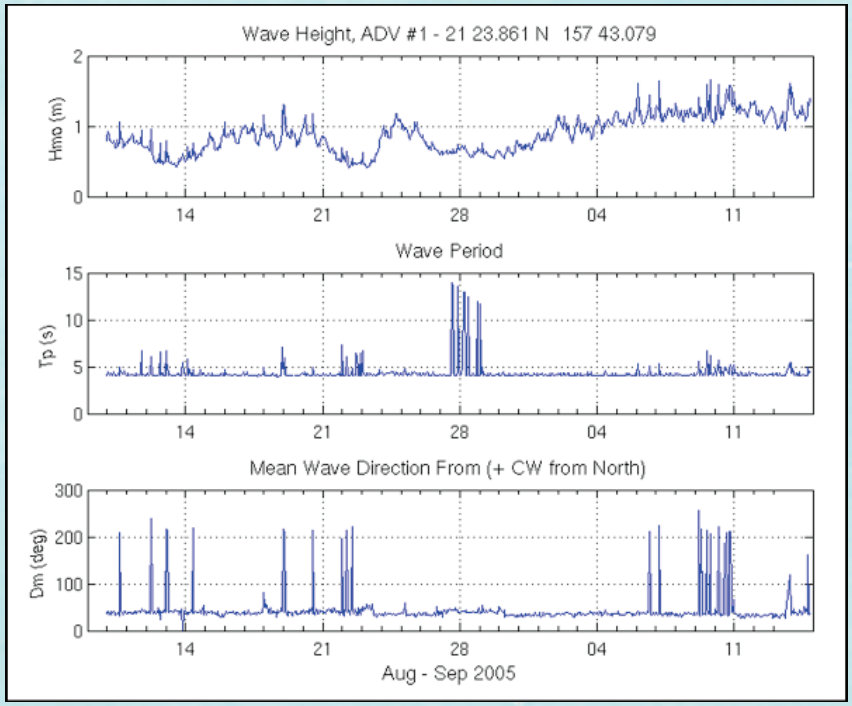

Figure 7. Wave height, period, and direction for ADCP No. 1.

Figure 7 is a plot wave height (Hmo), peak period (Tp), and mean direction (Dm) for ADV No. 1. Figure 8 compares Hmo for the three ADVs and shows ADV No. 3 as having the smallest wave heights. Current directions for ADV No. 2 appear to be mainly north or south which may be due to placing the gauge between coral heads that restricts flows to those directions.

The field data is being utilized to calibrate and verify the results of ongoing wave transformation and water circulation modeling. Bathymetric data used in the generation of model grids were derived from various sources. National

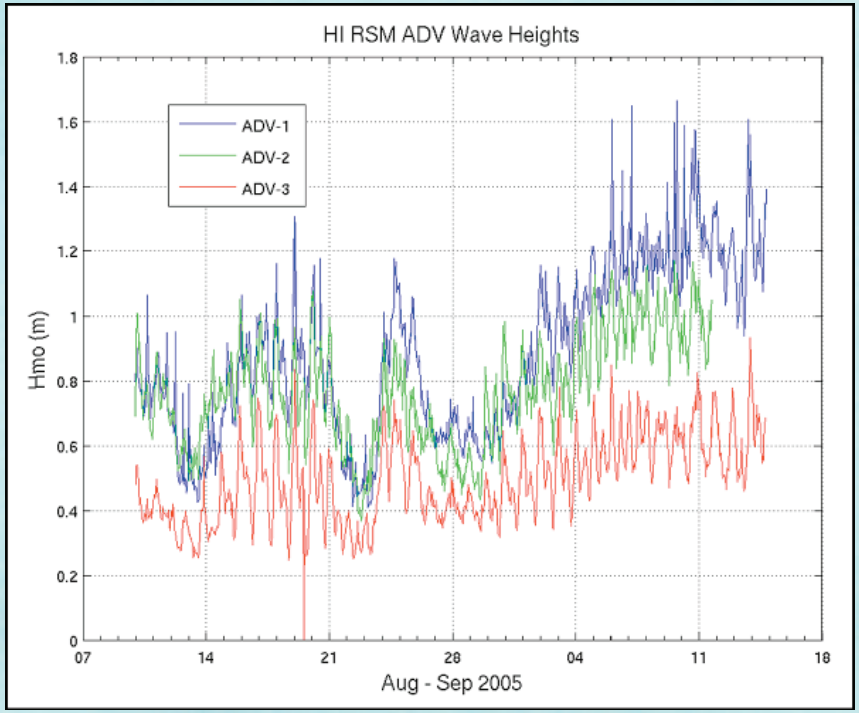

Figure 8. Wave height (Hmo) comparison of the three ADVs.

Geophysical Data Center data sets including ETOPO2 and GEODAS were used in the deep ocean while National Oceanic and Atmospheric Administration (NOAA) digital nautical charts and SHOAL were used for intermediate and nearshore waters, respectively. Grid element size for the circulation model ranged from 75 miles to 80 feet. Bathymetric data were interpolated onto the circulation model grid and hand-edited to ensure accuracy.

Tidal constituents from an established database were used to force the model boundary water levels as well as hindcast winds procured from Ocean Weather, Inc. Tide levels generated by the model compared favorably to NOAA tide gauge data from Kaneohe (bamboo god) Bay and Honolulu (calm bay) Harbor. Wave transformation modeling was conducted over a grid incorporating the SEO region as well as additional area both longshore and makai (oceanward). A directional wave gauge (University of Hawaii/Coastal Data Information Program (CDIP) gauge 098) has been operational at the boundary of the grid from August 2000 to the present and has provided valuable boundary conditions for use in model calibration/verification with nearshore field gauge data acquired as

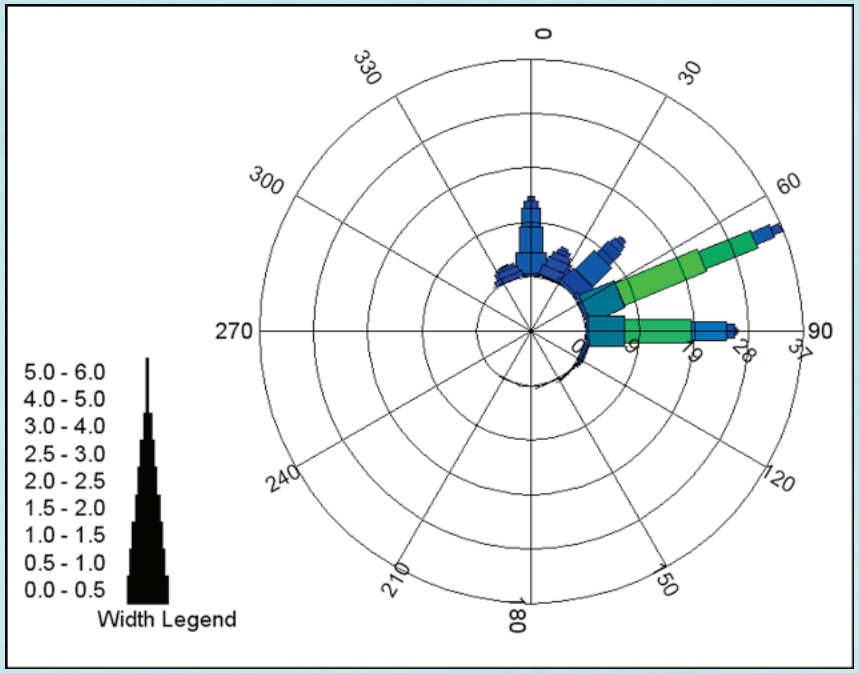

Figure 9. Wave rose for UH/CDIP bouy in RSM demo area.

previously described. As shown in Figure 9, waves recorded by the University of Hawaii gauge were generally from the northeast quadrant and ranged in height from 0.5 to 1.5 meters. Wave periods were on the order of 6 to 16 seconds. Currently, the wave transformation and water circulation modeling is being refined based upon comparison to the field data. Once calibrated, the models will be used to hindcast the wave/wind/tide induced water circulation within the SEO/RSM study area for the year 2004.

The historical shoreline change analysis being conducted for SEO/RSM by the University of Hawaii consists of determining the rate of shoreline change at 20-meter intervals alongshore over the period of early 20th century to 2005. NOAA "T" sheets dating from the early 20th century are being orthorectified using modern GPS ground control and used in comparison with four to eight orthorectified aerial photographs from the post-World War II era to determine a long-term rate of shoreline change. Reweighted weighted least median of squares linear regression technique is being used to determine the long-term trend of historical change. This technique eliminates outlier points from the linear regression and combines measurement and positional uncertainties with regression uncertainties in calculating the standard deviation of the trend.

New aerial photographs from 2005 with a scale of 1:8400 digitally scanned at 10 microns will be acquired for the study. These aerials will cover a coastal strip approximately 800 to 1,000 meters wide centered on the shoreline. Stereo-photogrammetry using orthorectified pairs of photos, with GPS ground control, will be used to create coastal digital terrain models (DTMs). These DTMs will be digitally combined with offshore SHOALS data (where such data exist) to create a seamless topographic/bathymetric DEM for the region. Historical photography and "T" sheets will be orthorectified using the 2005 DEM so that all derived shoreline data are based on orthorectified positions, thus minimizing positional errors. Root mean square positional error of final orthorectified photographs is typically about 1 to 2 meters. Using topographic field profiles to measure beach and dune volume shoreline change rates can be converted to rates of sand volume change over time. Along with historical shoreline change data presented at a 20-meter interval along the entire region a sediment budget for the period of study (approximately 80 years) will be produced.

Sediment Trend Analysis (STA) is a technique that derives patterns of net sediment transport from relative changes in grain-size distributions of aquatic sediments. STA also determines the dynamic behavior or stability (i.e., erosion, dynamic equilibrium, accretion or deposition) of the sediments. Sediment Trend Analysis is used to derive the following information:

- Grain size characteristics of surficial sediment encompassing the entire area of study
- Sediment sources and sinks
- Zones of influence of sediment sources

- Sediment transport pathways
- Sediment stability (i.e., erosion, accretion, dynamic equilibrium, etc.)
- Links between intertidal or beach areas and offshore sediments

For the SEO/RSM study, STA will be utilized as another means to identify sediment pathways in the vicinity of Wailea Point. Sediment sampling is to consist of acquisition of 250 grab samples by the University of Hawaii, analysis of the sediment samples by the CHL and the ultimate use of STA methodology by the University of Hawaii to qualitatively describe how sand moves around and offshore of Wailea Point.

Comparison and correlation of the field data, numerical model results, historical shoreline change analysis, and STA will unlock the mystery of sediment transport within the Wailea Point subregion of the SO/RSM study area. Given an accurate understanding of sediment transport and coastal processes in and around Wailea Point, stakeholders and decision-makers will be able to forge realistic goals in the management of beach resources along the Lanikai and Bellows Air Force Stations shorelines. With a regional sediment management plan in hand, the remaining question will be "Loa'a One? (Got Sand?)".

Loa'a One? (Got Sand?)